

# Politecnico di Torino

*Master's Degree in Civil Engineering*



Master's degree Thesis

## *Numerical Modelling of an Underground Cavern in jointed rock mass*

Supervisors:

Prof. **Daniele Peila**

Prof. **Monica Barbero**

External Supervisor:

Ing. **Giovanni Quaglio**

Candidate:

**Lorenzo Emidio D'Imperio**

*July 2021*



# ***Abstract***

In this dissertation the study of the behavior and the stability of an underground cavern in jointed rock granite has been carried out. For this purpose, different analyses were developed, using Finite Element Method software for the modelling in two and three dimensions of the cavern. The main purpose of this master thesis was to create different continuum numerical models which could represent the weathered rock mass using different approaches.

One possible approach followed in this project as means to incorporate the influence of joints on rock mass strength in numerical analysis was by modelling rock masses as equivalent continuum with reduced deformation and strength properties. This model was considered as reference in the present dissertation.

Another way to model jointed rock masses was through the introduction of special elements such as joint elements, also known as interface elements. In this way, it was possible to implement different continuum models with joints following the joint systems formulated by Dershowitz in 1985. All these models were compared, the continuum model with joints “Cross jointed” was indicated as the one that better represents the weathered rock mass. It was found that this model was the one that exhibiting the more similar behaviour and results compared to the equivalent continuum model.



# ***Acknowledgments***

First, I would like to thank the institutions of the Politecnico di Torino and in particular the Professor Daniele Peila and Monica Barbero thanks to whom I was able to carry out this thesis. A special thanks to Giovanni Quaglio for having supported me during the internship and in the developing of this project, he provided the data and gave me important suggestions during the study. An endless thank you to my family, who has always supported me in any way during these years. A special thank you to my girlfriend Annie for her constant and indispensable presence to face every challenge in the best way.



# Contents

<b>1.</b>	<b>INTRODUCTION.....</b>	<b>1</b>
1.1	RESEARCH DESCRIPTION AND OBJECTIVES .....	1
1.2	THESIS OVERVIEW .....	2
<b>2.</b>	<b>CONTEXT OF THE WORK .....</b>	<b>4</b>
2.1	PROJECT CONTEXT .....	4
2.2	GEOLOGY DESCRIPTION .....	5
2.3	CAVERN ENGINEERING OVERVIEW .....	7
2.3.1	<i>Cavern design.....</i>	<i>7</i>
2.3.2	<i>Cavern construction.....</i>	<i>14</i>
<b>3.</b>	<b>CONTINUUM MODEL IN 2D.....</b>	<b>20</b>
3.1	GEO-MECHANICAL CHARACTERISATION .....	20
3.2	CONTINUUM MODEL USING $RS_2$ .....	31
<b>4.</b>	<b>CONTINUUM MODEL WITH JOINTS IN 2D .....</b>	<b>36</b>
4.1	GEO-MECHANICAL CHARACTERIZATION OF JOINTS.....	36
4.2	CONTINUUM MODEL WITH JOINTS USING $RS_2$ .....	41
4.2.1	<i>Joint Networks overview.....</i>	<i>43</i>
4.2.2	<i>Model 1-Joint network CROSS JOINTED .....</i>	<i>46</i>
4.2.3	<i>Model 2-Joint Network PARALLEL STATISTICAL.....</i>	<i>49</i>
4.2.4	<i>Model 3-Joint Network PARALLEL DETERMINISTIC.....</i>	<i>50</i>
4.2.5	<i>Model 4-Joint network VENEZIANO.....</i>	<i>51</i>
4.2.6	<i>Model 5-Joint Network BAECHER.....</i>	<i>55</i>
4.2.7	<i>Model 6-Joint Network VORONOI.....</i>	<i>57</i>
<b>5.</b>	<b>CONTINUUM MODEL IN 3D.....</b>	<b>61</b>
5.1	CONTINUUM MODEL USING $RS_3$ .....	61
<b>6.</b>	<b>CONTINUUM MODEL WITH JOINTS IN 3D .....</b>	<b>69</b>
6.1	CONTINUUM MODEL WITH JOINTS USING $RS_3$ .....	69
<b>7.</b>	<b>RESULTS AND CONCLUSIONS.....</b>	<b>77</b>
7.1	TWO-DIMENSIONAL MODEL'S RESULTS .....	77
7.2	THREE-DIMENSIONAL MODEL'S RESULTS .....	88

7.3	CONCLUSIONS.....	96
7.4	FUTURE RESEARCH.....	99
8.	<b>REFERENCES .....</b>	<b>101</b>

# List of figures

FIGURE 2.1: STEREOGRAM AND CAVERN ORIENTATION.....	8
FIGURE 2.2: COST CURVES AGAINST CAVERN SPAN AND HEIGHT FOR DIFFERENT ROCK CONDITIONS (O.J. BERTHELSEN, 1992). .....	9
FIGURE 2.3: STANDARD ROOF ARCH SHAPE (O.J. BERTHELSEN, 1992).....	9
FIGURE 2.4 ILLUSTRATION OF FAILURE MODES (MODIFIED FROM MARTIN ET AL, 1999).....	11
FIGURE 2.5: TYPICAL ROOF SUPPORT WITH PATTERN BOLTING (O.J. BERTHELSEN, 1992).....	14
FIGURE 2.6: TYPICAL EXCAVATION STAGES FOR TOP HEADINGS IN CAVERNS (O.J. BERTHELSEN, 1992).....	15
FIGURE 2.7: TYPICAL EXCAVATION STAGES FOR A LARGE CAVERN (O.J. BERTHELSEN, 1992). .....	16
FIGURE 2.8: FULLY GROUTED BOLTS SCHEME (O.J. BERTHELSEN, 1992).....	19
FIGURE 3.1: REFERENCE GUIDE FOR ROCK QUALITY DESIGNATION (NGI, 2015) .....	21
FIGURE 3.2: REFERENCE GUIDE FOR JOINT SET NUMBER J <sub>N</sub> (NGI, 2015) .....	23
FIGURE 3.3: REFERENCE GUIDE FOR JOINT ROUGHNESS NUMBER J <sub>R</sub> (NGI, 2015).....	23
FIGURE 3.4: REFERENCE GUIDE FOR JOINT ALTERATION NUMBER J <sub>A</sub> (NGI, 2015) .....	24
FIGURE 3.5: REFERENCE GUIDE FOR JOINT WATER REDUCTION FACTOR J <sub>W</sub> (NGI, 2015) .....	25
FIGURE 3.6: REFERENCE GUIDE FOR STRESS WATER REDUCTION FACTOR SRF (NGI, 2015) .....	25
FIGURE 3.7: WEATHERING DEGREE CHART (J.B. MASSEY, 1988).....	27
FIGURE 3.8: RATIO OF HORIZONTAL TO VERTICAL STRESS FOR DIFFERENT DEFORMATION MODULI BASED UPON SHEOREY'S EQUATION. (SHEOREY, 1994).....	29
FIGURE 3.9: ROCK SUPPORT CHART (NGI, 2015) .....	30
FIGURE 3.10: CONVERSION FROM ACTUAL Q-VALUES TO ADJUSTED Q-VALUES FOR DESIGN OF WALL SUPPORT (NGI, 2015).....	30
FIGURE 3.11: CONTINUUM MODEL.....	31
FIGURE 3.12: CONTINUUM MODEL GEOMETRY .....	32
FIGURE 4.1: HOEK & BROWN LINEARIZATION GRANITE Q=0,7 .....	38
FIGURE 4.2: HOEK & BROWN LINEARIZATION GRANITE Q=0,2.....	38
FIGURE 4.4: CONCEPTUAL MODEL FOR ROCK JOINT SYSTEM (DERSHOWITZ, 1985).....	45
FIGURE 4.5: JOINT SYSTEM MODELS (DERSHOWITZ, 1985).....	46
FIGURE 4.6: 3D ORTHOGONAL MODEL (DERSHOWITZ, 1985).....	47
FIGURE 4.7: 2D ORTHOGONAL MODEL (DERSHOWITZ, 1985).....	47
FIGURE 4.8: MODEL 1-CROSS JOINTED.....	48
FIGURE 4.9: MODEL 2-PARALLEL STATISTICAL .....	50
FIGURE 4.10: MODEL 3-PARALLEL DETERMINISTIC .....	51

FIGURE 4.11: TWO-DIMENSIONAL VENEZIANO MODEL (DERSHOWITZ, 1985) .....	53
FIGURE 4.12: TWO-DIMENSIONAL VENEZIANO MODEL (DERSHOWITZ, 1985) .....	53
FIGURE 4.13: MODEL 4 VENEZIANO .....	54
FIGURE 4.14: THREE-DIMENSIONAL BAECHER MODEL (DERSHOWITZ, 1985).....	55
FIGURE 4.15: TWO-DIMENSIONAL BAECHER MODEL (DERSHOWITZ, 1985).....	56
FIGURE 4.16: MODEL 5 BAECHER.....	57
FIGURE 4.17: THREE-DIMENSIONAL BAECHER MODEL (DERSHOWITZ, 1985).....	58
FIGURE 4.18: TWO-DIMENSIONAL BAECHER MODEL (DERSHOWITZ, 1985).....	59
FIGURE 4.19: MODEL 6 VORONOI .....	60
FIGURE 5.1: CONTINUUM MODEL IN 3D GEOMETRY .....	63
FIGURE 5.2: CAVERN GEOMETRY IN GEOSTATIC CONDITION.....	64
FIGURE 5.3: THIRD STAGE OF CAVERN'S EXCAVATION .....	65
FIGURE 5.4: EIGHTH STAGE OF CAVERN'S EXCAVATION.....	65
FIGURE 5.5: FINAL STAGE OF CAVERN'S EXCAVATION .....	66
FIGURE 5.6: 3D CONTINUUM MODEL RESTRAINTS.....	67
FIGURE 5.7: 3D CONTINUUM MODEL MESH.....	67
FIGURE 5.8: 3D CONTINUUM MODEL .....	68
FIGURE 6.1: CONTINUUM MODEL WITH JOINTS 3D GEOMETRY .....	71
FIGURE 6.2: CAVERN GEOMETRY IN GEOSTATIC CONDITION.....	72
FIGURE 6.3: THIRD STAGE OF CAVERN'S EXCAVATION .....	73
FIGURE 6.4: EIGHTH STAGE OF CAVERN'S EXCAVATION.....	73
FIGURE 6.5: FINAL STAGE OF CAVERN'S EXCAVATION .....	74
FIGURE 6.6: 3D CONTINUUM MODEL WITH JOINTS RESTRAINTS .....	75
FIGURE 6.7: 3D CONTINUUM MODEL WITH JOINTS MESH .....	75
FIGURE 6.8: 3D CONTINUUM MODEL WITH JOINTS.....	76
FIGURE 7.1: $\Sigma_1$ EXCAVATION BOUNDARIES .....	78
FIGURE 7.2: $\Sigma_3$ EXCAVATION BOUNDARIES .....	78
FIGURE 7.3: TOTAL DISPLACEMENT EXCAVATION BOUNDARIES .....	79
FIGURE 7.4: STRENGTH FACTOR WITH UBIQUITOUS JOINTS EXCAVATION BOUNDARIES .....	79
FIGURE 7.5: ELEMENTS YIELDED CONTINUUM MODEL .....	80
FIGURE 7.6: ELEMENTS YIELDED MODEL 1 CROSS JOINTED.....	80
FIGURE 7.7: ELEMENTS YIELDED MODEL 2 PARALLEL STATISTICAL .....	80
FIGURE 7.8: ELEMENTS YIELDED MODEL 3 PARALLEL DETERMINISTIC.....	81
FIGURE 7.9: ELEMENTS YIELDED MODEL 4 VENEZIANO .....	81
FIGURE 7.10: ELEMENTS YIELDED MODEL 5 BAECHER.....	81

FIGURE 7.11: ELEMENTS YIELDED MODEL 6 VORONOI .....	82
FIGURE 7.12: COMPARISON CONTINUUM MODEL AND MODEL 1 CROSS JOINTED- $\Sigma_1$ .....	83
FIGURE 7.13: COMPARISON CONTINUUM MODEL AND MODEL 1 CROSS JOINTED-SIGMA $\Sigma_3$ .....	84
FIGURE 7.14: COMPARISON CONTINUUM MODEL AND MODEL 1 CROSS JOINTED-TOTAL DISPLACEMENT .....	84
FIGURE 7.15: COMPARISON CONTINUUM MODEL AND MODEL 1 CROSS JOINTED-YELDED ELEMENTS .....	84
FIGURE 7.16: AXIAL FORCE BOLTS EQUIVALENT CONTINUUM .....	86
FIGURE 7.17: AXIAL FORCE BOLTS MODEL 1 CROSS JOINTED.....	86
FIGURE 7.18: 3D-CONTINUUM MODEL $\Sigma_1$ [kPA] .....	89
FIGURE 7.19: COMPARISON 2D-3D CONTINUUM MODEL $\Sigma_1$ [kPA].....	89
FIGURE 7.20: 3D-CONTINUUM MODEL $\Sigma_3$ [kPA] .....	90
FIGURE 7.21 COMPARISON 2D-3D CONTINUUM MODEL $\Sigma_3$ [kPA].....	90
FIGURE 7.22: 3D-CONTINUUM MODEL TOTAL DISPLACEMENT [M].....	91
FIGURE 7.23 COMPARISON 2D-3D CONTINUUM MODEL TOTAL DISPLACEMENT [M] .....	91
FIGURE 7.24: 3D-CONTINUUM MODEL WITH JOINTS $\Sigma_1$ [kPA].....	93
FIGURE 7.25: COMPARISON 2D-3D CONTINUUM MODEL WITH JOINTS $\Sigma_1$ [M] .....	93
FIGURE 7.26: 3D-CONTINUUM MODEL WITH JOINTS $\Sigma_3$ [kPA].....	94
FIGURE 7.27: COMPARISON 2D-3D CONTINUUM MODEL WITH JOINTS $\Sigma_3$ [M] .....	94
FIGURE 7.28: 3D-CONTINUUM MODEL WITH JOINTS TOTAL DISPLACEMENTS [M].....	95
FIGURE 7.29: COMPARISON 2D-3D CONTINUUM MODEL WITH JOINTS TOTAL DISPLACEMENT [M] .....	95
FIGURE 7.30: COMPARISON 2D-3D MODELS $\Sigma_1$ [M] .....	98
FIGURE 7.31: COMPARISON 2D-3D MODELS $\Sigma_3$ [M] .....	98
FIGURE 7.32: COMPARISON 2D-3D MODELS TOTAL DISPLACEMENT [M] .....	99

# List of Tables

TABLE 3.1 SUMMARY OF THE DESCRIBED CORRELATIONS BETWEEN Q PARAMETERS AND RQD VALUES .....	26
TABLE 3.2 WEATHERING DEGREE-UCS (O.J. BERTHELSEN, 1992) .....	28
TABLE 3.3 CONSTANT FIELD STRESS (CONTINUUM MODEL) .....	33
TABLE 3.4 MATERIAL PROPERTIES (CONTINUUM MODEL).....	34
TABLE 3.5 SUPPORT CROWN BOLTS FULLY BONDED PROPERTIES (CONTINUUM MODEL).....	35
TABLE 3.6 SUPPORT WALL BOLTS FULLY BONDED PROPERTIES (CONTINUUM MODEL).....	35
TABLE 4.1: MOHR-COULOMB PARAMETERS.....	39
TABLE 4.2: SHEAR MODULUS .....	40
TABLE 4.3: JOINTS NORMAL STIFFNESS AND JOINTS SHEAR STIFFNESS.....	41
TABLE 4.4 MATERIAL PROPERTIES CONTINUUM MODEL WITH JOINTS.....	43
TABLE 4.5: MODEL 1 CROSS JOINTED PROPERTIES .....	48
TABLE 4.6: MODEL 1 CROSS JOINTED PROPERTIES .....	49
TABLE 4.7 MODEL 2 PARALLEL STATISTICAL PROPERTIES .....	50
TABLE 4.8 MODEL 3 PARALLEL DETERMINISTIC PROPERTIES.....	51
TABLE 4.9: MODEL 4 VENEZIANO PROPERTIES.....	54
TABLE 4.10: MODEL 5 BAECHER PROPERTIES.....	56
TABLE 4.11: MODEL 6 VORONOI PROPERTIES .....	59



# Chapter 1

## 1. INTRODUCTION

### 1.1 *Research description and objectives*

In the present dissertation the study of the behavior and the stability of an underground cavern in jointed rock granite was carried out. For this purpose, different analyses were developed, using FEM software for the modelling in two and three dimensions of the project. This work, started from an internship experience in which the analysis of an underground cavern was implemented. However, the site of interest and the main experimental data were not explicitly reported in this dissertation because sensitive data of this project could not be published yet. The main objective of this master thesis was to create different numerical models representing the jointed rock mass using different approaches and comparing them in order to reach as much as possible a solution that could fit and validate the reference equivalent continuum model set up during the internship in the best way possible. The equivalent continuum model was developed from the results obtained from experimental evidence. For this reason, it was taken as reference model and considered the target of the implementations.

One possible approach followed in this project for incorporating the influence of joints on rock mass strength in numerical analysis was modelling rock masses as equivalent continuum with reduced deformation and strength properties. Methods based on this approach are very useful, but they do not allow to model mechanisms involving movements such as: separation, slip and rotations of blocks.

Another way for modelling jointed rock masses was by introducing special elements such as joints, also known as interface elements. These elements can have either zero thickness or thin, finite thickness. Moreover, they can assume linear elastic behaviour or plastic response when stresses exceed the strengths of discontinuities. Due to the fundamental continuum analysis condition of displacement compatibility at element nodes, FEM programs do not allow the detachment of individual blocks. However, they are very useful for determining the onset of instability (collapse mechanisms) or large movements that cause block detachments.

In the following, the equivalent continuum models, and the continuum models with joints are used to model the stability of underground cavern in jointed rock granite, by using the RS2 and RS3 FEM software of the Rocscience suite.

### **1.2 Thesis Overview**

Chapter 2 contextualises the project and allows the reader to take confidence with the topic. The geology of the site of interest is presented, moreover a general discussion about the cavern design and construction methods that can be adopted in the realization of an underground facility as the one object of study is reported.

Chapter 3 reports the two-dimensional equivalent continuum model set up, and the description of how it is possible to derivate the geo-mechanical properties of the rock mass. Moreover, the project settings of the finite element equivalent continuum model have been explained in the detail.

Chapter 4 shows the two-dimensional continuum model with joints, the description of the geo-mechanical properties of joints and the joint systems, the analysis and derivation of the input parameter for the continuum model with joints to be implemented.

Chapter 5 provides the three-dimensional equivalent continuum model, in particular a description of how the model was implemented with the geometrical features, the cavern design sequences, and all the parameters adopted.

Chapter 6 deals instead with the three-dimensional continuum model with joints, describing of how the model was implemented with the geometrical features, the cavern design sequences, and all the parameters adopted.

Finally, in Chapter 7, results and conclusions were pointed out with the comparison between the two-dimensional and the three-dimensional models. Then, the chapter also reports some thoughts regarding further future research.

## Chapter 2

### 2. CONTEXT OF THE WORK

#### 2.1 *Project context*

Since the earliest times, largely opportunistic use has been made of naturally occurring caves for habitation and primitive industry. The use of man-made underground space has been recorded from all the early and great civilizations.

The project under analysis describes an underground cavern in jointed rock granite. This cavern results part of a more complicated series of cavern that will determine an underground sewage treatment system plant; the cavern area is situated below a small mountain with a cover of about 300 m. In general, caverns are similar to tunnels in terms of engineering principles. The differences between them are their physical dimension and their application. Perhaps, cavern usually have larger cross section than tunnels. Moreover, tunnels are used essentially to enhance connectivity, whereas caverns are usually associated with a specific usage, which might include storage, industrial process, commercial activities and possibly habitation.

The primary drivers for cavern developments are often lack of space, security requirement and the need to reduce environmental impacts. However, it is necessary that geological conditions must be suitable; as where hard rock lies close to surface, development of rock caverns will be preferred.

## **2.2 Geology description**

The site of interest was not explicitly declared in the present dissertation due to fact that it was not possible to report sensitive data, however a brief general geological description of the area was proposed in the following.

Knowledge of the geology is the starting point for all geotechnical investigations of cavern developments. A variety of rock types of igneous, sedimentary, and metamorphic origins were found in the site of interest. Of these, the igneous rocks, principally granite and the various volcanic rock types, have the greatest potential for cavern development and comprise the 80% of the rock in the studied location. The igneous rocks are mainly granite and volcanic rocks.

Discontinuities in the granites are generally widely spaced, even more than 2 m. Sheeting joints are often present near the surface. The granitic rocks are normally composed of feldspar, quartz and biotite but vary in grain size, texture, composition, and color. Granodiorite and quartz monzonite in the form of sheet-like plutons, stocks and dykes are present in many zones. Many of the above-mentioned rocks have been faulted and sheared. Perhaps, the studied area was subjected to significant different phases of intrusions that are strongly controlled by a NE-SW trend; the intrusions are elongated along this direction. Tectonic activity has continued after the intrusions of these rocks, which have been subsequently faulted, jointed and intruded by dykes, always following NE-SW orientation, which is the dominant trend in the zone of interest.

The whole area of the cavern zone is mainly composed of equigranular medium-grained with some porphyritic fine-grained granite. The main trends of the joints are NE-SW and NW-SE, as previously mentioned the dyke swarms also follow these trends, with NE also being the dominant trend of the minor intrusions and dykes. The volcanic rocks in the proximity of the major faults are significantly sheared and altered.

This may result in a significant change in the geotechnical properties. Faulted rocks may be weathered at considerable depths. The knowledge of the faulting pattern is very important because it can be used to minimize the risk of encountering unforeseen critical ground conditions during the excavation of the cavern. Moreover, it also allows an early optimization of the cavern orientation with regards to the joint sets and potential instability. However, no major faults have been identified crossing the proposed sewage treatment works cavern site, although some lineaments, representing minor faults, cross the proposed cavern site. Adjacent to the faults, the frequency of tectonic joints may increase, and the rock may be very closely jointed. Joints will control the most common instabilities mechanisms underground in the vicinity of the cavern site.

The geotechnical characterization was carried out considering the data derived from in situ surveys, in particular from boreholes. The Rock Quality Designation and the Weathering grade were derived. As first assessment, RQD distribution can be used to understand the distribution of the jointing degree of rock masses. In fact, RQD is a rough measure of the degree of jointing or fracture in a rock mass, measured as a percentage of the drill core in lengths of 10 cm or more.

High quality rock has an RQD more than 75%, low quality less than 50%. Given that the shallower portion of the rock mass may mislead the statistical evaluation of the jointing boreholes, the analysis was focused on the cavern complex elevation from 20 m a.s.l to 60 m a.s.l.

Result indicates that a large percentage of the cavern rock mass is composed by low jointed rock mass, therefore with a RQD larger than 75%. A more detailed description of the rock characterization is proposed in the chapter 3.

## **2.3 Cavern engineering overview**

This paragraph was inserted in the dissertation with the goal to give general information regarding Cavern engineering.

### **2.3.1 Cavern design**

First, concerning the cavern design the stability and serviceability of the excavation must be guaranteed, as a cavern should be designed to obtain the basis requirements of stability during the construction and during its design life. Instabilities in caverns, such as cave-in, rock fall and failure of structural supports can result in damage to underground facilities, in the case under study the sewage system. Moreover, a cavern is designed and built to last for a service life during which it can be maintained in a practical and economically viable manner. Support elements such as bolts, and shotcrete should be designed to be sufficiently durable and robust to prevent local deterioration of the rock mass during time.

The choice of the location and the orientation for a cavern development is one of the most important decisions in the design process, its stability is influenced by the orientation of joints affecting the rock mass. A minimum rock cover must be guaranteed to give adequate normal stress on the discontinuities such that the roof and wall could be self-supporting; in the case under examination there was a large rock cover therefore this was not an issue. However, weakness zones were present, and they had to be carefully considered, in the mechanical characterization of the rock mass. The cavern orientation of the project was  $11^\circ$  North, and the goal was to have as much as possible the longitudinal axis of the cavern oriented along the bisector line of the largest intersection angle of the strikes of the two dominant sets of discontinuities as reported in figure 2.1.

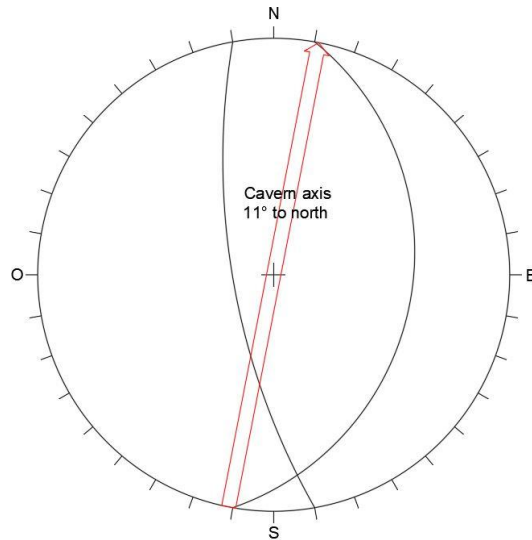


*Figure 2.1: Stereogram and cavern orientation*

Generally, the geometry and layout of a system of caverns are based on optimizing the requirements given by the cavern usage. The main parameters to be considered are the cavern size, the shape and the spacing between caverns. It is necessary to consider that the rock mass is a discontinuous material, and that the basic concept for a cavern is that the shape of the opening should conform to the rock structures and stress conditions.

In fact, the compressive stresses in the rock mass that bound the excavation, must be distributed in such a way that the span of the cavern can be self-supporting as far as possible. This condition can be reached by giving the cavern space a simple form with an arched roof to reduce the zone of tensile stresses in the crown. Moreover, the cross section of a cavern should be optimized to produce the lowest combined excavation and support costs. Support costs increase with cavern span, excavation rates reduce with cavern height. Of course, it is important to find a good balance between these important parameters.

In the figure 2.2 the cost curves for different rock conditions against cavern span and height is reported.

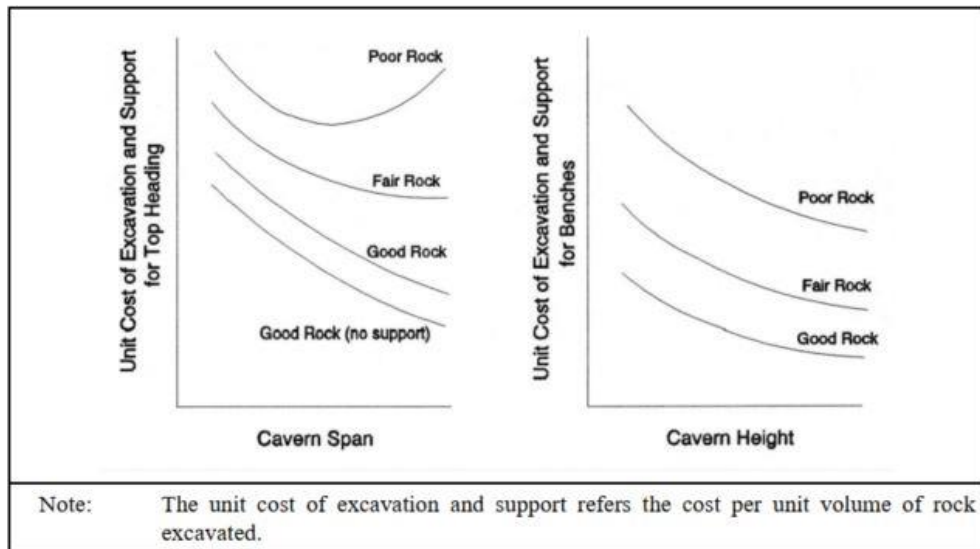


*Figure 2.2: Cost Curves against Cavern Span and Height for Different Rock Conditions (O.J. Berthelsen, 1992).*

The starting point for the design of the shape of a cavern roof is the assumption of a standard roof arch height of  $1/5$  of the cavern span (O. J. Berthelsen, Guide to Cavern Engineering, 1992), how reported in figure 2.3. In the case of this dissertation the span of the cavern was about 30 m and the roof arch measured 6 m, therefore it was perfectly aligned with the previous advises.

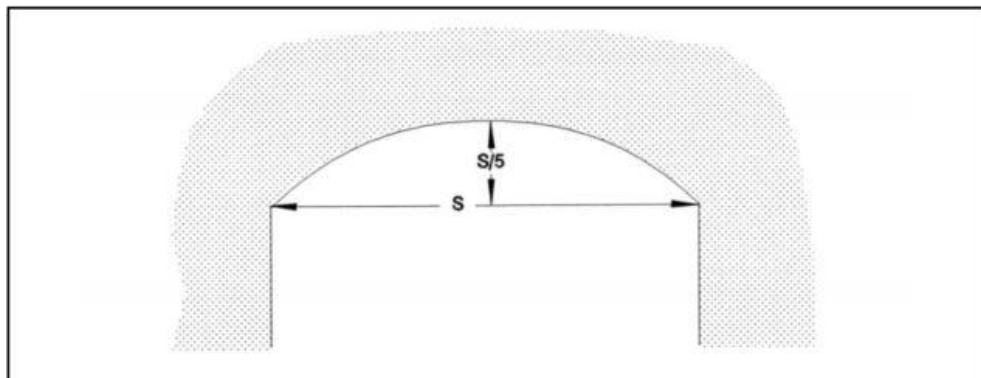


*Figure 2.3: Standard Roof Arch Shape (O.J. Berthelsen, 1992).*

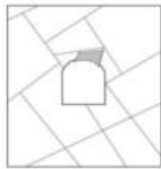
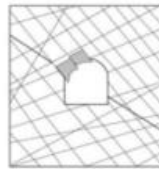
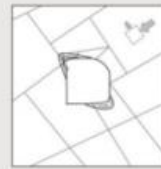
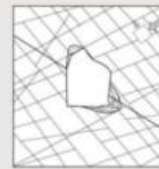
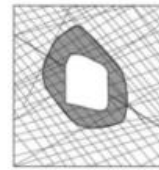
Then, it is also important to keep in mind that wall stability is a function of the wall height, therefore high walls are to be avoided because they tend to be unstable. Moreover, typical pillar widths between caverns are between half and full cavern span or height. While in case of vertical separation of parallel cavern located above each other, the distance should not be less than the largest span or height of the

adjacent caverns. Furthermore, the excavation of an upper cavern before a lower cave is recommended, this to avoid the risk of damaging the roof support installed in the lower cavern by the vibrations generated by the excavation of the upper cavern.

Another aspect to carefully consider in caverns are the junctions between caverns and their tunnels and shafts. In fact, the junctions often result in zones of stress concentration and intruding corners which are dangerous for cavern stability.

Rock mass classification is essential in cavern engineering and follows logically from the general assumption that rock can generally be considered as a structural material for the purpose of cavern construction. Anyway, this topic will be treated more in the detail in chapter 3, contextualized in the case under analysis.

Another important issue is the failure modes in caverns, which depend on the characteristics of the rock mass, the strength of the intact rock and discontinuities and the in-situ stresses. Two types of failure modes are expected in cavern: the structurally controlled failure and the stress-induced failure. The first one is the dominating type of instability for cavern at modest depth and involves kinematically sliding along adverse joints or block falls. The second one, characterized by slabbing, rock bursting and squeezing will occur when rock materials are subjected to high external or in-situ stress, therefore in deep caverns. The project under study was interested by the stress induced failure since it was situated at about 300 m from the free surface of the mountain. In figure 2.4 an illustration of the failure modes is highlighted.

	Massive ( $RMR > 75$ )	Moderately Fractured ( $50 > RMR > 75$ )	Highly Fractured ( $RMR < 50$ )
Low In-Situ Stress ( $\sigma_1 / \sigma_c < 0.15$ )	 <p>Linear elastic response.</p>	 <p>Falling or sliding of blocks and wedges.</p>	 <p>Unravelling of blocks from the excavation surface.</p>
Intermediate In-Situ Stress ( $0.15 > \sigma_1 / \sigma_c > 0.4$ )	 <p>Brittle failure adjacent to excavation boundary.</p>	 <p>Localised brittle failure of intact rock and movement of blocks.</p>	 <p>Localised brittle failure of intact rock and unravelling along discontinuities.</p>
High In-Situ Stress ( $\sigma_1 / \sigma_c > 0.4$ )	 <p>Failure Zone Brittle failure around the excavation.</p>	 <p>Brittle failure of intact rock around the excavation and movement of blocks.</p>	 <p>Squeezing and swelling rocks. Elastic/plastic continuum.</p>

*Figure 2.4 Illustration of Failure Modes (modified from Martin et al, 1999)*

For the purpose of facing high in situ stress, temporary and permanent supports are required in the cavern’s excavation. Temporary support is mandatory to control deformations and secure safe working conditions for the workers, should be installed shortly after excavation and removal of spoil are completed. Permanent support is required to maintain stable rock conditions in an excavation during the service life of a cavern.

In the following part, a brief overview of different types of support that can be used in cavern engineering is proposed.

Rock anchors (cable bolts) are required for permanent stabilization of caverns with large spans or with poor quality rock mass, typical lengths of anchors vary between 10 and 30 m, a good point for anchors is that they can be pre-stressed to a high tension.

Forepoling is a means of reinforcing a rock mass ahead of an excavation face with long bolts called forepoles or spiles. This support system is particularly indicated to poor quality rock masses.

Canopy tubes are adopted as pre-support to enhance roof and face stability during excavation in poor ground and consists in perforated steel pipes that can be jointed together and drilled into the ground in longitudinal direction of an excavation. Canopy tubes are normally applied with lattice arches or steel ribs. In fact, they act as beams bridging unsupported ground in the longitudinal direction between a transverse support and an excavation face or between two transverse supports.

Steel ribs or lattice arches used with shotcrete are implemented as immediate support measures where poor ground conditions are expected. Steel ribs are usually made of straight or bent I- or H-beams, bolted together to form a circular or pitched arch with vertical side supports. While lattice arches are lightweight support members comprising steel reinforcement bars that are usually linked together in a triangular shape.

Shotcrete creates a semi-stiff lining on excavated faces, it should have adequate shear and moment bearing capacity to prevent collapse of excavated surfaces.

Finally, the permanent lining may be installed in a cavern with pre-cast or cast in place concrete lining but could be very expensive. Therefore, in condition with suitable rock mass, groundwater control and initial rock support/reinforcement works, it is possible and more cost effective to provide, using high pressure jetting a one or multi pass shotcrete lining structure for a cavern. In the case under analysis a systematic bolts pattern was design as means to fulfil the stability of the underground excavation.

Furthermore, rock bolting is the most common method to rock support, as it is convenient and flexible to use, rock bolts may be used for both temporary support and permanent support. The common length ranges between 2 and 6 m. In rock tunnelling and in cavern construction, with the term bolt is intended both tensioned bolts and fully grouted un-tensioned bolts. In the last mentioned, stress is induced when movement occurs along the discontinuity stabilized. In a jointed rock mass, dilation occurs as movement along a discontinuity causes riding-up on the asperities. It is important to provide that the bonded length must be adequate on the side of the discontinuity, since at this stage tension and shear are induced in the bolt.

Rock bolts, used as roof and wall supports, are normally applied in two ways such as spot bolts as means to secure isolated loose blocks, and systematic pattern bolting to achieve a general increase of stability, as reported in figure 2.5. In general, the bolts should be long enough to obtain adequate anchorage in a stable rock mass beyond the block. Systematic bolting was applied in the cavern under analysis, and it was used to achieve a general increase in stability holding a rock mass together and allowing to form a natural arch. Bolt spacings and length for caverns are designed using empirical design rules, for example the Q-system or the RMR system.

The formula (2.1) proposed by Barton et al (1977) should be used for an initial assessment of rock bolt length. In the equation, the length of rock bolts,  $L$ , can be estimated from the excavation width,  $B$ , and the excavation support ratio (ESR) as follows (for wall support,  $B$  should be replaced by the cavern height,  $H$ , in the equation):

$$L = 2 + \frac{0.15B}{ESR} \quad (2.1)$$

Where:

$L$  = bolt length (in m)

$B$  = cavern span for roof support (use cavern height,  $H$ , for wall support in m)

ESR = excavation support ratio, representing the safety requirement for the use of the cavern space (Barton & Grimstad, 2014; NGI, 2015).

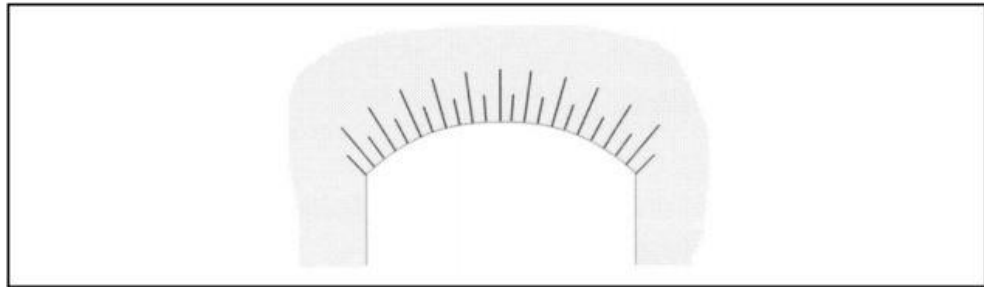


*Figure 2.5: Typical Roof Support with Pattern Bolting (O.J. Berthelsen, 1992).*

### 2.3.2 Cavern construction

In this paragraph, some considerations related to the cavern construction were exposed. Mostly the one that could also be applied in the realisation of the cavern analysed in the present dissertation.

Firstly, Drill and blast methods dominate the construction of underground space in rock, this mainly due to fact that it is the only cost-effective method of forming large caverns in hard rock. Different methods are commonly employed in cavern construction such as: face blasting with horizontal drillholes for top heading excavation; benching with horizontal drillholes for side benches to provide good control of the excavation profile along the walls; benching with vertical drillholes for central benches. All these three methods are commonly used in cavern construction. Drill and blast technique is an iterative procedure consisting in the following parts: probe drilling; pre-grouting of rock mass if required; drilling of blast holes; charging with explosives; detonation; ventilation; scaling; mucking-out and temporary support works after rock mapping and design verification.

The typical equipment used for cavern construction is the drilling jumbos capable of drilling up to 2 m per minute in rock with uniaxial compressive strength up to 160 MPa. Scaling is normally pursued by hydraulic hammers mounted on excavators. Mucking-out is performed by wheel loaders and trucks. Then, Shotcrete is placed using computerised robots which can spray up to a height of 14 m, while drilling for rock bolt is usually carried out by a drilling jumbo.

The Top Heading of a cavern excavation should normally be excavated first using tunnelling techniques, in this way the cavern roof access could be easier to install support works. The secured roof gives safe working conditions for the excavation of the lower levels of the cavern. Then, the lower levels may be excavated using quarrying techniques, such as benching which are cheaper than tunnelling. It is normally economical to excavate a face as large as possible up to 200 m<sup>2</sup>, however often different factors such as poor rock conditions or presence of weak rock may limit the size of the top heading to 100-120 m<sup>2</sup>. The number of sections of the top heading depends on the span of the cavern and the maximum practical size of heading. In figure 2.6 are shown typical excavation stages for a top heading excavation in hard rock conditions for different ranges of cavern span.

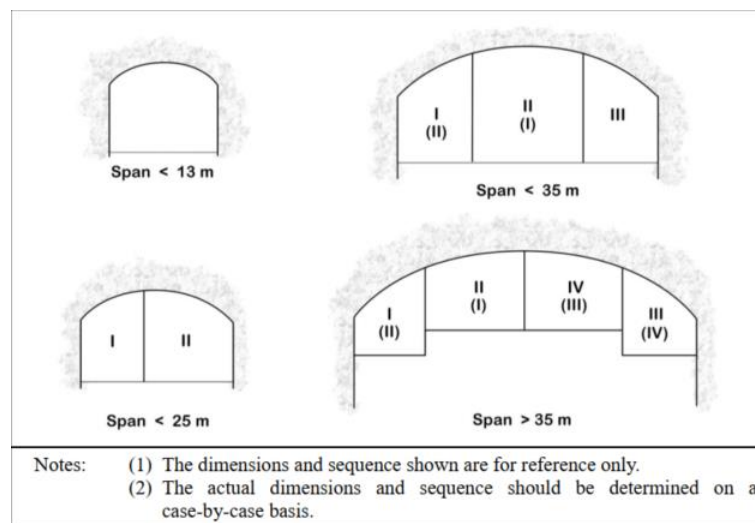


*Figure 2.6: Typical Excavation Stages for Top Headings in Caverns (O.J. Berthelsen, 1992).*

There are various options for the timing of the excavation of the second and subsequent sections of a top heading. The main options available are either to drive one section prior to completion, followed by the excavation of the subsequent stages, or to allow each section to lead subsequent sections by a small distance. In the case under study with a span of 30 m the top heading was excavated in 2 stages, and the section was excavated until its completion.

The Bench excavation results being cheaper because the large free surfaces allow the use of quarrying principles rather than tunnelling technology, in this way it is possible to reduce drilling and explosive costs. Support costs for benching are low because the roof has already been supported and only wall supports need to be done. Bench excavation may be carried out with vertical drillholes as in quarrying operation, or with horizontal drillholes as in tunnelling using drilling jumbos. A cavern excavation should be divided into benches of a suitable height. In the cavern project under analysis four different bench excavations were developed with a height of about 6.5 m each. In the figure 2.7 are shown typical excavation stages for a large cavern.

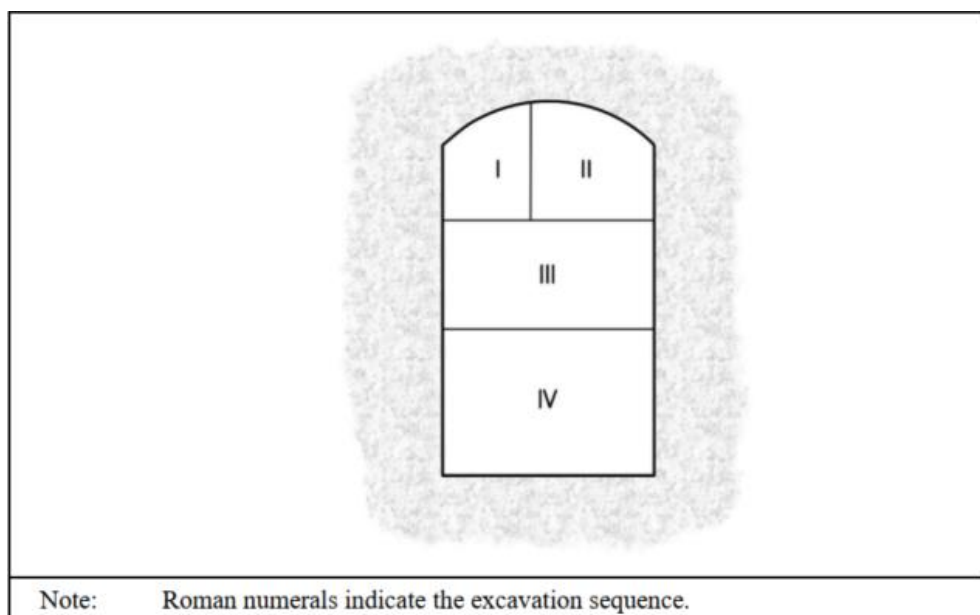


*Figure 2.7: Typical Excavation Stages for a Large Cavern (O.J. Berthelsen, 1992).*

Moreover, blast holes are drilled using jumbos with hydraulic percussion drills, rate of drilling is, in general, of the order of 2 m per minute for standard drills in granitic and volcanic rocks and can be higher in weaker rocks. Drillholes are normally between 45 and 51 mm in diameter, the length of the drillholes is commonly 4 to 6 m.

For what regards explosives and charging, different types of detonators are available: electric, non-electric and electronic detonators. Electric detonators are typically used to initiate a blast and have seldomly been used to ignite individual blast holes. This is because there are safety issues related to the possibility of prematurely triggering electric detonators. On the contrary, Non-electric detonators are initiated by a shock tube and are commonly used to initiate blast holes. Electronic detonators have an accurate programmable timing system which enables a wide variety of possible delay timing in a blast round and allows better prediction and control of the blast induced vibrations. However, the cost of these detonators is considerably higher than non-electric detonators. For main production blasting the mostly used explosives are the low-cost bulk based on ammonium nitrate mixed on site with fuel oil (ANFO).

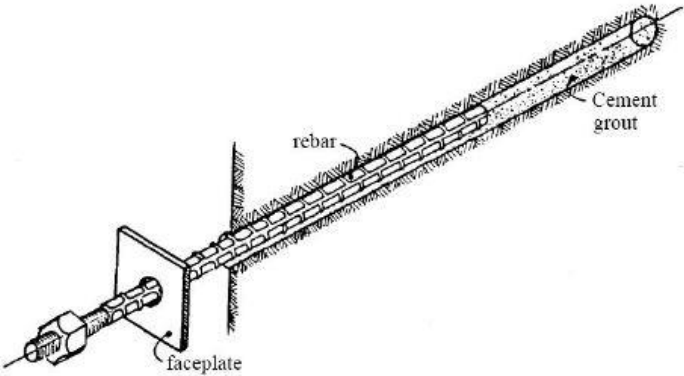
Furthermore, charging of explosives should only start after the drilling of all holes has been completed. After checking the holes for blockages, the holes are bottom primed. Non-electric detonators are placed following the blast pattern, whilst electronic detonators are placed in the holes either in a pre-programmed state or to be programmed later. Non-ferrous tamping rods should be used to place the detonator and booster into the back of the hole. Then the main explosive is charged (cartridges, bulk emulsion or ANFO) followed by stemming, normally in the form of 10 mm aggregate. The detonators are then connected to form a controlled blasting system. Detonation must be done remotely after clearance of workers and equipment. Contour holes are normally lightly charged to prevent excessive overbreak. The large relief holes in the center of a blast pattern are left uncharged to act as a free face.

After blasting and ventilation, the roof and sidewalls should be scaled. Then mucking procedures take place using diesel powered trucks or electric device using crushers and conveyors in order to limit pollution emission. Finally, as mentioned in the previous part, the rock support must be implemented.

Rock bolting is the most common method for rock support. They may be used both for temporary support at a working face and for permanent support. Lengths are commonly in the range of 2 to 6 m. Rock bolts may be used for both crown and wall support. The bolts may be anchored at the far end and tensioned or may be fully grouted bolts without tensioning. Typically, rock bolts are centralized in a hole with stabilizers, such as plastic items, and then fully encapsulated in grout, which is normally a cementitious product with a maximum grain size of 3 mm.

Drillholes should be properly cleaned and the drillhole diameter should be sufficient to allow a grout pipe to be inserted and for the grout to fill the annulus around a bolt, in this way it is provided a good bond between the rock and the bolt. In the figure 2.8 a scheme of the fully grouted bolt is reported, with the Pros and Cons of this technology. This typology of bolts was used in the support design of the cavern under analysis how it was reported in paragraph 3.2.

In the zone under analysis, for full face blasting a weekly excavation rate of 70 m/week can be achieved with two blasts per day, six days per week with a 5.8 m drill/pull length. While the production rate for rock support is for rock bolting 6 to 15 bolts per hour, highly dependent on the bolt length, working conditions and rock quality.

Type	Description
Grouted rock bolt	<p><i>Pros</i></p> <ul style="list-style-type: none"> <li>• Materials are easy to obtain and inexpensive.</li> <li>• Grout provides corrosion protection.</li> <li>• It is simple to install.</li> <li>• It performs well in weak, broken, poor quality rock and poorly drilled holes because the grout will flow into the voids.</li> </ul> <p><i>Cons</i></p> <ul style="list-style-type: none"> <li>• The grout setting time could be slow, i.e. lack of immediate support.</li> <li>• Pumping grout, especially overhead, may require a particular procedure.</li> <li>• A longer bond zone than other bolt types depending on the rock type may be required.</li> <li>• Installation can be time consuming, requires two grouting periods for pre-stressed bolts (bond zone and unbonded zone).</li> <li>• Grouting operation may tend to be more expensive than some other bolt types due to time and manpower.</li> <li>• Installation cannot be automated.</li> </ul> 

*Figure 2.8: Fully grouted bolts scheme (O.J. Berthelsen, 1992).*

In the next chapter a detailed discussion of the numerical modelling of the cavern excavation was then proposed.

## Chapter 3

### 3. CONTINUUM MODEL IN 2D

Numerical modelling is a powerful tool in the design of cavern structures. In the present thesis it was decided to apply continuum numerical modelling, to study the behaviour of a cavern in jointed granite. In particular, continuum models based on Finite Element Method were adopted. This approach related the conditions at nodal points, which must be stated within elements, moreover the physical model being numerically discretized within the region of interest. In this way it was possible to handle material heterogeneity and non-linearity.

In this first model the discontinuities were considered by modifying the overall material properties to implicitly incorporate the effect of the discontinuities, i.e. an equivalent continuum was implemented. This model was the object of the internship carried out by the author and was the starting point of the current argumentation.

#### 3.1 *Geo-mechanical characterisation*

As mentioned above, the cavern was situated at 300 m depth, presenting a span of 30 m and an overall height of about 32 m. The cavern was excavated in mainly good rock granite, although two main sets of discontinuities intersecting the cavern.

The mechanical characterisation was carried out by using data coming from site investigation, principally borehole tests. These are sensible data and cannot be reported in this dissertation. From the BHs the RQD (Rock Quality Designation) and the Weathering degree were defined.

As first assessment, RQD distribution could be used to understand the distribution of the jointing degree of rock masses. In fact, RQD is a rough measure of the degree of jointing or fracture in a rock mass, as reported in the table in figure 3.1. It is measured as a percentage of the drill core in lengths of 10 cm or more. High quality rock has and RQD more than 75%, low quality less than 50%.

Results indicated that a large percentage of the cavern rock mass was characterized by a RQD larger than 75%. However, some weak zones were present. Starting from the RQD the Q value was derived.

I RQD (Rock Quality Designation)			RQD
A	Very poor	(> 27 joints per m <sup>3</sup> )	0-25
B	Poor	(20-27 joints per m <sup>3</sup> )	25-50
C	Fair	(13-19 joints per m <sup>3</sup> )	50-75
D	Good	(8-12 joints per m <sup>3</sup> )	75-90
E	Excellent	(0-7 joints per m <sup>3</sup> )	90-100
Note: I) Where RQD is reported or measured as ≤ 10 (including 0) the value 10 is used to evaluate the Q-value II) RQD-Intervals of 5, i.e. 100, 95, 90, etc., are sufficiently accurate			

*Figure 3.1: Reference guide for Rock quality designation (NGI, 2015)*

The Q-system was developed by the Norwegian Geotechnical Institute and the original version is described by Barton et al (1974).

This empirical method is based on the rock quality designation RQD and five additional parameters, which account for the number of discontinuity sets, the discontinuity roughness and alteration (infilling), the amount of water and adverse features associated with loosening, high stress, squeezing and swelling.

The Q value is expressed by the relation (3.1):

$$Q = \frac{RQD}{J_n} \times \frac{J_r}{J_a} \times \frac{J_w}{SRF} \quad (3.1)$$

Where:

RQD = rock quality designation

$J_n$  = joint set number

$J_r$  = joint roughness number

$J_a$  = joint water reduction number

$J_w$  = joint water reduction number

SRF = stress reduction factor

The numerical value of Q ranges from 0.001 for exceptionally poor-quality squeezing ground to 1000 for exceptionally good quality and massive rock.

The six parameters can be estimated from site investigation results and verified during excavation. The parameters are grouped in the following three quotients:

- $RQD/J_n$ , that represents the degree of jointing or block size;
- $J_r/J_a$ , which represents the inter-block shear strength;
- $J_w/SRF$ , which consists of two stress parameters representing an empirical factor describing the active stresses.

For the evaluation of the joint set number ( $J_n$ ), the table reported in figure 3.2 can be used. In the case study a rating from 4 to 6 was applied depending on RQD, as two main family of discontinuities and random joints were present.

2 Joint set number		$J_n$
A	Massive, no or few joints	0.5-1.0
B	One joint set	2
C	One joint set plus random joints	3
D	Two joint sets	4
E	Two joint sets plus random joints	6
F	Three joint sets	9
G	Three joint sets plus random joints	12
H	Four or more joint sets, random heavily jointed "sugar cube", etc	15
J	Crushed rock, earth like	20

Note: I) For tunnel intersections, use  $3 \times J_n$   
 II) For portals, use  $2 \times J_n$

*Figure 3.2: Reference guide for joint set number  $J_n$  (NGI, 2015)*

Moreover, to evaluate the joint roughness, the table in figure 3.3 can be adopted. The joint roughness depends on the nature of the joint wall surfaces, if they are undulating, planar, rough, or smooth. A rating from 1.5 to 2 was applied depending on RQD.

3 Joint Roughness Number		$J_r$
<b>a) Rock-wall contact, and</b>		
<b>b) Rock-wall contact before 10 cm of shear movement</b>		
A	Discontinuous joints	4
B	Rough or irregular, undulating	3
C	Smooth, undulating	2
D	Slickensided, undulating	1.5
E	Rough, irregular, planar	1.5
F	Smooth, planar	1
G	Slickensided, planar	0.5
Note: I) Description refers to small scale features and intermediate scale features, in that order		
<b>c) No rock-wall contact when sheared</b>		
H	Zone containing clay minerals thick enough to prevent rock-wall contact when sheared	1
Note: I) Add 1 if the mean spacing of the relevant joint set is greater than 3 m (dependent on the size of the underground opening)		
II) $J_r = 0.5$ can be used for planar slickensided joints having lineations, provided the lineations are oriented in the estimated sliding direction		

*Figure 3.3: Reference guide for joint roughness number  $J_r$  (NGI, 2015)*

Then, for the joint alteration number, the table in figure 3.4 can be consulted. The joint infill is significant for joint shear strength, when dealing with joint infill, two factors are important: thickness and strength. These parameters depend on the

mineral composition of the rock mass. A rating from 1 to 3 was applied depending on RQD, 1 for the higher values and 3 for lower values of RQD.

4 Joint Alteration Number		$\Phi_r$ approx.	$J_a$
<b>a) Rock-wall contact (no mineral fillings, only coatings)</b>			
A	Tightly healed, hard, non-softening, impermeable filling, i.e., quartz or epidote.		0.75
B	Unaltered joint walls, surface staining only.	25-35°	1
C	Slightly altered joint walls. Non-softening mineral coatings; sandy particles, clay-free disintegrated rock, etc.	25-30°	2
D	Silty or sandy clay coatings, small clay fraction (non-softening).	20-25°	3
E	Softening or low friction clay mineral coatings, i.e., kaolinite or mica. Also chlorite, talc, gypsum, graphite, etc., and small quantities of swelling clays.	8-16°	4
<b>b) Rock-wall contact before 10 cm shear (thin mineral fillings)</b>			
F	Sandy particles, clay-free disintegrated rock, etc.	25-30°	4
G	Strongly over-consolidated, non-softening, clay mineral fillings (continuous, but <5 mm thickness).	16-24°	6
H	Medium or low over-consolidation, softening, clay mineral fillings (continuous, but <5 mm thickness).	12-16°	8
J	Swelling-clay fillings, i.e., montmorillonite (continuous, but <5 mm thickness). Value of $J_a$ depends on percent of swelling clay-size particles.	6-12°	8-12
<b>c) No rock-wall contact when sheared (thick mineral fillings)</b>			
K	Zones or bands of disintegrated or crushed rock. Strongly over-consolidated.	16-24°	6
L	Zones or bands of clay, disintegrated or crushed rock. Medium or low over-consolidation or softening fillings.	12-16°	8
M	Zones or bands of clay, disintegrated or crushed rock. Swelling clay. $J_a$ depends on percent of swelling clay-size particles.	6-12°	8-12
N	Thick continuous zones or bands of clay. Strongly over-consolidated.	12-16°	10
O	Thick, continuous zones or bands of clay. Medium to low over-consolidation.	12-16°	13
P	Thick, continuous zones or bands with clay. Swelling clay. $J_a$ depends on percent of swelling clay-size particles.	6-12°	13-20

*Figure 3.4: Reference guide for joint alteration number  $J_a$  (NGI, 2015)*

Furthermore, for the evaluation of the joint water reduction factor the table in figure 3.5 can be chosen. Joint water may soften or wash out the mineral infill and thereby reduce the friction on the joint planes.

The determination of the joint water reduction is based on inflow and water pressure observed in an underground opening. A value of 1, dry excavation or minor inflow, was considered in this case.

5 Joint Water Reduction Factor		$J_w$
A	Dry excavations or minor inflow ( humid or a few drips)	1.0
B	Medium inflow, occasional outwash of joint fillings (many drips/"rain")	0.66
C	Jet inflow or high pressure in competent rock with unfilled joints	0.5
D	Large inflow or high pressure, considerable outwash of joint fillings	0.33
E	Exceptionally high inflow or water pressure decaying with time. Causes outwash of material and perhaps cave in	0.2-0.1
F	Exceptionally high inflow or water pressure continuing without noticeable decay. Causes outwash of material and perhaps cave in	0.1-0.05
Note: I) Factors C to F are crude estimates. Increase $J_w$ if the rock is drained or grouting is carried out II) Special problems caused by Ice formation are not considered		

Figure 3.5: Reference guide for joint water reduction factor  $J_w$  (NGI, 2015)

Finally, as means to evaluate the Stress reduction factor table in figure 3.6 is available. In general, the SRF describes the relation between stress and rock strength around an underground opening. The effects can be observed as spalling, slabbing, deformation, squeezing, dilatancy and block release. In this assessment a value of 1 has been set.

6 Stress Reduction Factor			SRF	
<b>a) Weak zones intersecting the underground opening, which may cause loosening of rock mass</b>				
A	Multiple occurrences of weak zones within a short section containing clay or chemically disintegrated, very loose surrounding rock (any depth), or long sections with incompetent (weak) rock (any depth). For squeezing, see 6L and 6M		10	
B	Multiple shear zones within a short section in competent clay-free rock with loose surrounding rock (any depth)		7.5	
C	Single weak zones with or without clay or chemical disintegrated rock (depth $\leq$ 50m)		5	
D	Loose, open joints, heavily jointed or "sugar cube", etc. (any depth)		5	
E	Single weak zones with or without clay or chemical disintegrated rock (depth > 50m)		2.5	
Note: I) Reduce these values of SRF by 25-50% if the weak zones only influence but do not intersect the underground opening				
<b>b) Competent, mainly massive rock, stress problems</b>				
		$\sigma_2/\sigma_1$	$\sigma_3/\sigma_2$	
F	Low stress, near surface, open joints	>200	<0.01	2.5
G	Medium stress, favourable stress condition	200-10	0.01-0.3	1
H	High stress, very tight structure. Usually favourable to stability. May also be unfavourable to stability dependent on the orientation of stresses compared to jointing/weakness planes*	10-5	0.3-0.4	0.5-2 2-5*
J	Moderate spalling and/or slabbing after > 1 hour in massive rock	5-3	0.5-0.65	5-50
K	Spalling or rock burst after a few minutes in massive rock	3-2	0.65-1	50-200
L	Heavy rock burst and immediate dynamic deformation in massive rock	<2	>1	200-400
Note: ii) For strongly anisotropic virgin stress field (if measured): when $5 \leq \sigma_1/\sigma_3 \leq 10$ , reduce $\sigma_2$ to 0.75 $\sigma_2$ . When $\sigma_1/\sigma_3 > 10$ , reduce $\sigma_2$ to 0.5 $\sigma_2$ , where $\sigma_c$ = unconfined compression strength, $\sigma_1$ and $\sigma_3$ are the major and minor principal stresses, and $\sigma_2$ = maximum tangential stress (estimated from elastic theory) iii) When the depth of the crown below the surface is less than the span; suggest SRF increase from 2.5 to 5 for such cases (see F)				
<b>c) Squeezing rock; plastic deformation in incompetent rock under the influence of high pressure</b>				
		$\sigma_2/\sigma_c$	SRF	
M	Mild squeezing rock pressure	1-5	5-10	
N	Heavy squeezing rock pressure	>5	10-20	
Note: iv) Determination of squeezing rock conditions must be made according to relevant literature (i.e. Singh et al., 1992 and Bhasin and Grimstad, 1996)				
<b>d) Swelling rock; chemical swelling activity depending on the presence of water</b>			SRF	
O	Mild swelling rock pressure		5-10	
P	Heavy swelling rock pressure		10-15	

Figure 3.6: Reference guide for stress water reduction factor SRF (NGI, 2015)

From the current analysis, Q values were calculated, resulting into more than 90% of the rock mass at the cavern elevation showed a Q value > 5.9, while only almost the 5% featured a Q value < 1.9; this means that the underground excavation was generally developed in good rock conditions. However, some weak areas were present. In the table 3.1 is reported the summary of the described correlations between Q parameters and RQD values.

Evaluation of the Q parameter						
RQD [%]	Jn	Jr	Ja	Jw	SRF	Q
100	4	2	1	1	1	33
90	4	2	1	1	1	20
80	4	2	2	1	1	9
70	4	1,5	2	1	1	6
60	5	1,5	2	1	1	4
50	5	1	2	1	1	1,5
40	5	1	3	1	1	0,8
30	6	1	3	1	1	0,5
20	6	1	3	1	1	0,3
10	6	1	3	1	1	0,1

*Table 3.1 Summary of the described correlations between Q parameters and RQD values*

The derived Q value were adopted to estimate the m and s factors in the Hoek & Brown failure criterion (Hoek et al, 2002, Hoek & Diederichs, 2006) using the relations (3.2), (3.3), (3.4), (3.5):

$$GSI = 9 \ln Q' + 44 \quad (3.2)$$

$$m_b = m_i e^{\left(\frac{GSI-100}{28-14D}\right)} \quad (3.3)$$

$$s = e^{\left(\frac{GSI-100}{28-14D}\right)} \quad (3.4)$$

$$E_m = E_i \left( 0.02 + \frac{1 - \frac{D}{2}}{1 + e^{\left(\frac{60+15D-GSI}{11}\right)}} \right) \quad (3.5)$$

Where:

GSI = Geological Strength Index

$Q' = RQD/J_n \times J_r/J_a$

$m_i$  = material constant

$m_b$  = reduced value of material constant

$s$  = rock mass constant

$D$  = disturbance factor

$E_m$  = rock mass modulus

$E_i$  = intact rock modulus

After the determination of the  $Q$  and the Hoek & Brown parameters, it was necessary to derive the weathering degree of the igneous rocks of the site of interest. In closely jointed volcanic rock, the weathering zone thickness can be on the order of magnitude of centimetres, whereas in the granite the thickness can be several tens of meters. The figure 3.7 shows the main characteristic associated to each weathering degree.

4. MATERIAL WEATHERING/ALTERATION		
<u>Decomposition Term</u>	<u>Grade Symbol</u>	<u>Typical Characteristics</u>
Residual Soil	VI	Original rock texture completely destroyed; can be crumbled by hand and finger pressure into constituent grains.
Completely Decomposed	V	Original rock texture preserved; can be crumbled by hand and finger pressure into constituent grains; easily indented by point of geological pick; staves in water; completely discoloured compared with fresh rock.
Highly Decomposed	IV	Can be broken by hand into smaller pieces; makes a dull sound when struck by hammer; not easily indented by point of pick; does not stake in water; completely discoloured compared with fresh rock.
Moderately Decomposed	III	Cannot usually be broken by hand; easily broken by hammer; makes a dull or slight ringing sound when struck by hammer; completely stained throughout.
Slightly Decomposed	II	Not broken easily by hammer; makes a ringing sound when struck by hammer; fresh rock colours generally retained but stained near joint surfaces.
Fresh Rock	I	Not broken easily by hammer; makes a ringing sound when struck by hammer; no visible signs of decomposition (i.e. no discolouration).

*Figure 3.7: Weathering degree chart (J.B. Massey, 1988)*

In the table 3.2 it is summarized the correspondence among the intact rock compressive strength and weathering degree classification. These values were taken from literature concerning the typical uniaxial compressive strength and weathering degree of the site.

WEATHERING DEGREE	UCS	
	max	min
I	175	125
II	104	60
III	42	24
IV	5	1
V	1	0,25

*Table 3.2 Weathering degree-UCS (O.J. Berthelsen, 1992)*

Then, another consideration must be given regarding the stress conditions. The state of stress can be computed with the following relations:

$$\sigma_v = z * \gamma \quad (3.7)$$

$$\sigma_h = \sigma_v * k_0 \quad (3.8)$$

$$\sigma_z = \nu \cdot (\sigma_v + \sigma_h) \quad (3.9)$$

Where:

$z$  = depth of the cavern

$\gamma$  = unit weight of the rock

$k_0$  = coefficient of earth pressure

The assumption of plane strain conditions was adopted for the relation 3.9.

For the assessment of the coefficient of earth pressure it was possible to use the graph reported in figure 3.8. In which knowing the depth and the elastic modulus the  $k_0$  could be derived.

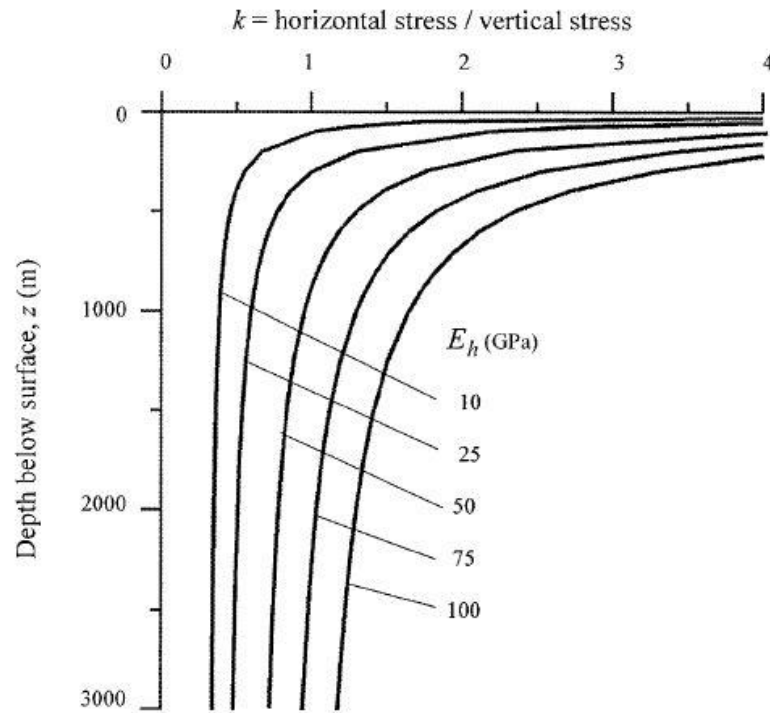
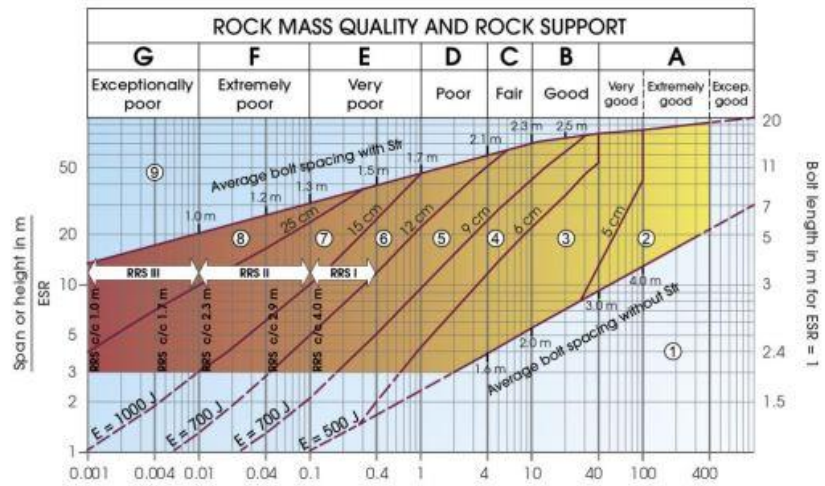


*Figure 3.8: Ratio of horizontal to vertical stress for different deformation moduli based upon Sheorey's equation. (Sheorey, 1994)*

The Q-value can be also used to preliminarily choose the type of reinforcement that is expected to be considered for the support of the underground excavation. In the support chart shown in figure 3.9, the Q-values are plotted along the horizontal axis and the equivalent dimension along the vertical axis on the left side. For a given combination of Q-value and span or height in m, a given type of support has been used and the support chart is divided into areas according to the type of reinforcement.

The support chart is based on empirical data, it can be a guideline for the design of support of underground excavation. In the case of bolts their length can be also derived and depends on the span or wall height of the underground opening and on the degree of the rock mass quality. Figure 3.9 shows the rock support chart provided by the NGI.



**Support categories**

- ① Unsupported or spot bolting
- ② Spot bolting, **SB**
- ③ Systematic bolting, fibre reinforced sprayed concrete, 5-6 cm, **B+Sfr**
- ④ Fibre reinforced sprayed concrete and bolting, 6-9 cm, **Sfr (E500)+B**
- ⑤ Fibre reinforced sprayed concrete and bolting, 9-12 cm, **Sfr (E700)+B**
- ⑥ Fibre reinforced sprayed concrete and bolting, 12-15 cm + reinforced ribs of sprayed concrete and bolting, **Sfr (E700)+RRS I +B**
- ⑦ Fibre reinforced sprayed concrete >15 cm + reinforced ribs of sprayed concrete and bolting, **Sfr (E1000)+RRS II+B**
- ⑧ Cast concrete lining, **CCA** or **Sfr (E1000)+RRS III-B**
- ⑨ Special evaluation

Bolts spacing is mainly based on  $\varnothing 20$  mm  
 E = Energy absorption in fibre reinforced sprayed concrete  
 ESR = Excavation Support Ratio  
 Areas with dashed lines have no empirical data

**RRS - spacing related to Q-value**

- I** Si30/6  $\varnothing 16 - \varnothing 20$  (span 10m)  
D40/6+2  $\varnothing 16-20$  (span 20m)
- II** Si35/6  $\varnothing 16-20$  (span 5m)  
D45/6+2  $\varnothing 16-20$  (span 10m)  
D55/6+4  $\varnothing 20$  (span 20m)
- III** D40/6+4  $\varnothing 16-20$  (span 5m)  
D55/6+4  $\varnothing 20$  (span 10 m)  
Special evaluation (span 20 m)

Si30/6 = Single layer of 6 rebars,  
30 cm thickness of sprayed concrete  
 D = Double layer of rebars  
 $\varnothing 16$  = Rebar diameter is 16 mm  
 c/c = RSS spacing, centre - centre

Figure 3.9: Rock support chart (NGI, 2015)

When the Q-system is used for wall support, the height of the walls must be used instead of the span. The actual Q-value is adjusted as shows figure 3.10.

In rock masses of good quality	$Q > 10$	Multiply Q-values by a factor of 5.
For rock masses of intermediate quality	$0.1 < Q < 10$	Multiply Q-values by a factor of 2.5. In cases of high rock stresses, use the actual Q-value.
For rock masses of poor quality	$Q < 0.1$	Use actual Q-value.

Figure 3.10: Conversion from actual Q-values to adjusted Q-values for design of wall support (NGI, 2015)

### 3.2 Continuum model using RS<sub>2</sub>

The equivalent continuum model has been set up using the finite element method software RS<sub>2</sub>. Knowing the geometry of the cavern, the orientation of the joint sets it was possible to draw the 2D section of the underground construction site. In the figure 3.11 the adopted model was represented.

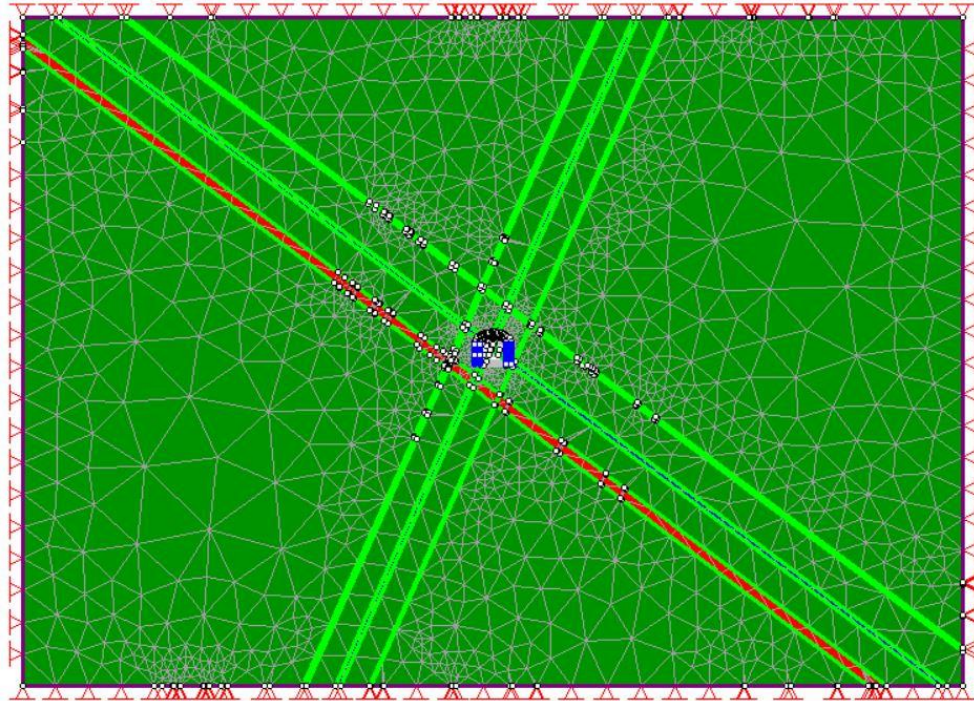


*Figure 3.11: Continuum model*

Furthermore, also the material properties derived from the geo-mechanical analysis were inserted as means to characterise the rock mass.

The following assertions were addressed when modelling the project on RS<sub>2</sub>:

- Project settings:

In this first step, it was important to notice the use of eight stages: the first one representing the geostatic conditions, in the second one the cavern's excavation started. It was decided to divide the excavation in six different steps as suggested in section 2.3.2. Then after the digging phases a final stage was realized.

- Geometry:

As the cavern present about a 30x30 dimension, it was decided to use a boundary measuring 10 times the cavern dimension in each direction from the cavern (nearly 300x300). Using the data from the in-situ investigations and from the literature of the geology of the site of interest, it was possible to draw the zones, indeed joints, characterized by the presence of weaker granite. Two of these zones crossed the cavern section, they were strips of about 5 m spacing. Other zones of discontinuities were modeled in the same way in the project, they were all parallel to each other but with different spacing. The discontinuities in the current equivalent continuum model were implemented as regions defined by boundary materials with reduced deformation and strength properties as reported in table 3.5. The geometry of the model is represented in the figure 3.12.

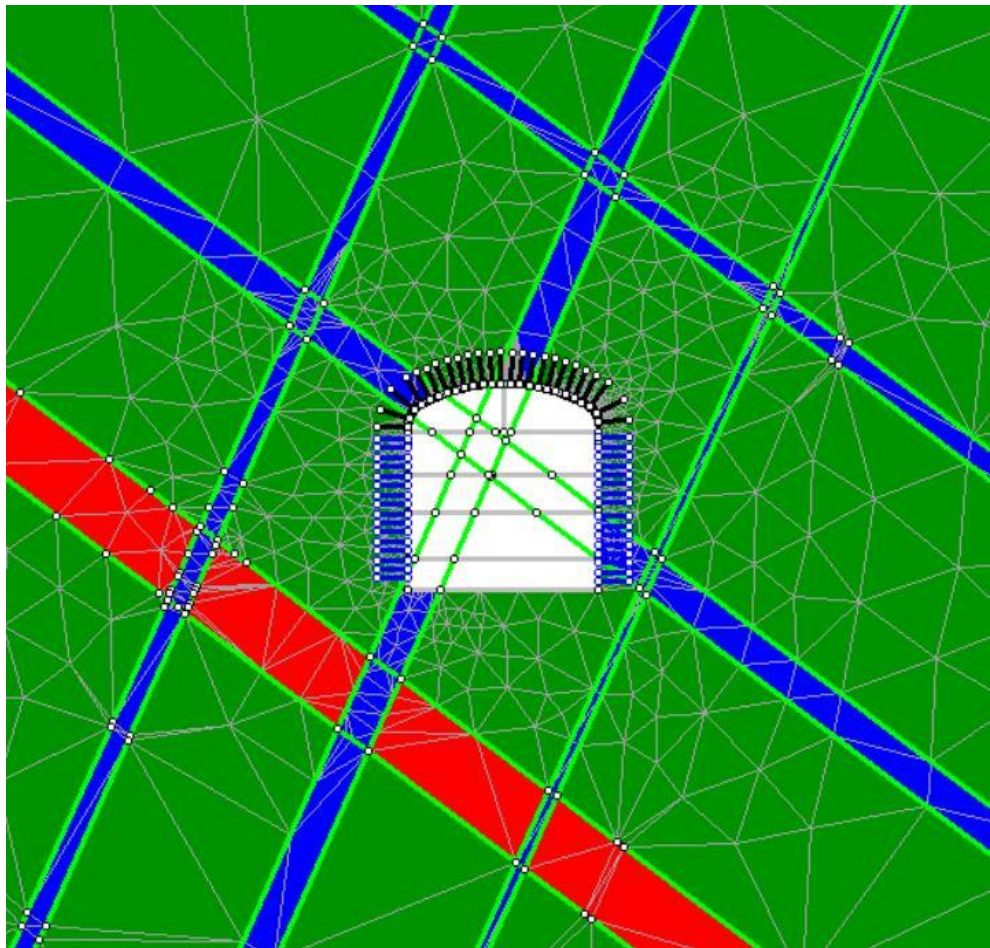


*Figure 3.12: Continuum model geometry*

- Mesh:

For the realization of the mesh, 3 noded triangular elements mesh with 300 elements were conceived. Moreover, in the zone of the excavation the density of the mesh was increased to obtain better results.

- Loading:

Due to fact that the project deals with a deep excavation, constant field stress conditions were applied using the relations reported in section 3.1.1 and reported in the table 3.3. From the Sheorey graph reported in figure 3.8 a  $k_0=0.67$  was derived. Moreover, also stress relief was applied as to simulate the excavation.

Constant field stress	
$\sigma_1$ [kPa]	8100
$\sigma_3$ [kPa]	5400
$\sigma_z$ [kPa]	4050

*Table 3.3 Constant field stress (continuum model)*

- Material:

Three different materials were modelled following the Q parameters: the granite with good strength properties, and two jointed granites. The presence of weathered regions has been represented using long thin areas modelled with different materials characterized by lower mechanical properties. In figure 3.12 these regions are reported in blue and red, while the granite in green. The Q values were derived following the considerations proposed in section 3.1.1 and reported in the table 3.1. More than 90% of the rock mass presented a  $Q > 5.9$  then for the granite was decided to use a  $Q=5.9$ , adopting a precautionary approach. While for the fractured granite  $Q=0.7$  and  $Q=0.2$  were assumed following the boreholes data from site investigation.

The failure criterion applied for the materials was the Generalized Hoek & Brown, and the elastic-perfectly plastic law was assumed. In figure 3.4 the material properties for the equivalent continuum model are reported.

Material Properties			
	Granite	Jointed Granite	Jointed Granite
Q	5,9	0,7	0,2
$\gamma$ [kN/m <sup>3</sup> ]	27	27	27
$\nu$ [-]	0,3	0,3	0,3
E [kPa]	1,04x10 <sup>7</sup>	3,42x10 <sup>6</sup>	1,63x10 <sup>6</sup>
$\sigma_{cr}$ -UCS [kPa]	175000	42000	5000
mb	7,66883	3,89072	2,62672
s	0,011744	0,001422	0,000419
a	0,502841	0,510622	0,522344

*Table 3.4 Material properties (continuum model)*

- Support:

Using the Q system support chart, it was possible to derive the typology of supports required for the stabilisation of the underground cavern under analysis. A systematic pattern of fully bonded bolts was chosen, the dextra Astec thread hollow bar 32x13 with different spacing between the crown and the wall due to fact that the crown was more solicited by the vertical loads.

Then, a layer of 15-20 cm of shotcrete should be applied to the excavation, but in this model was chosen, in a precautionary way to use only the bolts to assure the stability of the cavern. This because the shotcrete layer increases the stability of the structure, but this is not immediate after its application.

Then, during the realization of the work, it is advised to apply the abovementioned shotcrete layer to increase the stability and guarantee a smooth surface to the underground structure. The bolts properties are collected and reported in the table 3.5 and 3.6.

Support crown bolts fully bonded	
Bolt diameter [mm]	32
Bolt Modulus E [kPa]	4,50E+07
Tensile capacity [kN]	282
Residual Tensile Capacity [kN]	282
Out of plane spacing [m]	1,8

*Table 3.5 Support crown bolts fully bonded properties (continuum model)*

Support wall bolts fully bonded	
Bolt diameter [mm]	32
Bolt Modulus E [kPa]	4,50E+07
Tensile capacity [kN]	282
Residual Tensile Capacity [kN]	282
Out of plane spacing [m]	2

*Table 3.6 Support wall bolts fully bonded properties (continuum model)*

The results of the equivalent continuum model are deeply discussed in the chapter 7 in which this model and the continuum model with joints were compared and analysed.

## Chapter 4

### 4. CONTINUUM MODEL WITH JOINTS IN 2D

In the chapter 3, to account for the influence of joints on rock mass strength, in the numerical analysis modelling of rock masses was carried out as equivalent continuum with reduced deformation and strength properties.

Instead, in the 4<sup>th</sup> chapter another way for modelling jointed rock masses is adopted, introducing special elements such as joint elements, sometimes also known as interface elements, to the continuum model. These elements can have either zero thickness or be of thin finite thickness. Moreover, they can assume linear elastic behaviour or plastic response when stresses exceed the strengths of discontinuities.

#### 4.1 *Geo-mechanical characterization of joints*

In this paragraph the geo-mechanical characterization of joints was developed. To derive the joint properties the assumption of using the characteristics of the rock mass reported in table 3.3, in the previous chapter, was made.

The modelling of joints required the definition of a shear strength criterion, and elastic properties such as the joint normal stiffness and the joint shear stiffness. Different types of shear strength criterion can be adopted in RS2: Mohr Coulomb, Barton-Bandis and Geosynthetic Hyperbolic. In the case under study, it was chosen to apply the Mohr-Coulomb criterion.

The strength criterion is a function which define a locus of points, in the space or in a plane, representative of the state of stress that induces the failure in the

material. The parameters of M-C criterion are the cohesion  $c$ , the friction angle  $\varphi$ , and the tensile strength. It is expressed by the well-known equation (4.1):

$$\tau' = c + \sigma' \tan \varphi \quad (4.1)$$

As means to apply the Mohr-Coulomb slip criterion, the friction angle and the cohesion must be derived. Using the non-linear generalized Hoek & Brown criterion (4.2) and the linearization process it was possible to obtain  $\varphi$  and  $c'$  of the materials under analysis.

$$\sigma_1' = \sigma_3' + \sigma_{ci} \left( m \frac{\sigma_3'}{\sigma_{ci}} + s \right)^\alpha \quad (4.2)$$

Where  $m$  is a coefficient related to the lithotype,  $s$  represents the fracturing degree of the rock mass while  $\sigma_{ci}$  corresponds to the uniaxial compressive strength of the studied rock mass.

Then it was possible to transit towards Mohr – Coulomb's approach, written in terms of principal stresses in (4.3):

$$\sigma'_1 = C_0 + N_\varphi \sigma'_3 \quad (4.3)$$

The coefficients  $C_0$  and  $N_\varphi$  were found to be related to the  $c$ , cohesion term, and  $\varphi$ , rock's friction angle using the relations (4.4).

$$\begin{cases} N_\varphi = \frac{1 + \sin \varphi}{1 - \sin \varphi} = \tan^2 \left( 45^\circ + \frac{\varphi}{2} \right) \\ C_0 = 2c \cdot \frac{\cos(\varphi)}{(1 - \sin(\varphi))} = \sigma_{ci} \end{cases} \quad (4.4)$$

Therefore, using the material properties derived in the previous chapter and reported in the table 3.3, it was possible to apply the Hoek & Brown criterion and the procedure above mentioned to obtain the graphs highlighted in figure 4.1 and 4.2. Clearly, these properties were calculated only for the weathered granite characterised by the discontinuities (Q=0.2 and Q=0.7).

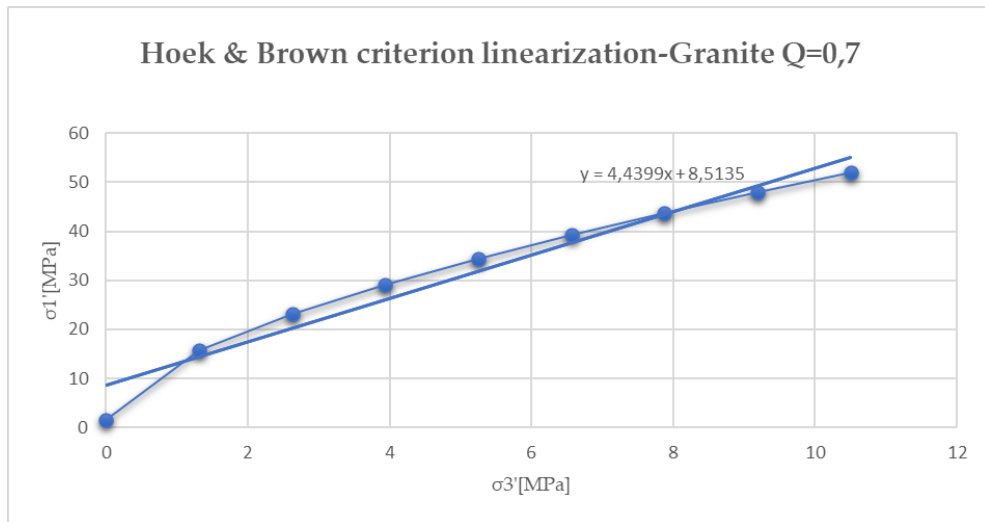


*Figure 4.1: Hoek & Brown Linearization Granite Q=0,7*

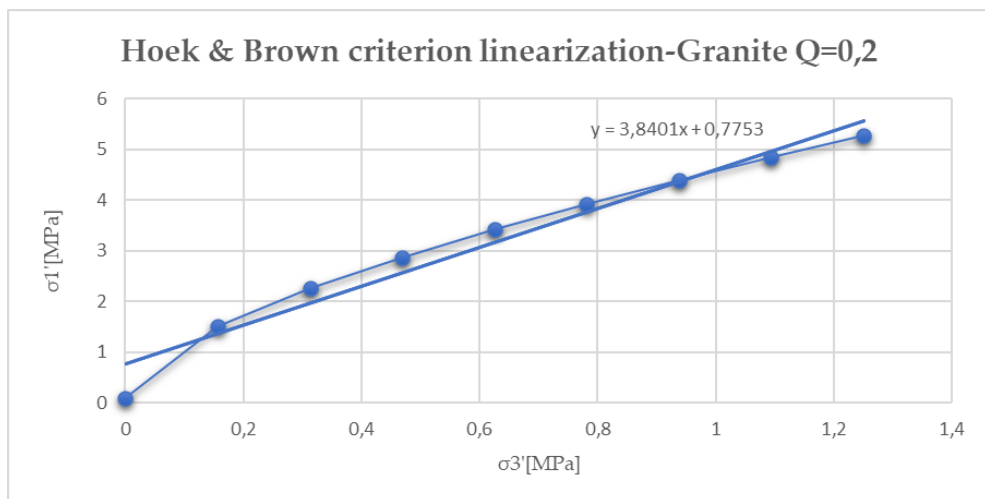


*Figure 4.2: Hoek & Brown Linearization Granite Q=0,2*

Using the derived graph, it was possible to obtain, with the relations 4.4, the Mohr-Coulomb parameters shown in table 4.1.

Mohr-Coulomb parameters	Jointed granite Q=0,7	Jointed granite Q=0,2
$\phi$ [°]	39	36
C'[kPa]	2000	200

*Table 4.1: Mohr-Coulomb parameters*

Therefore, after the determination of the Mohr Coulomb parameters, it was necessary to derive stiffness of joints.

The stiffness of a rock joint describes the overall stress-deformation characteristic, both in the normal and tangential sense. The normal stiffness is defined as the normal stress per unit closure of the joint, and the shear stiffness is the ratio of the peak shear stress to the shear displacement at this peak.

The normal stiffness following (Barton 1972) relation can be estimated from rock mass modulus, intact rock modulus and joint spacing using the equation 4.5.

$$\frac{1}{E_m} = \frac{1}{E_i} + \frac{1}{k_n L} \quad (4.5)$$

Where:

$E_m$  = rock mass modulus

$E_i$  = intact rock modulus

$K_n$  = joint normal stiffness

$L$  = mean joint spacing

This assumes joint sets referring to an average spacing  $L$ , oriented perpendicularly to the direction of loading. The equation 4.5 can be re-arranged to give, the joint normal stiffness relation 4.6 (Barton 1972).

$$k_n = \frac{E_i E_m}{L(E_i - E_m)} \quad (4.6)$$

The same reasoning can be adopted to derive an expression for the joint shear stiffness:

$$k_s = \frac{G_i G_m}{L(G_i - G_m)} \quad (4.7)$$

Where:

$G_m$  = rock mass shear modulus

$G_i$  = intact rock mass shear modulus

$K_s$  = joint shear stiffness

$L$  = mean joint spacing

In order to derive the shear modulus, the equation 4.8 was adopted:

$$G = \frac{E}{2(1 + \nu)} \quad (4.8)$$

Using the relations abovementioned, it was possible to obtain the shear modulus of the rocks, reported in table 4.2 and moreover the joint normal stiffness and the joint shear stiffness, how it is shown in the table 4.3. The mean joint spacing was derived from the geometry of the discontinuities and the obtained value was  $L=32$  m.

	Jointed granite $Q=0,7$	Jointed granite $Q=0,2$
G [Kpa]	$2,23 \times 10^6$	$1,06 \times 10^6$

*Table 4.2: Shear modulus*

	Jointed granite Q=0,7	Jointed granite Q=0,2
$k_n$ [kPa/m]	$1,59 \times 10^5$	$6,04 \times 10^4$
$k_s$ [kPa/m]	$1,04 \times 10^5$	$3,93 \times 10^4$

*Table 4.3: Joints normal stiffness and joints shear stiffness*

## 4.2 Continuum model with joints using RS<sub>2</sub>

Knowing the geometry of the cavern, the orientation and inclination of the joint sets it was possible to draw the 2D section of the underground construction site as previously done for the continuum model.

Six different models were set up to obtain a large simulation of the joint's behaviour. The general settings, such as the geometry, the mesh, the loading, the material properties, and the supports were the same for all the models. What characterises each model was the implementation of the joints, and particularly six different joint networks were developed. In the following paragraph the general properties are collected, then a joint's network introduction is proposed.

The following general assertions were addressed when modelling the projects on RS<sub>2</sub>:

- Project settings:

In this first step, it was important to notice the use of height stages: the first one representing the geostatic conditions, while in the second one the cavern's excavation starts. It was decided to divide the excavation in six different parts as suggested in the section 2.3.2. Then after the digging phases a final stage was realized.

- Geometry:

The same geometry assumed in the previous model was used in these simulations.

- Mesh:

For the realization of the mesh, 3 noded triangular elements mesh with 300 elements were conceived. Moreover, in the zone of the excavation the density of the mesh was increased to obtain better results, using the increase density tool provided by the software.

- Loading:

Due to fact that the project deals with a deep excavation, constant field stress conditions were applied using the relations reported in section 3.1.1, reported in the table 3.2. Moreover, also stress relief was applied in order to better simulate the excavation.

- Material:

Analogously with the equivalent continuum model, the same properties for the granite characterized by  $Q=5.9$  were adopted.

However, differently from the approach followed in the section 3.2, in this model inside the long thin areas characterized by lower mechanical properties the weathered rock mass was simulated using joint networks.

The joint systems are two-dimensional networks of joint boundaries, that simulate pattern of joints in the rock mass. They present the joints properties described in table 4.1, 4.2 and 4.3.

These joint networks were added to the strips, where jointed granite was present. The material properties of the strips were different to the one reported in table 3.3, because the weakness of the rock mass was described by the joints. Therefore, the parameter of the intact rock ( $GSI=100$ ,  $m_b=m_i$ ,  $s=1$ ,  $\alpha=0,5$ ) were applied to the rock mass, while the parameters derived from the characteristic of the weathered rock mass were applied to the joints. This means that the material in the

strips was considered as intact but with the presence of joints that described the weakness of the rock mass.

In the table 4.4 all the material properties used for the continuum model with joints are reported.

Material properties			
	Granite	Jointed Granite	Jointed Granite
Q	5,9	0,7	0,2
$\gamma$ [kN/m <sup>3</sup> ]	27	27	27
$\nu$ [-]	0,3	0,3	0,3
E [kPa]	$1,04 \times 10^7$	$3,42 \times 10^6$	$1,63 \times 10^6$
$\sigma_{ci}$ -UCS [kPa]	175000	42000	5000
mb	7,66883	7,66883	7,66883
s	0,011744	1	1
a	0,502841	0,5	0,5
Joint properties			
G [kPa]		$2,23 \times 10^6$	$1,06 \times 10^6$
$\phi$ [°]		39	36
C' [kPa]		2000	200
L [m]		32	32
kn [kPa/m]		$1,59 \times 10^5$	$6,04 \times 10^4$
ks [kPa/m]		$1,04 \times 10^5$	$3,93 \times 10^4$

*Table 4.4 Material properties continuum model with joints*

- Support:

The same support system was implemented regarding to the equivalent continuum model.

#### 4.2.1 Joint Networks overview

Joint networks, or joint system models were constructed by specifying combinations of joint geometric characteristics (such as joint shape, size, location, orientation, and planarity) to get a complete and consistent representation of joint

geometry. Rock joints could be viewed conceptually as two-dimensional elements within a three-dimensional region, the rock mass, as reported in figure 4.4. The purpose of joint system modelling is to describe both the two-dimensional geometric characteristics, such as size and shape, and the three-dimensional characteristic of location and orientation of these two-dimensional features within the three-dimensional region. All joint geometric characteristics may be defined either deterministically or stochastically. Stochastic characteristics must be described by distributional information (Dershowitz, 1985).

Joint shapes in rock masses depend upon different factors related to joint formation, however joint networks are limited to regular, convex mathematical shapes, which are more tractable for analysis and simulations. Where joints extend beyond the scale of the problem being evaluated or traverse the entire rock mass joints are referred to unbounded or infinite size. Instead, for bounded joints, joint size may be represented by joints area, or by joint radius or joint edge dimensions. Furthermore, joints are generally planar, however they can also have curve or undulatory shapes. To facilitate joint system modelling, joints are generally assumed as planar.

The joint location can be specified by the centre or end points of jointing, and could be either a regular following deterministic process, or a stochastic process. Regular jointing may be either uniform or regular series (exponential or geometric series of progressively increasing spacings between joints). One of the simplest assumptions for joint location is the regular grid with constant distances. The most common used stochastic process by definition of joint location is the Poisson process, in which joints are located independently according to a uniform distribution in  $x$ ,  $y$ , and  $z$  axes.

Joint orientation is mainly described by the relationship between the orientations of all joints within a rock mass. Orientation mainly requires stochastic

representation. One class of deterministic joint orientations is the parallel jointing, in which all joints have the same orientation. Joints sets are indicated as group of joints with the same or similar joints. For stochastic approaches, joint orientations are specified by a probability distribution. In this occasion joint set term is indicated to refer to a group of joints defined by a single distribution about a mean value.

It was possible to implement the joint network in RS2. In fact, the software allows to generate 2-dimensional networks of joint boundaries, to simulate patterns of natural or induced jointing in rock masses.

In the figure 4.4 the conceptual model for Rock Joint system is reported.

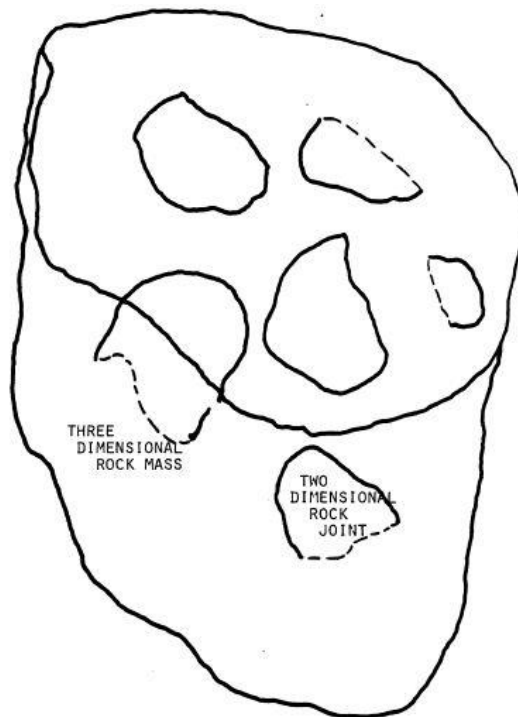


*Figure 4.4: Conceptual model for Rock Joint System (Dershowitz, 1985)*

In the next paragraphs the six continuum models with joints have been reported, related to six different joints network implemented in the RS<sub>2</sub> software: Cross Jointed, Parallel Statistical, Parallel Deterministic, Baecher, Veneziano and Voronoi (polygons model). The joint system models are reported in the figure 4.5. With RS<sub>2</sub> was not possible to use the Dershowitz Polygon model.

JOINT SYSTEM MODELS

Model Number and Name	Joint Shape	Joint Size	Termination at Intersect.	Co- Planarity	Orientation of sets
1. Orthogonal	Rectangle	Bounded	no	----	Parallel
		Unbounded	yes	yes	Parallel
		Unbounded	no	yes	Parallel
2. Baecher	Circle	Bounded	no	no	Stochastic
3. Veneziano	Polygon	Bounded	in joint planes only	yes	Stochastic
4. Dershowitz	Polygon	Bounded	yes	yes	Stochastic
5. Mosaic Tesselation	Polygon	Bounded	yes	yes	Systematic Stochastic

*Figure 4.5: Joint system models (Dershowitz, 1985)*

#### 4.2.2 Model 1-Joint network CROSS JOINTED

The Cross Jointed joint network model, or orthogonal model, allows to define a network which consists of two sets of parallel joints (e.g. bedding planes with cross joints) intersecting to form rectangular or trapezoidal blocks. The spacing of the joint planes can be defined as random variables (assigned statistical distributions). The bedding joint planes are assumed to be continuous (infinite), while the cross joints intersect the bedding planes at intervals defined by the spacing distribution.

The cross joints do not have to be perpendicular to the bedding planes but may intersect them at any angle. In figures 4.6 and 4.7 representations of the three-dimensional orthogonal model and the two-dimensional Orthogonal model are proposed.

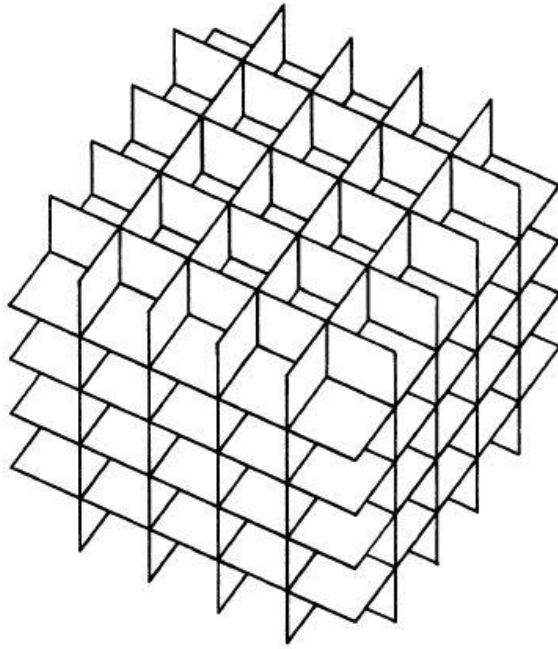


*Figure 4.6: 3D Orthogonal model (Dershowitz, 1985)*

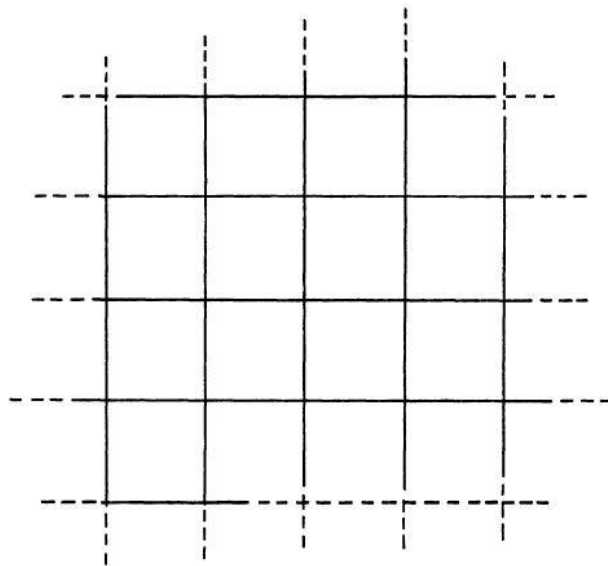


*Figure 4.7: 2D Orthogonal model (Dershowitz, 1985)*

The first model implemented with Cross Jointed network is reported in figure 4.8 and the relative properties are reported in table 4.5, for the joint characterised by

Q=0.7 (in the red zone in the figure 4.8) and 4.6 for the joints with Q=0.2 (in the blue zone in figure 4.8).

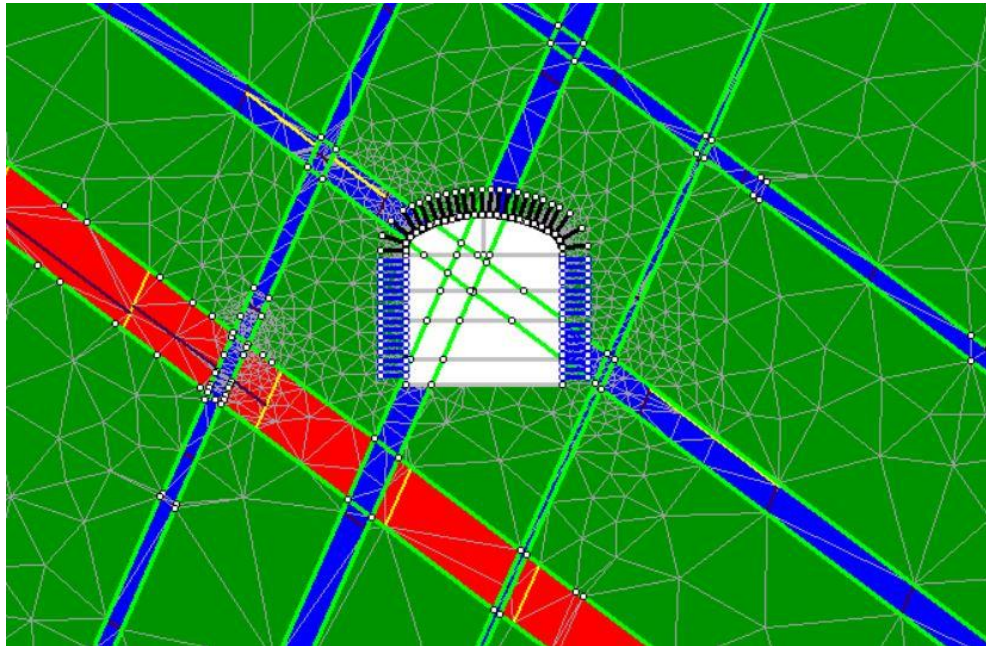


*Figure 4.8: Model 1-cross jointed*

Model 1 Joint Network Cross Jointed	
Bedding Joint property	Joint Q=0,2
Cross Joint Property	Joint Q=0,7
Orientation	
Trace plane	No
Bedding inclination [°]	66
Cross Joint Inclnation [°]	-37
Bedding spacing	
Mean [m]	32
Distribution	Normal
Cross Joint Spacing	
Mean [m]	32
Distribution	Normal

*Table 4.5: Model 1 Cross Jointed properties*

Model 1 Joint Network Cross Jointed	
Bedding Joint property	Joint Q=0,7
Cross Joint Property	Joint Q=0,2
Orientation	
Trace plane	No
Bedding inclination [°]	66
Cross Joint Inclination [°]	-37
Bedding spacing	
Mean [m]	32
Distribution	Normal
Cross Joint Spacing	
Mean [m]	32
Distribution	Normal

*Table 4.6: Model 1 Cross Jointed properties*

### 4.2.3 Model 2-Joint Network PARALLEL STATISTICAL

The Parallel Statistical joint network model allows to define a network of parallel joints with user-defined statistical distributions for the joint spacing, length and persistence. For this model, the spacing can be defined as a random variable by adopting a statistical distribution.

In figure 4.9 it is reported the geometry of the Parallel Statistical joint network model, in which joints of determined length, it was taken as reference value 100 m following the indication from boreholes, a spacing of 32 m was adopted with the normal statistical distribution. All the properties of this model are collected in the table 4.7.

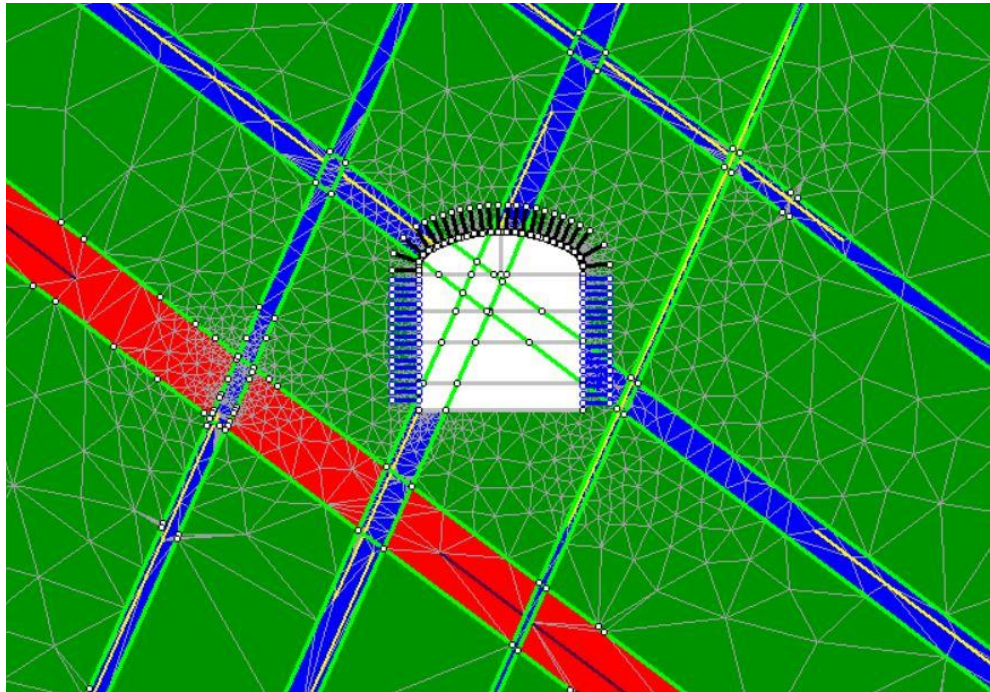


*Figure 4.9: Model 2-Parallel statistical*

Model 2 Joint Network Parallel Statistical		
	Joint Q=0,7	Joint Q=0,2
Inclination [°]	-37	66
Spacing [m]	32	32
Distribution	Normal	Normal
Length [m]	100	100
Mean persistence	0,5	0,5
Distribution	Normal	Normal

*Table 4.7 Model 2 Parallel Statistical properties*

#### 4.2.4 Model 3-Joint Network PARALLEL DETERMINISTIC

The Parallel Deterministic joint network model allows to define a network of parallel joints with a fixed spacing and orientation. In this case deterministic refers to the fact that the spacing, length and persistence of the joints is assumed to be constant (exactly known with no statistical variation). However, the Parallel Deterministic model allows randomness of the joint location. By means of having different results with respect to the previous model, and therefore having the possibility to obtain

better comparison between models, in this case it was chosen to use an infinite length for the joints. Thus, the joints extension was continuous across the region.

Figure 4.10 reports the model's geometry, while the table 4.8 the model's properties.

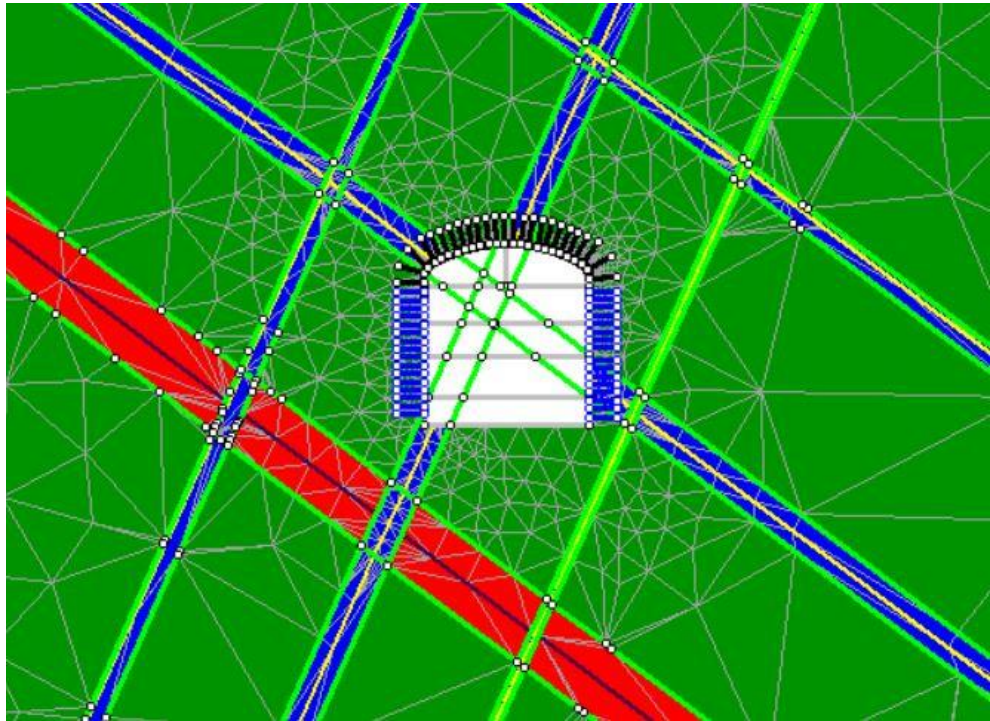


*Figure 4.10: Model 3-parallel deterministic*

Model 3 Joint Network Parallel Deterministic		
	Joint Q=0,7	Joint Q=0,2
Inclination [°]	-37	66
Spacing [m]	32	32
Length [m]	INF	INF

*Table 4.8 Model 3 Parallel Deterministic properties*

#### 4.2.5 Model 4-Joint network VENEZIANO

The Veneziano joint network model, in a two-dimensional trace plane, is based on the Poisson line process. Perhaps, it adapts the Poisson process to generate

joints of finite length (Dershowitz, 1985). To have a complete analysis, the Poisson point process and line process have been briefly reported in the following section.

The Poisson point process is a method adopted to derive random locations for joints in two-dimensional and three-dimensional space. This system assumes that the location of joints must be independent from one another. Thus, these locations follow uniform random distribution along the coordinate axes. Moreover, The Poisson line process is based on the fact that a joint of infinite extent passes through each joint location originated by a Poisson point process.

The Veneziano model follows the present steps:

- Generation of infinite joint lines, each of which passing through a point located according to a Poisson point process, so points in the trace plane following a uniform distribution. The orientations of the lines may be constant or vary according to some orientation distribution.
- Division of each joint line into segments of random lengths, adopting statistical distribution.

With the Veneziano model, the joint shapes are polygonal, and the size of joints are determined by the intensity of the Poisson line process.

A portion of these segments are joints and the remainder as intact rock bridges. The proportion of joints to intact rock bridges is determined by the length persistence, that is the ration between the joint length and the sum of joint length and rock bridge length.

In the figures 4.11 and 4.12 the three-dimensional and two-dimensional representations of the Veneziano model are reported.

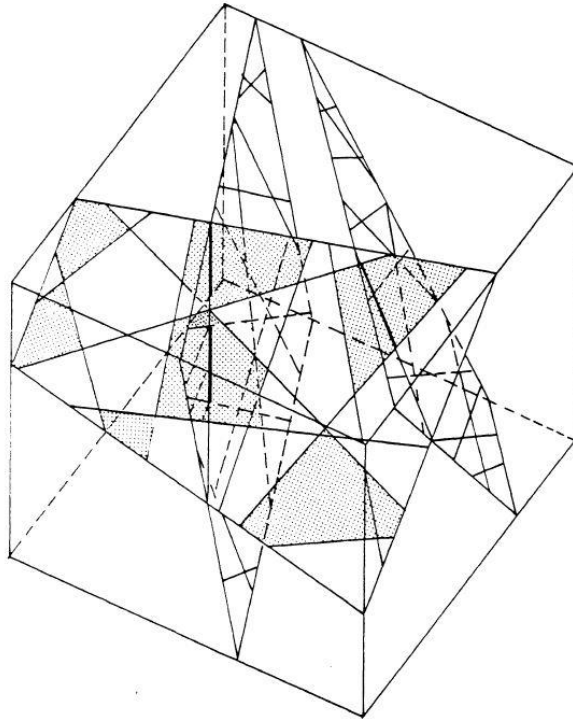


*Figure 4.11: Two-dimensional Veneziano Model (Dershowitz, 1985)*

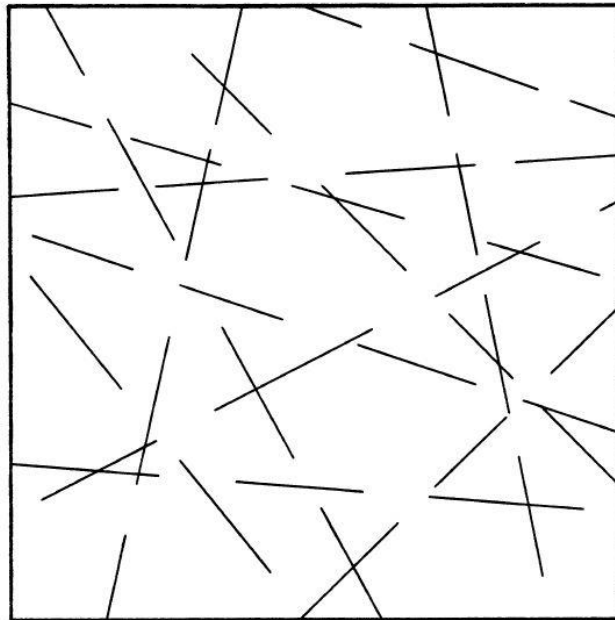


*Figure 4.12: Two-dimensional Veneziano Model (Dershowitz, 1985)*

As a result of the use of joint lines in generating joints, joints in a Veneziano network tend to be coplanar. This attitude differentiates Veneziano model from Baecher model in which joints, instead are independent segments.

In the table 4.9 were shown the properties adopted for the Veneziano joint network model, while in the figure 4.13 the developed model is reported.

Model 4 Joint Network Veneziano		
	Joint Q=0,7	Joint Q=0,2
Orientation		
Inclination [°]	-37	66
Distribution	Normal	Normal
Length [m]		
Mean length [m]	100	100
Distribution	Normal	Normal
Length persistence		
Mean	0,5	0,5

*Table 4.9: Model 4 Veneziano properties*

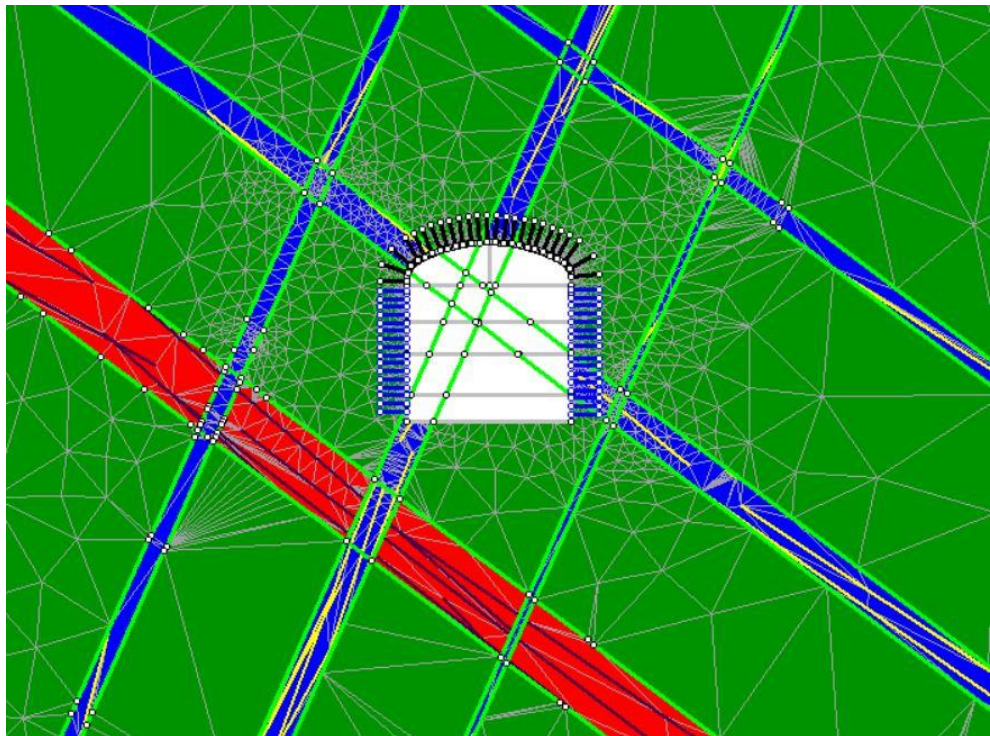


*Figure 4.13: Model 4 Veneziano*

#### 4.2.6 Model 5-Joint Network BAECHER

The Baecher joint network model can generate intricate joint networks. In this model, joints are assumed to have finite trace lengths, following some statistical distribution. The joints' centres position are situated in the space according to a Poisson point process (points distributed in the trace plane according to a uniform distribution). The orientations of joints in a Baecher network can be constant or can vary according to an orientation distribution. The number of joints generated in a Baecher network is controlled by a joint intensity measure.

Moreover, the basic assumption of the Baecher model is the elliptical or circular joint shapes. In the figure 4.14 it is reported the three-dimensional shape of this model. This allows the model to be determined by joint terminations at the intersection of joints, due to fact that intersections among planar joints are always line segments. The above-mentioned consideration was instead clarified in the imagine 4.15 with the two-dimensional Baecher Model.

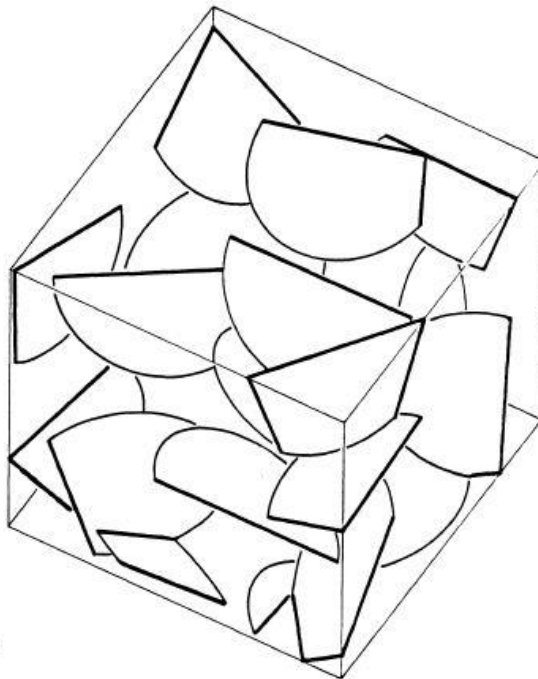


*Figure 4.14: Three-dimensional Baecher Model (Dershowitz, 1985)*

In two dimensions, a Baecher model is then defined by joint segments in a plane.

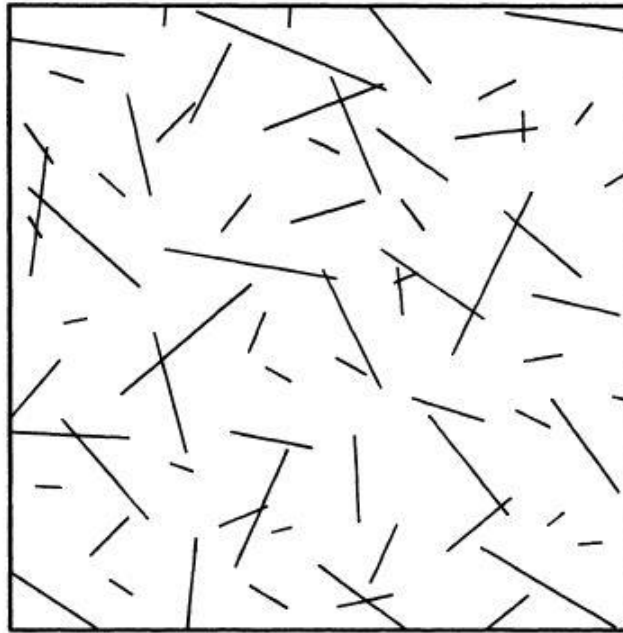


*Figure 4.15: Two-dimensional Baecher Model (Dershowitz, 1985)*

Therefore, the model has been implemented and in the table 4.10 all the material's properties are collected.

Model 5 Joint Network Baecher		
	Joint Q=0,7	Joint Q=0,2
Orientation		
Inclination [°]	-37	66
Distribution	Normal	Normal
Length [m]		
Mean length [m]	100	100
Distribution	Normal	Normal
Length persistence		
Mean	0,5	0,5

*Table 4.10: Model 5 Baecher properties*

Figure 4.16 shows the representation of the fifth model derived with the Baecher joint network.

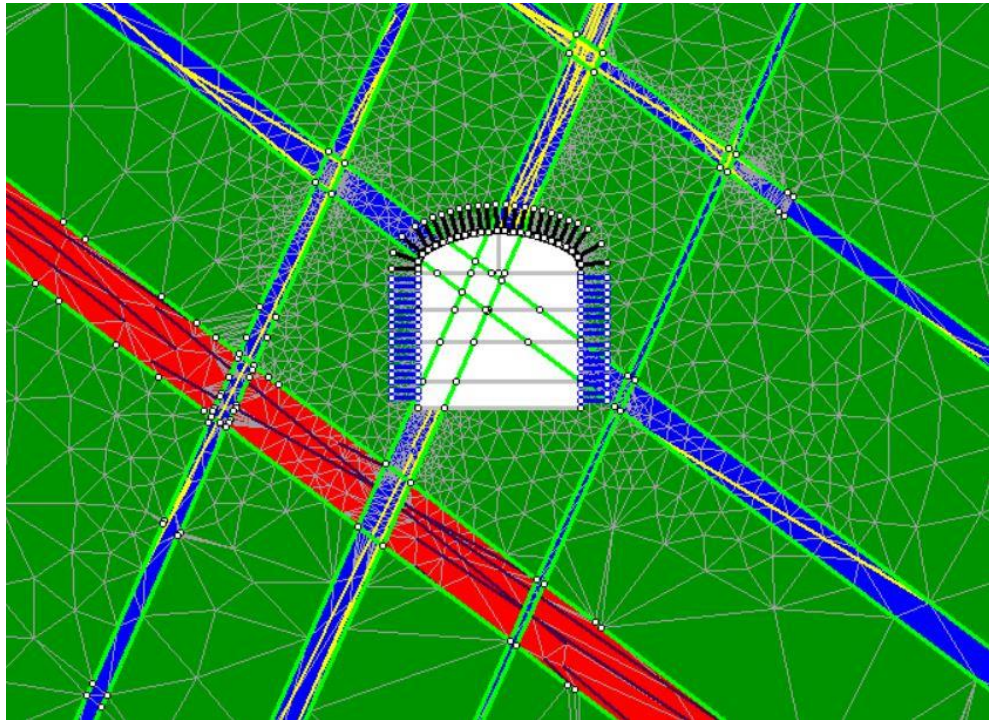


*Figure 4.16: Model 5 Baecher*

#### 4.2.7 Model 6-Joint Network VORONOI

Voronoi two-dimensional mosaic tessellation is a process that randomly subdivides a plane into non-overlapping convex polygons. A Voronoi joint network consists of joints that are defined by the bounding segments of these polygons (Dershowitz, 1985).

The Voronoi tessellation starts with a Poisson point process, in which it is defined the generators or seeds. The Voronoi cell corresponding to each generator is the planar region closer to the generator than to any other generator.

The bounding segments of this region are lines that are equidistant to the seed and adjacent generator. Seeds generated through a Poisson point process are generally not evenly distributed in space.

Some points may lie very close to each other, while others are far apart. As a result, it may be desirable to make the distribution of seeds more regular. When this is done, the resulting Voronoi cells become more regular in shape.

In the figures 4.17 and 4.18 the three-dimensional and two-dimensional representation of the Voronoi model are reported.

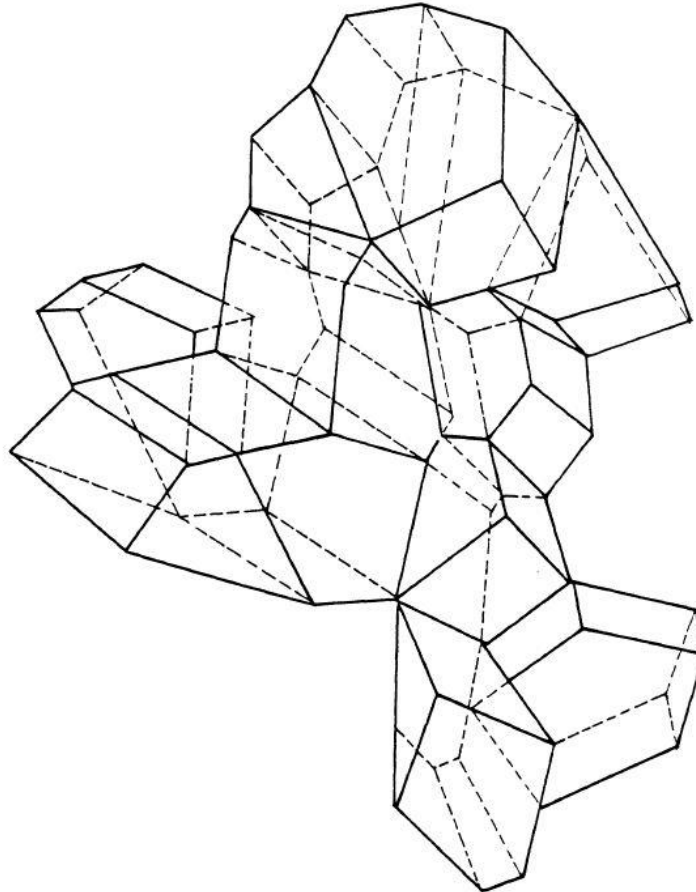


*Figure 4.17: Three-dimensional Baecher Model (Dershowitz, 1985)*

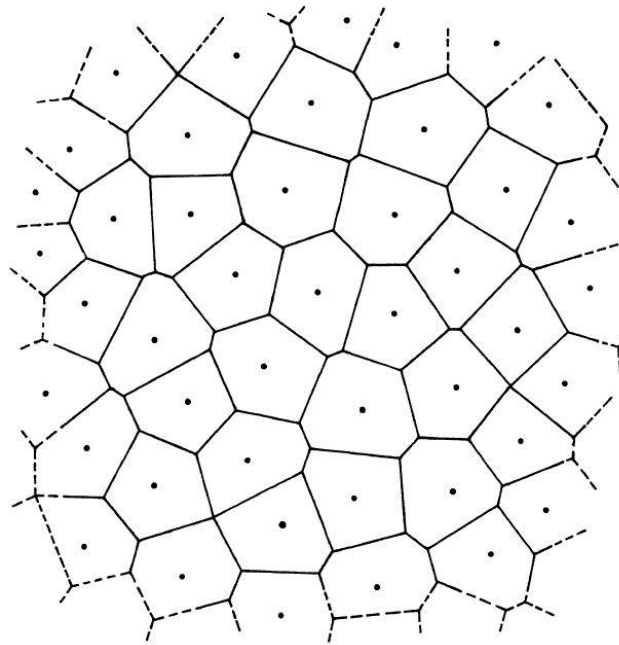


*Figure 4.18: Two-dimensional Baecher Model (Dershowitz, 1985)*

The mosaic tessellation system allows to model the joints which are not coplanar, giving more flexibility in joint modelling. Moreover, another feature is the generation of rock blocks first, followed by rock joints from the faces of the blocks.

In the RS<sub>2</sub> software, it was possible to adopt either the density of Voronoi seeds or the average length of the sides of Voronoi polygons. The Voronoi network is recommended for broken rock masses in which there are no preferred jointing directions. Therefore, it is not very efficient in modelling jointed granite. However, it was used in order to compare the results among the other models. In the table 4.11 the Voronoi model’s properties are reported, in the figure 4.19 the model geometry is shown.

Model 6 Joint Network Voronoi		
	Joint Q=0,7	Joint Q=0,2
Joint Density		
Density method	Average Joint Length	Average Joint Length
Average length [m]	100	100
Regularity of polygon shape		
Regularity	Irregular	Irregular

*Table 4.11: Model 6 Voronoi properties*

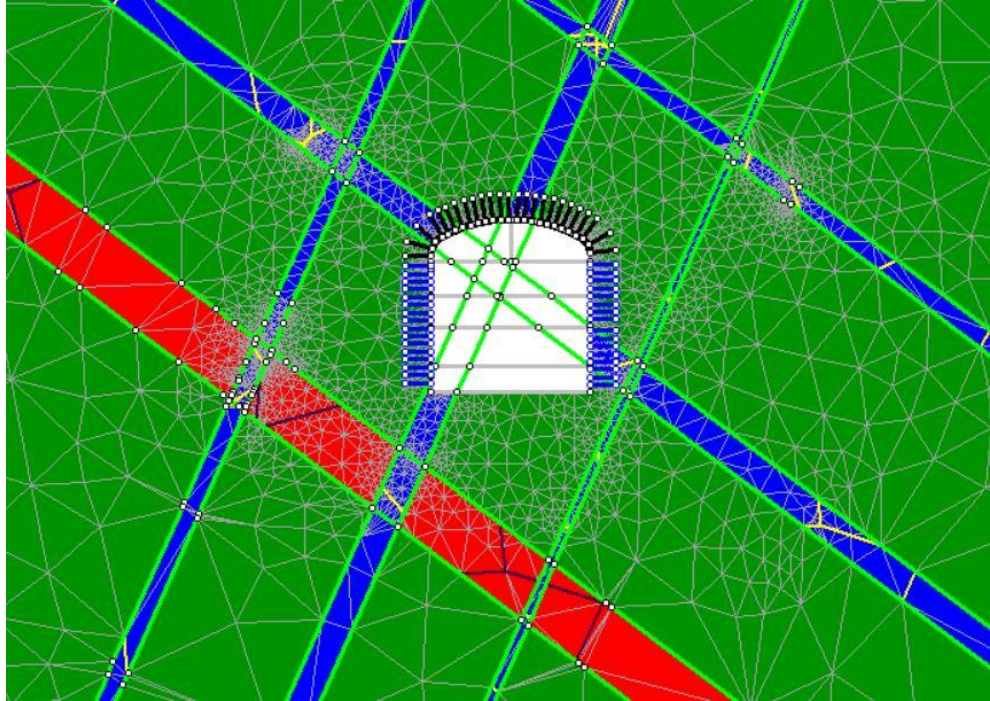


*Figure 4.19: Model 6 Voronoi*

All the results of the abovementioned six joint network models are deeply discussed in the chapter 7.

## Chapter 5

### 5. CONTINUUM MODEL IN 3D

In the present chapter, the implementation of the three-dimensional continuum model is dealt. For this purpose, the RS<sub>3</sub> software, of the Rocscience suite was used. RS<sub>3</sub> is designed for three-dimensional analysis of geotechnical structures for civil and mining applications. Applicable for both rock and soil, RS<sub>3</sub> is a general-purpose finite element analysis program used for underground excavations, tunnel and support design, surface excavation, foundation design, embankments, consolidation, groundwater seepage.

#### 5.1 *Continuum model using RS<sub>3</sub>*

The goal of these new analyses was to reproduce the model presented in the chapter three, using the current application. By considering the third dimension and moreover implementing in a proper way the excavation and the support installation sequences. Of course, the general properties of the materials and of the supports derived in the chapter three have been implemented also in this model, directly importing them using a particular feature of the software, which allows the import of the material and support properties from RS<sub>2</sub>.

Furthermore, it was chosen to study a limited portion of the cavern of 12 m depth, this because the goal of the study was to understand the behaviour of a part of the cavern in three-dimension and not to reproduce all the geometry of the cavern, that was actually part of a sewage system. Moreover, using a limited portion of the cavern excavation it was possible to understand the attitude during the development

of the project and for a computational point of view a reasonable time of computing was obtained.

The following general assertions were addressed when modelling the projects on RS<sub>3</sub>:

- Project settings:

In this first step, it was important to notice the use of twenty stages: the first one representing the geostatic conditions in which an elastic criterion was adopted in order to initialize the model, in the second one the cavern's excavation began. The sequence of the digging started from the portion of the cavern situated in the left of the crown. Then after the digging phases a final stage was realized.

- Geology:

The external boundary was the first step in the modeling of the project. It was decided to use an external box of 150x150 m, representing ten times the diameter of the underground structure. Following the continuum two-dimensional model, it was possible to draw the zones, indeed joints, characterized by the presence of weaker granite. Two of these zones crossing the cavern section, were strips of about 5 m spacing. Other zones of discontinuities were modeled in the project, as they were all parallel to each other but with different dimension. To do this, different planes were created, then extruded as means to obtain the three-dimensional feature, from these planes the zones characterized by a weathered granite were defined.

An important tool in the software is the Divide All, an important function to model creation. Analogously to subdividing external boundaries creating material regions in enclosed polylines in the two-dimensional software, Divide All splits three-dimensional external volume to smaller pieces, for material, support or loading assignments.

In the figure 5.1 the model geology and geometry are reported. So as to have the possibility of comparing as much as possible the two and three-dimensional models the same colors were used for the same materials, the materials properties are reported in table 3.4.

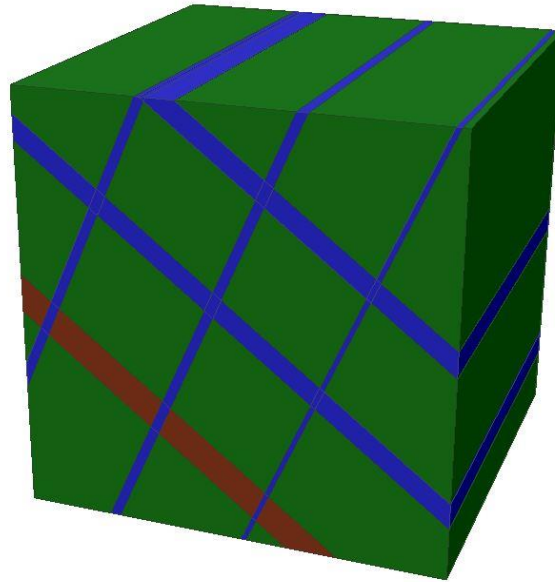


*Figure 5.1: Continuum model in 3D geometry*

- Cavern design:

In the RS<sub>3</sub> software, it was possible to use the tunnel/cavern design in order to implement the shape, the dimension, the construction sequence, and the supports of the excavation. Therefore, it was reproduced the cavern geometry as for the two-dimensional problem, with an overall height of the cavern of 32 m and a base of 30 m. Then, the cavern was divided in six zones, as in the 2D model for the excavation sequence. The chosen depth of the structure was of 12 m, just a portion of the cavern, in this way it was possible to understand the behavior during the excavation of the construction and the surrounding rock mass. In figure 5.2 it is shown the cavern geometry in geostatic conditions at the first stage.

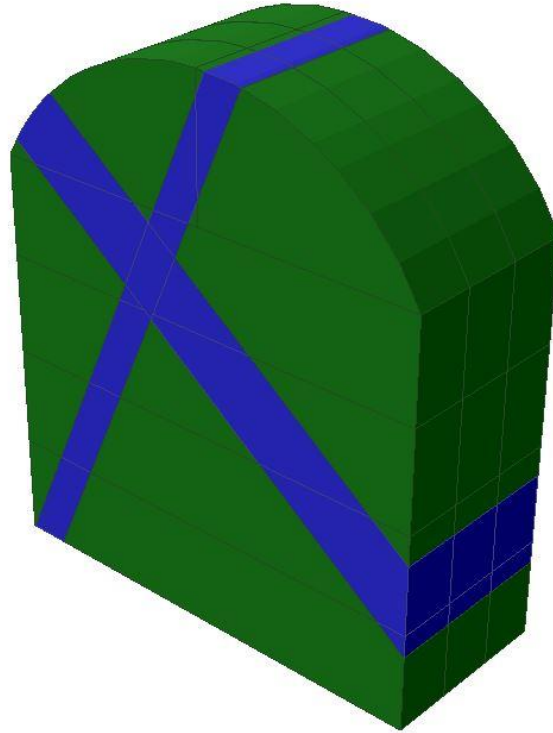


*Figure 5.2: Cavern geometry in geostatic condition*

Furthermore, for a depth of 12 m, three blasts of 4 m were implemented. Therefore, in general 20 stages were used, where the first one was meant for the initialization in geostatic condition setting elastic properties as means to avoid disturbances to the model. Then, for every region three stages were required, so 18 stages for the excavations, and the final stage for the final condition with all the volume excavated. The excavation started at the crown, in the left part, then after all the identified section has been excavated, it was possible to pass at the right-crown area, and subsequently downwards with the excavation of the 4 wall-regions. Simultaneously with the excavation of a portion of the cavern, the support system, was implemented. After the removal of an area in the following stage the same area was stabilized with a systematic pattern of bolts. The support system presented the same properties reported in table 3.5 and 3.6.

In the figure 5.3 it is shown the third stage of the model where the first region was excavated and supported, and the second region excavated. Then, in figure 5.4 all the crown is excavated and supported, and the first wall regions excavated.

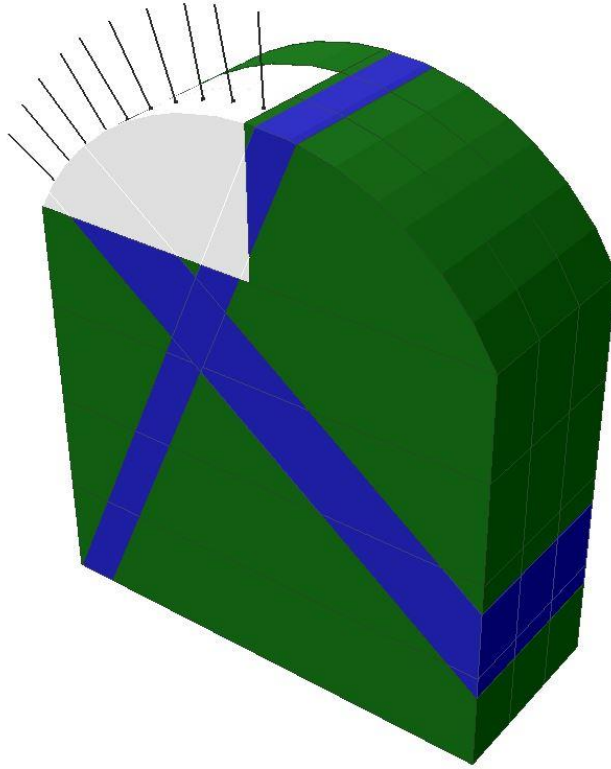


*Figure 5.3: Third stage of cavern's excavation*

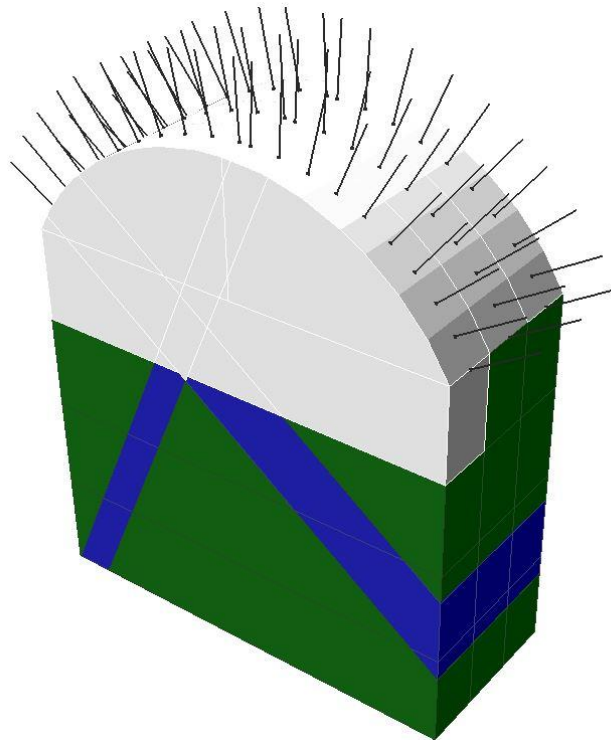


*Figure 5.4: Eighth stage of cavern's excavation*

Furthermore, in figure 5.5 the final configuration of the excavated cavern is reported.

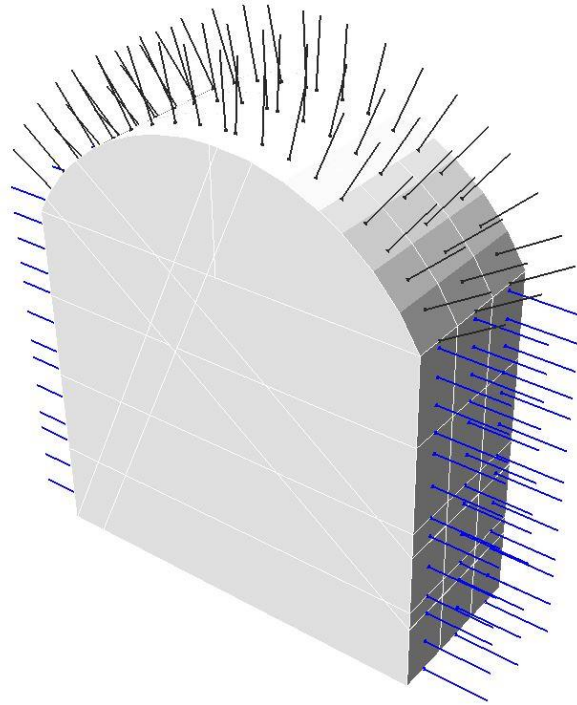


*Figure 5.5: Final stage of cavern's excavation*

- Loading:

Due to fact that the project deals with a deep excavation, constant field stress conditions were applied using the relations described in section 3.1.1, for the three-dimensional simulations the plane strain conditions were not considered, an isotropic  $k_0$  was assumed so the horizontal tension was assumed equal to the longitudinal one ( $\sigma_2 = \sigma_3$ ).

- Restraints:

Concerning the restraints, the model was completely implemented underground, so that the underground auto restrain were used. This option is a shortcut for automatically applying default restraint boundary conditions on the external boundary for underground models. The model constraints are shown in figure 5.6.

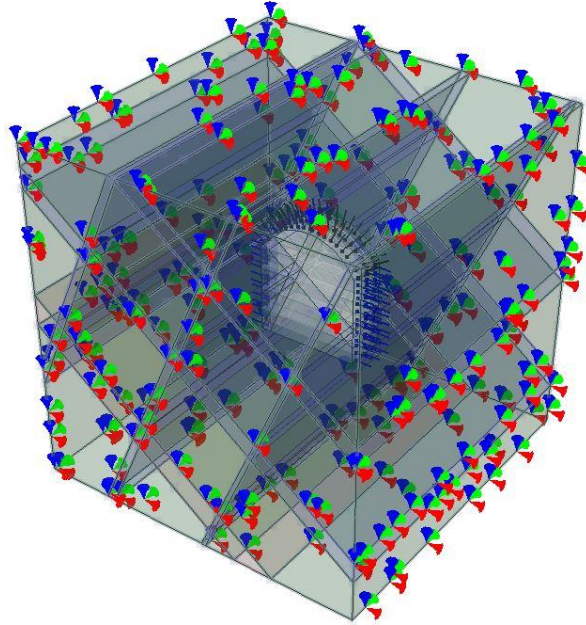


*Figure 5.6: 3D continuum model restraints*

- Mesh:

For the realization of the mesh, 4 noded tetrahedral graded elements mesh has been adopted. In figure 5.7 the meshed model is proposed.

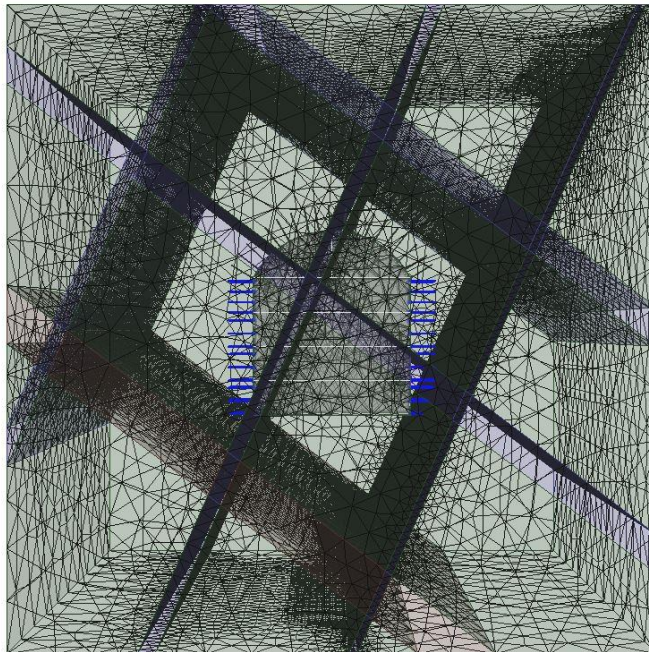


*Figure 5.7: 3D continuum model mesh*

Finally, in figure 5.8 the complete three-dimensional model with the external boundary, the strips of weathered granite, the excavated and supported cavern is presented. The results of this three-dimensional continuum model are then discussed in the chapter 7.

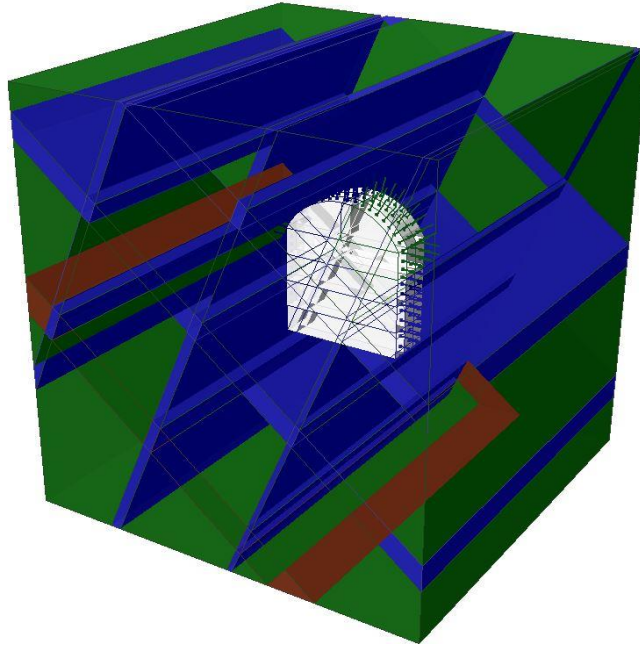


*Figure 5.8: 3D continuum model*

## Chapter 6

### 6. CONTINUUM MODEL WITH JOINTS IN 3D

In the present chapter, the implementation of the three-dimensional continuum model with joints is reported. To do so, the RS<sub>3</sub> software from the Rocscience suite was used. RS<sub>3</sub> is designed for three-dimensional analysis of geotechnical structures for civil and mining applications. It may be applied for both rock and soil, RS<sub>3</sub> is a general-purpose finite element analysis program used for underground excavations, tunnel and support design, surface excavation, foundation design, embankments, consolidation, and groundwater seepage.

#### 6.1 Continuum model with joints using RS<sub>3</sub>

The goal was to reproduce the model explained in the chapter four, using the Finite Element model application in three-dimensions. However, in RS<sub>3</sub>, the joint networks feature is not implemented. Anyway, it was possible to model joints element by means of obtaining a geometry closer to the one previously analysed.

Moreover, it was chosen to study a limited portion of the cavern of 12 m depth, in this way it was also possible to compare it with the continuum three-dimensional model. The following general assertions were addressed when modelling the projects on RS<sub>3</sub>:

- Project settings:

This first step was very similar to the one of the three-dimensional continuum model. Perhaps, it was noticed the use of twenty stages: the first one representing the geostatic conditions in which an elastic criterion was adopted as means to initialize

the model, in the second one the cavern's excavation began. The sequence of the digging started from the portion of the cavern located to the left part of the crown. Then after the digging phases a final stage was realized.

- Geology:

The external boundary was the first step in the modeling of the project. It was decided to use an external box of 150x150 m, representing ten times the diameter of the underground structure.

Then the joint implementation was required. In order to do this, different planes were created, these planes represented the discontinuities. To these planes, the joint properties were applied as means to determine continuum model with joints. Moreover, the same geometrical strips of the 3D continuum model were developed, but with  $GSI=100$   $m_b=m_i$ ,  $s=1$  and  $\alpha=0.5$  as done in the chapter 4, where the two-dimensional models with joints are implemented.

An important tool in this software is the Divide All, an essential function to model creation. Similarly, to subdividing external boundaries to create material regions in enclosed polylines in the two-dimensional software, Divide All splits three-dimensional external volume to smaller pieces, for material, support or loading assignments.

In figure 6.1 the model geology and geometry are reported, in yellow ( $Q=0.2$ ) and black ( $Q=0.7$ ) are highlighted the joints plane. The joints present the properties reported in table 4.1 and 4.3.

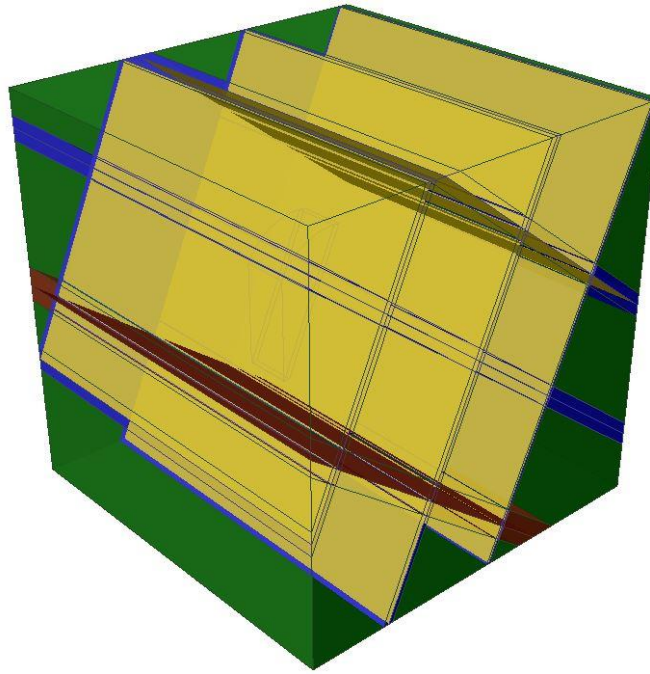


*Figure 6.1: Continuum model with joints 3D geometry*

- Cavern design:

The same procedure of the chapter 5 was pursued. Within, the RS<sub>3</sub> software, it was possible to use the tunnel/cavern design in order to implement the shape, the dimension, the construction sequence, and the supports of the excavation. Therefore, the cavern geometry was reproduced, as for the two-dimensional problem, with an overall height of the cavern of 32 m and a base of 30 m. Then, the cavern was divided in six zones, as in the 2D model for the excavation sequence. The chosen depth of the structure was of 12 m, just a portion of the cavern, in this way it was possible to understand the behavior during the excavation of the construction and the surrounding rock mass.

In figure 6.2 it is shown the cavern geometry in geostatic conditions at the first stage. Differently from the figure 5.2 in which regions of weathered granite were present, in this model joint planes in the blue and red strips were implemented.

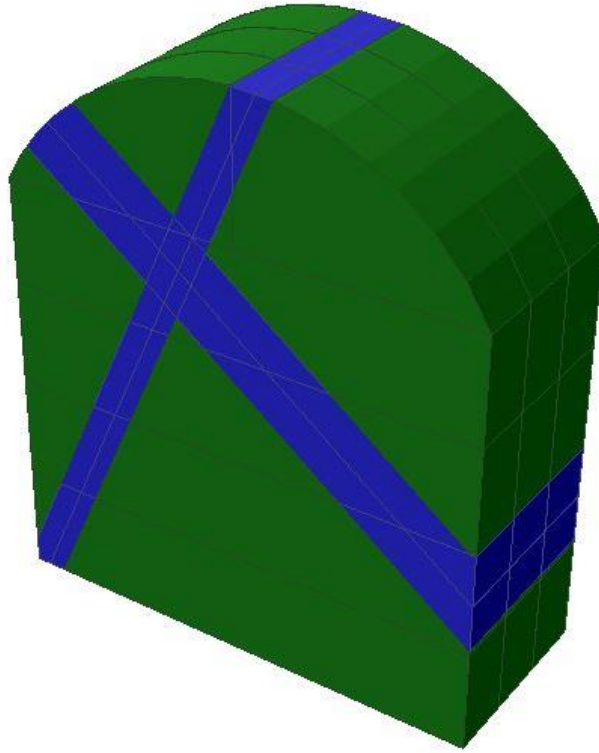


*Figure 6.2: Cavern geometry in geostatic condition*

Furthermore, for a depth of 12 m, three blasts of 4 m were designed. Therefore, in general, 20 stages were used, where the first one was meant for the initialization in geostatic condition setting elastic properties as means to avoid disturbances to the model. Then for every region three stages were required, 18 stages for the excavations, and the final stage for the final condition with all the volume excavated. The excavation started at the crown, in the left portion, then after all the identified region has been excavated, it was possible to pass to the right-crown area, and subsequently down with the excavation of the 4 wall-regions.

Simultaneously to the excavation of a portion of the cavern, the support system was implemented. After the removal of an area in the following stage the same area was stabilized with a systematic pattern of bolts. The support system presents the same properties reported in table 3.5 and 3.6.

In the figure 6.3 it is shown the third stage of the model where the first region was excavated and supported, and the second region excavated. Then, in figure 5.4 all the crown is excavated and supported, and the first wall regions excavated.

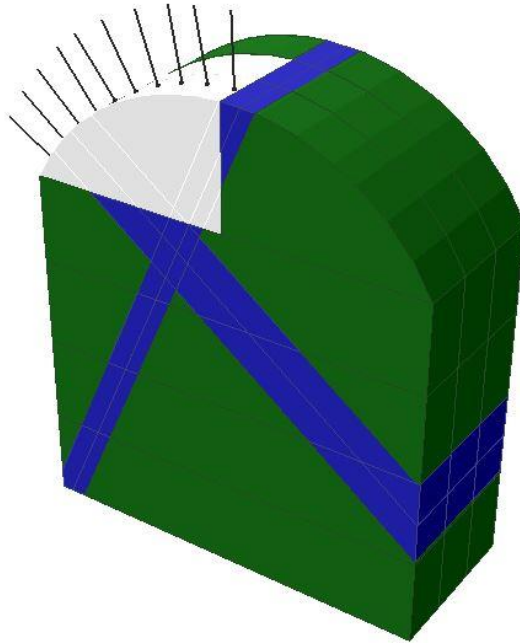


*Figure 6.3: Third stage of cavern's excavation*

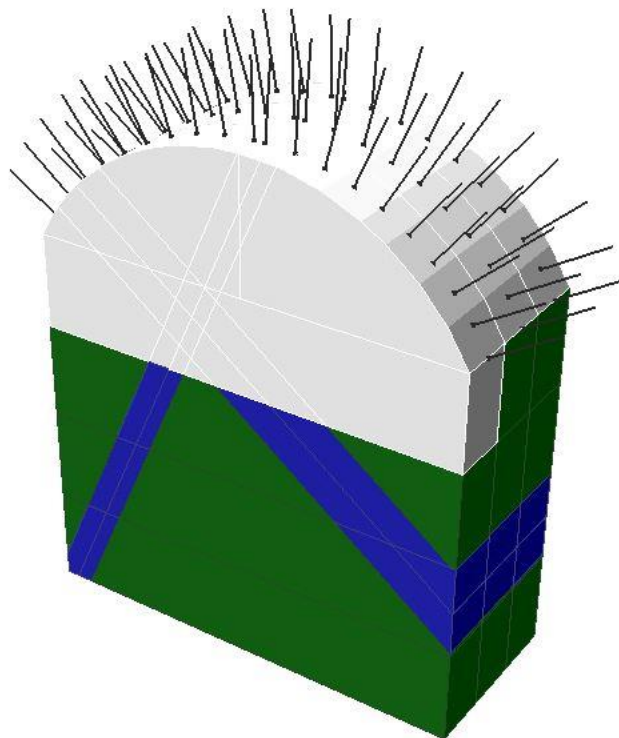


*Figure 6.4: Eighth stage of cavern's excavation*

Furthermore, in figure 6.5 the final configuration of the excavated and supported cavern is reported.

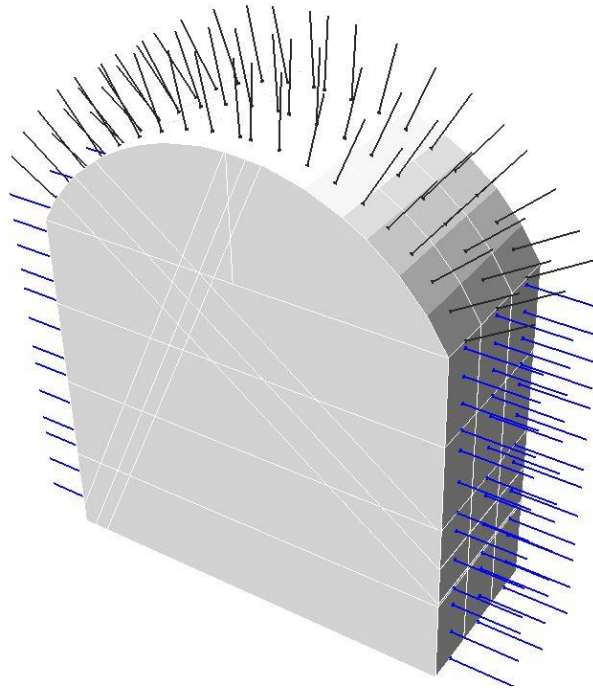


*Figure 6.5: Final stage of cavern's excavation*

- Loading:

Due to fact that the project deals with a deep excavation, constant field stress conditions were applied using the relations described in section 3.1.1, for the three-dimensional simulations the plane strain conditions were not considered, an isotropic  $k_0$  was assumed so the horizontal tension was assumed equal to the longitudinal one ( $\sigma_2 = \sigma_3$ ).

- Restraints:

For what concerned the current model, the underground auto restrain were used. This option is a shortcut for automatically applying default restraint boundary conditions on the external boundary for underground models. The model restrained is shown in figure 5.6.

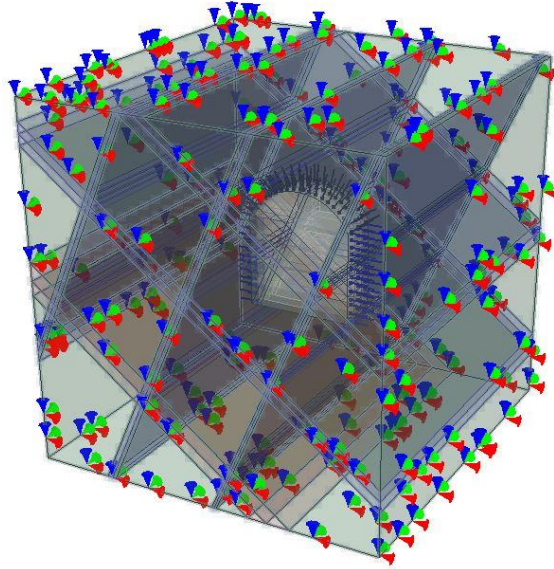


*Figure 6.6: 3D continuum model with joints restraints*

- Mesh:

For the realization of the mesh, 4 noded tetrahedral graded elements mesh is adopted. In figure 6.7 the meshed model is proposed.

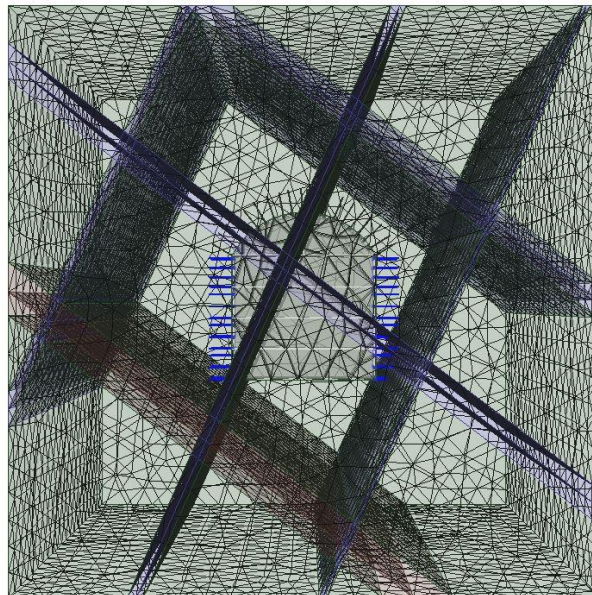


*Figure 6.7: 3D continuum model with joints mesh*

Finally, in figure 6.8 the complete three-dimensional model with the external boundary, the joints planes, the cavern's excavations, and supports are presented.

The results of this three-dimensional continuum model with joints are then discussed in the chapter 7.

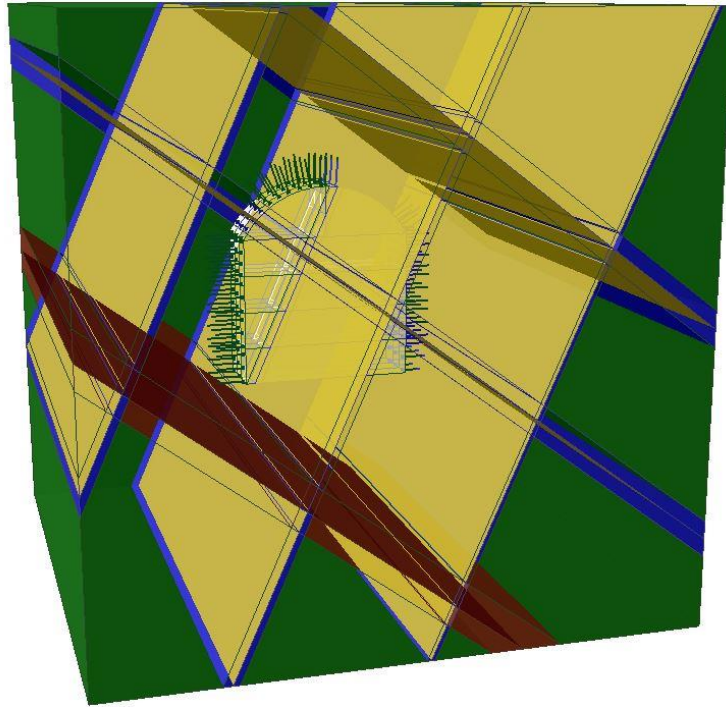


*Figure 6.8: 3D continuum model with joints*

## Chapter 7

### 7. RESULTS AND CONCLUSIONS

In the final chapter, the discussion of the results obtained by numerical analyses and some conclusions of the different proposed models realised with the software RS<sub>2</sub> and RS<sub>3</sub> are reported. In the first part a comparison between the two-dimensional models was proposed. Then this comparison was also extended to the three-dimensional models.

#### 7.1 *Two-dimensional model's results*

The comparison between the different models for the stability's analysis of the cavern was developed considering the major principal stress  $\sigma_1$ , the minor principal stress  $\sigma_3$ , the total displacement, and the strength factor with ubiquitous joints. These results were collected using a query in the interpret dialog of RS<sub>2</sub> around the boundary of the excavated cavern. A correlation between all the model was established, in order to understand which one of the continuous models with joints reported in the chapter 4 presented a more similar behaviour respect to the continuum model shown in the chapter 3, that was taken as the reference model. This, mainly due to fact that the continuum model was the object of the internship of the author and was validated by different analysis and field data investigations. In figures 7.1, 7.2, 7.3 and 7.4 the principal results are reported.

Regarding the Ubiquitous Joints, in general, these allow to plot strength factor contours which account for jointing in the rock mass. The term "ubiquitous" means that the joints may occur at any point in the rock mass, they do not have a fixed

## RESULTS AND CONCLUSIONS

location. The strength factor is calculated by dividing the rock strength, by the induced stress at every point in the mesh.

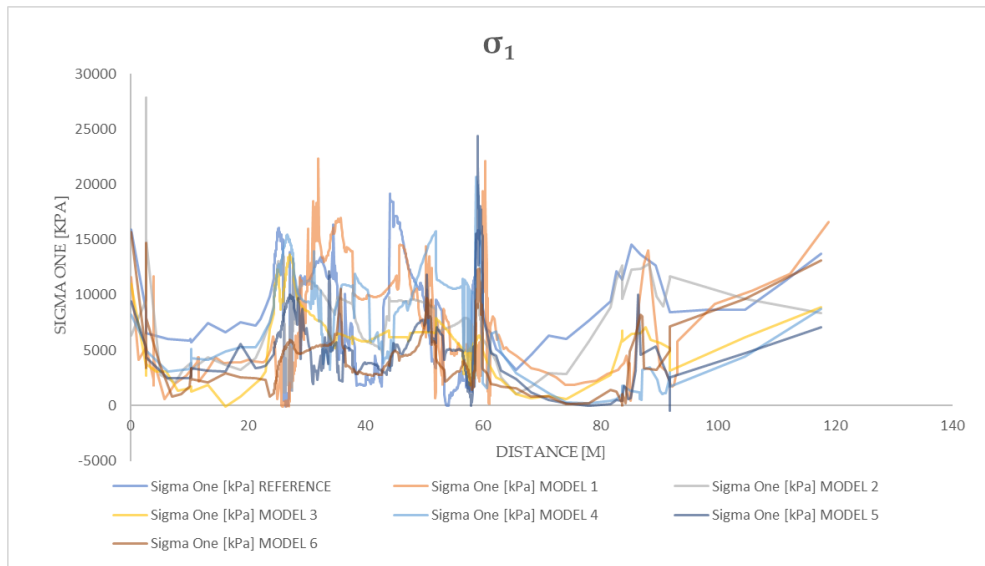


*Figure 7.1:  $\sigma_1$  excavation boundaries*

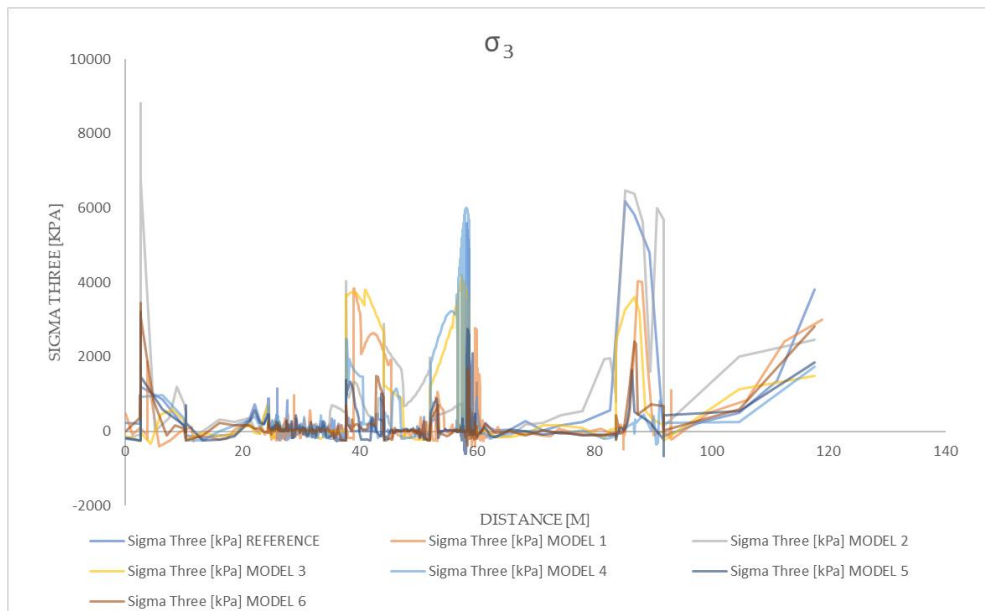


*Figure 7.2:  $\sigma_3$  excavation boundaries*

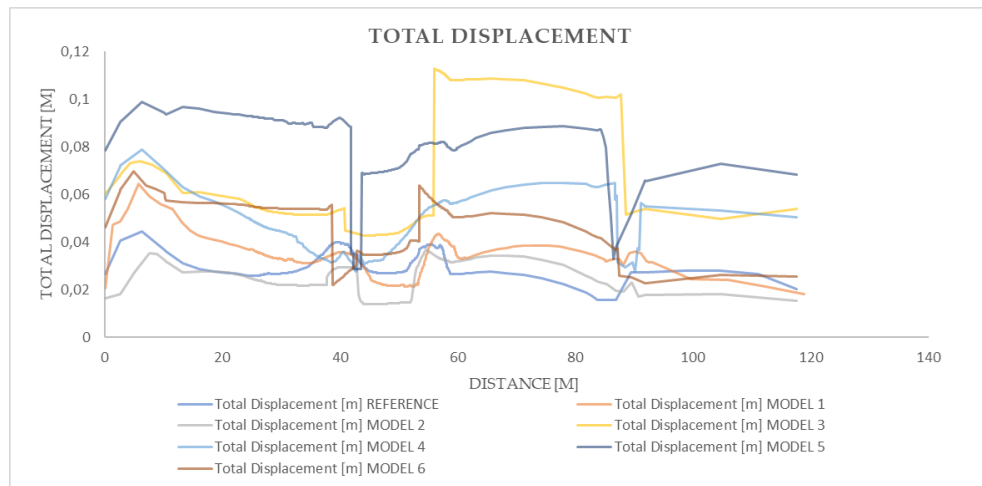


*Figure 7.3: Total displacement excavation boundaries*

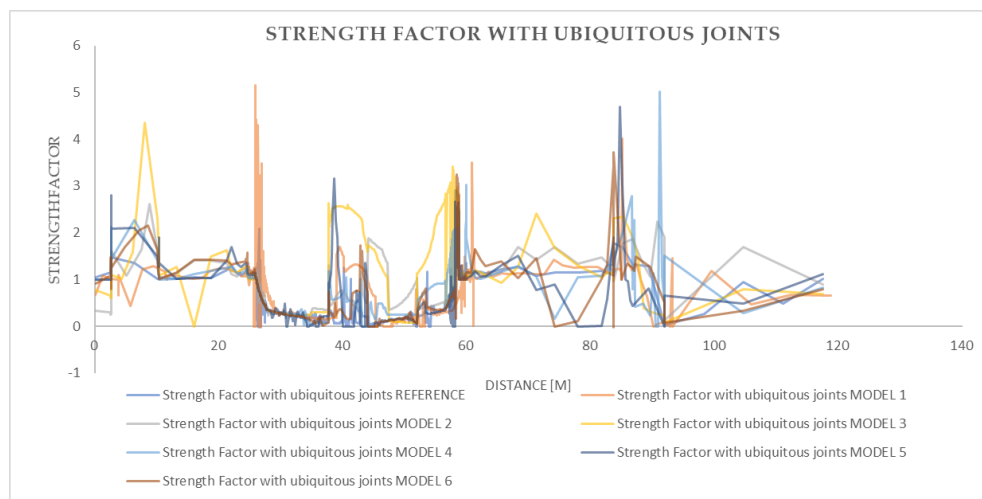


*Figure 7.4: Strength factor with ubiquitous joints excavation boundaries*

Furthermore, the yielded zones around the cavern were investigated. Consequently, the yielded elements contouring was used to analyze the degree of yielding in the rock mass around the excavation. In the RS<sub>2</sub> software the yielded zones were remarked using different colors, where red represents 100% yielding and blue 0% of yielding. In the following part, from figure 7.5 to figure 7.11, the yielded elements representations' are proposed around the excavation for each model.

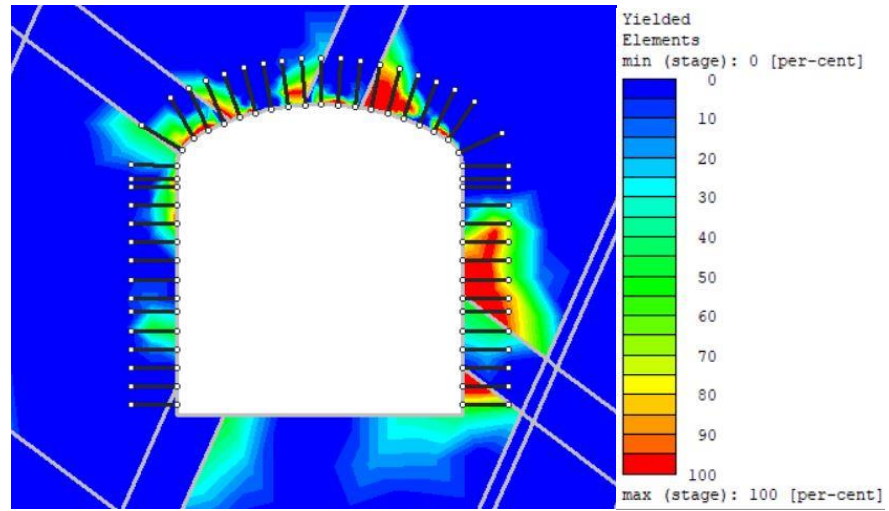


*Figure 7.5: Elements yielded Continuum model*

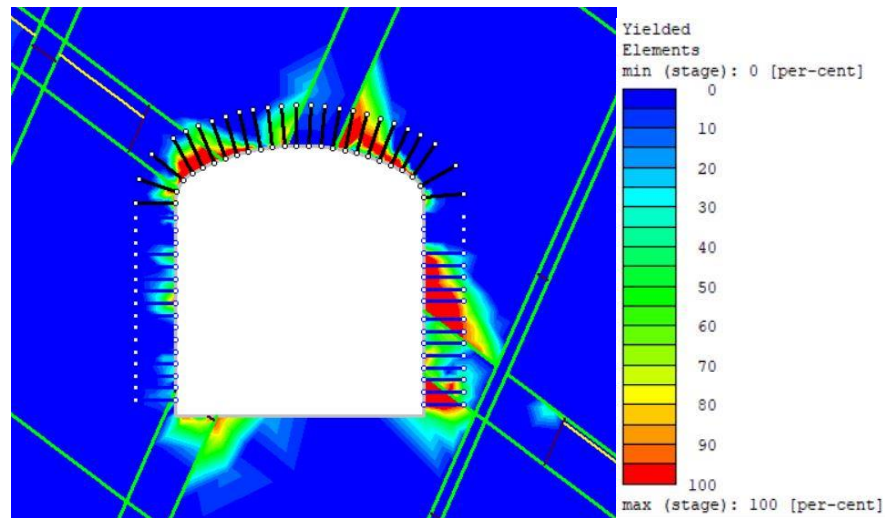


*Figure 7.6: Elements yielded Model 1 Cross jointed*

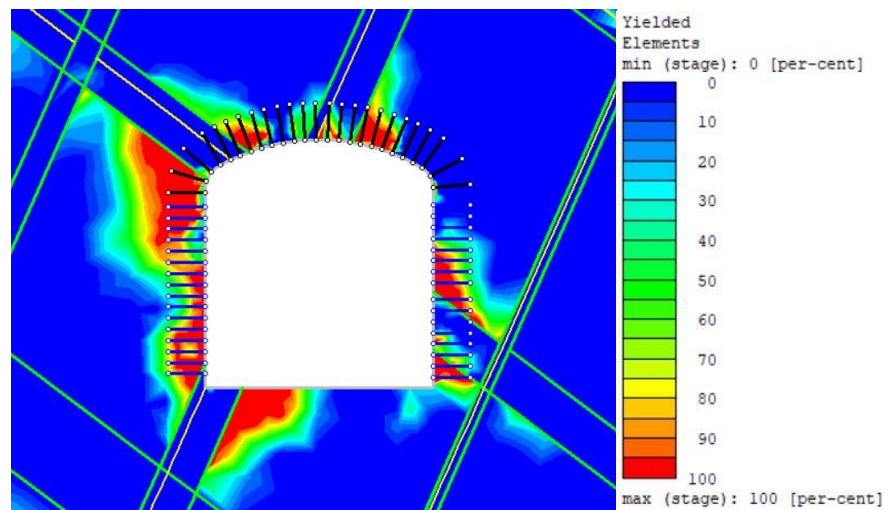


*Figure 7.7: Elements yielded Model 2 Parallel Statistical*

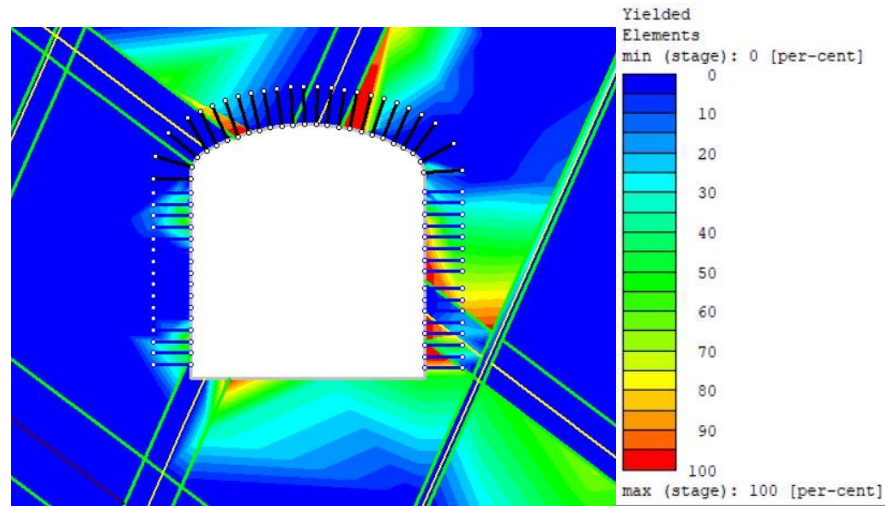


*Figure 7.8: Elements yielded Model 3 Parallel Deterministic*

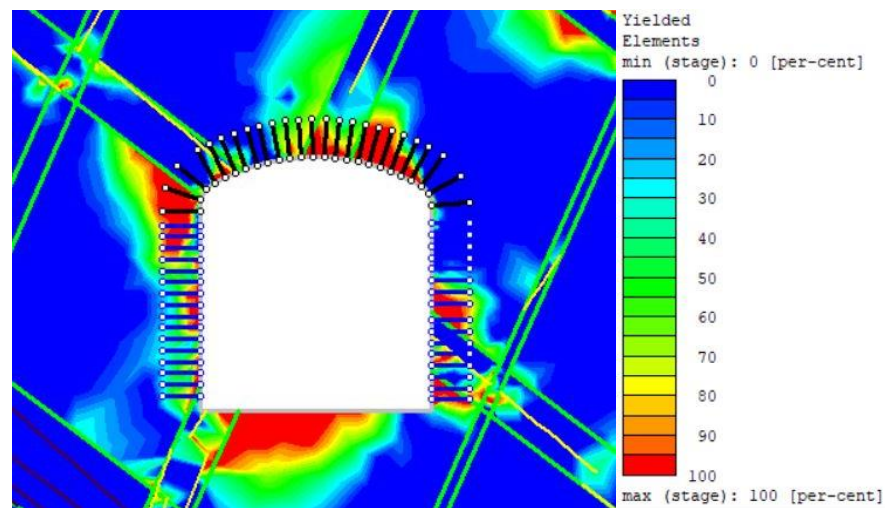


*Figure 7.9: Elements yielded Model 4 Veneziano*

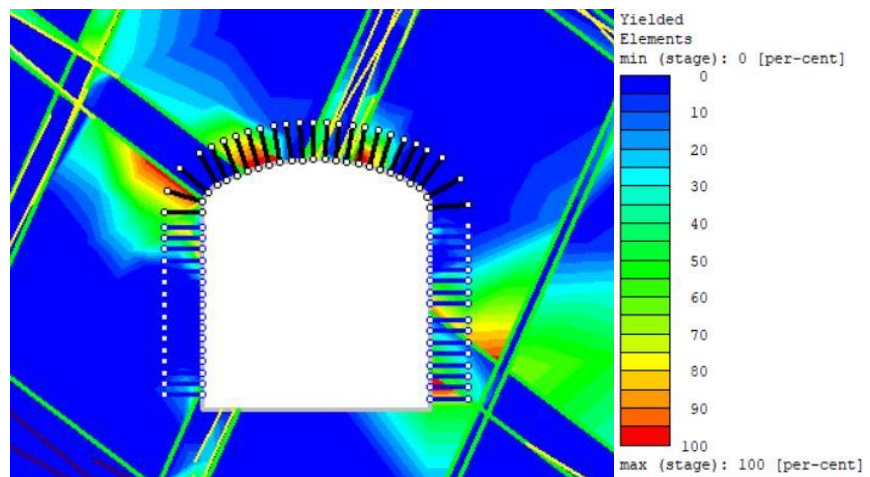


*Figure 7.10: Elements yielded Model 5 Baecher*

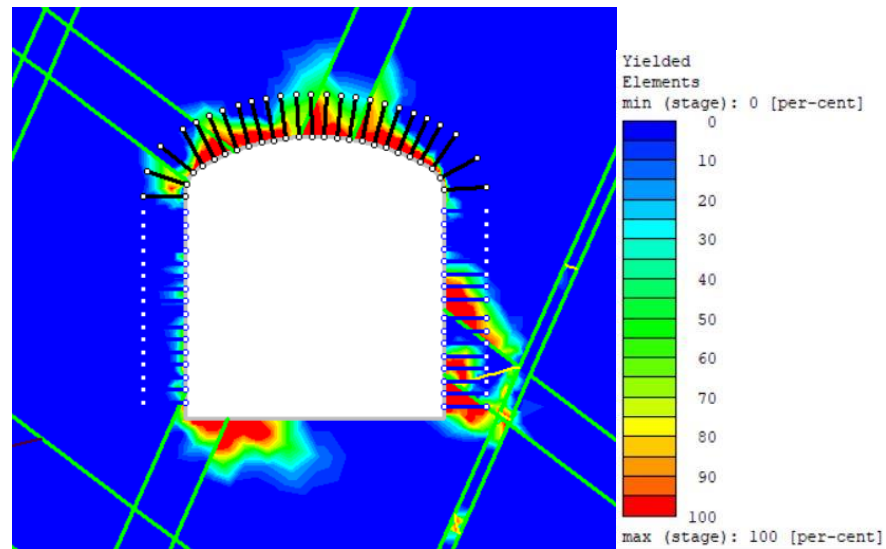


*Figure 7.11: Elements yielded Model 6 Voronoi*

From the results' analysis, it was pointed out that the continuum model with joints, that presents the more similar behaviour, compared to the continuum model set as Reference one, resulted the model 1 Cross Jointed network.

With this model it was experienced a closer attitude for what concern the principal outputs. This similarity may be due to several reasons described in the following.

The equivalent continuum model was developed from the results obtained based on surveys results. For this reason, it was taken as reference model and considered the target of the implementations. Thus, it can be considered as the model that better represents the real in-situ conditions.

Then, for what concern the model 1 Cross Jointed network, the fundamental assumption is that in this model, joints are defined in three mutually perpendicular sets of parallel joints. Therefore, rock blocks are intended as rectangular prisms. Joints may be either unbounded or bounded, although bounded joints are restricted to quadrilateral shapes. It is known that in the granite at the site of interest, the cracks tend to break the rock into roughly cube-shaped blocks, thus this natural shape is quite well represented by the Cross Jointed joint network model.

## RESULTS AND CONCLUSIONS

This increased the validity of the reference model, because representing the jointed rock mass in a different way (using joint networks) it was derived a similar result, consistently with the natural conditions. Therefore, it is possible to conclude that using an equivalent continuum with a good geotechnical characterisation is possible to obtain a fair approximation of the underground problem under investigation.

In the figure 7.12, 7.13, 7.14, and 7.15 the main results are compared between the Reference Model and the Model 1 Cross Jointed.

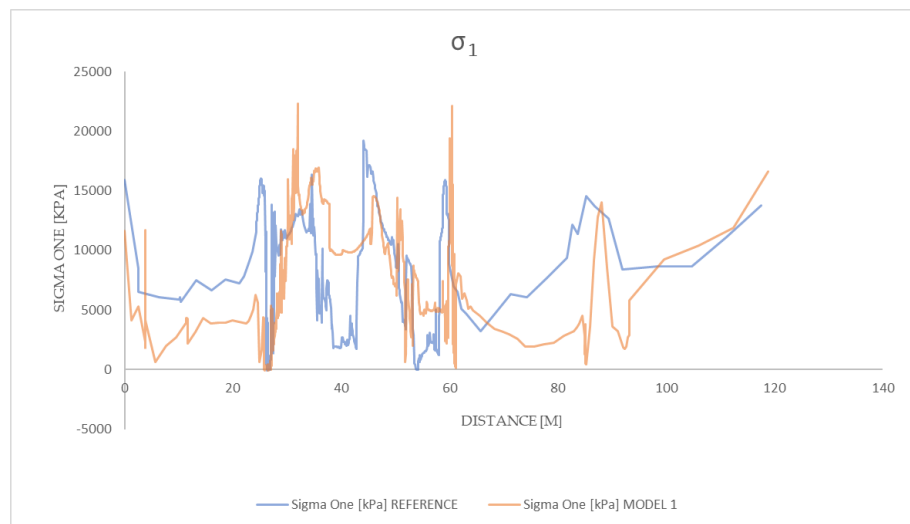


*Figure 7.12: Comparison Continuum Model and Model 1 Cross Jointed-  $\sigma_1$*

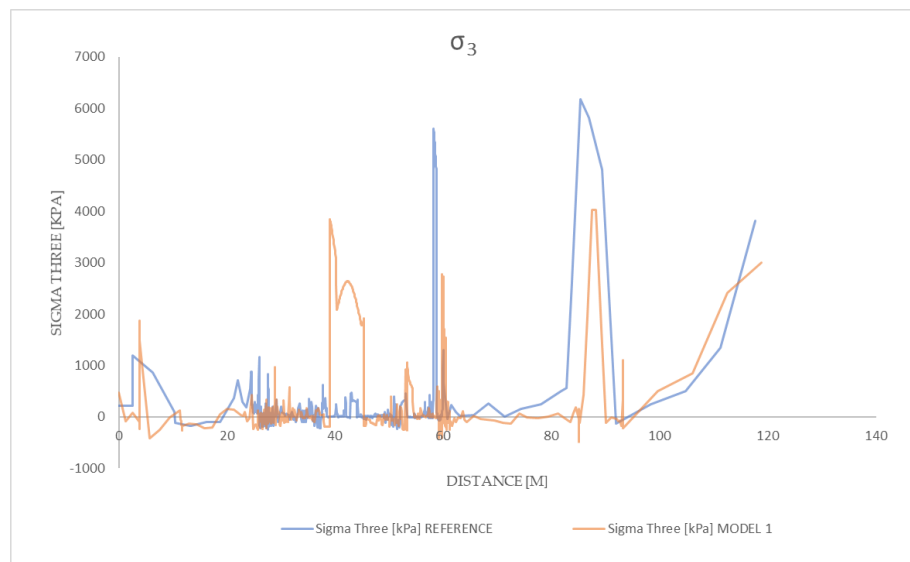


*Figure 7.13: Comparison Continuum Model and Model 1 Cross Jointed-Sigma  $\sigma_3$*

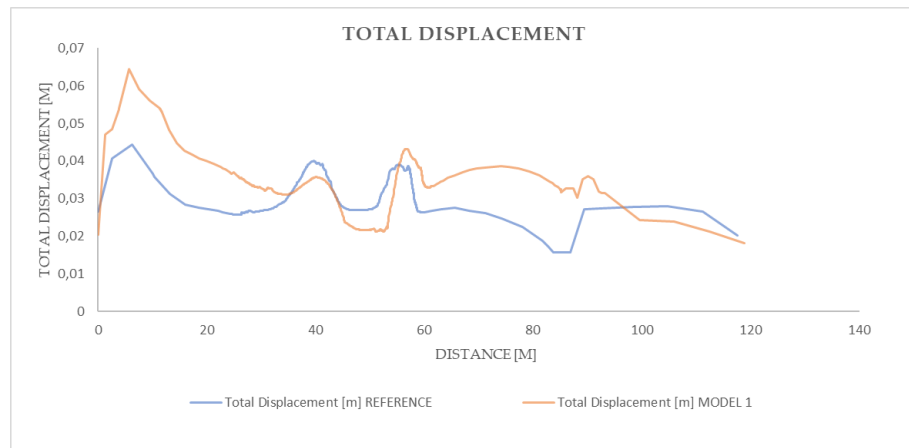


*Figure 7.14: Comparison Continuum Model and Model 1 Cross Jointed-Total displacement*

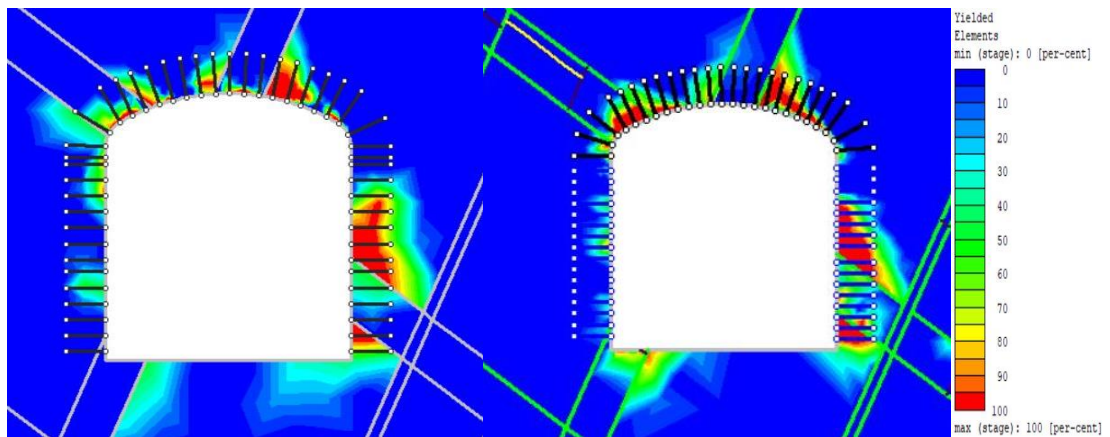


*Figure 7.15: Comparison Continuum Model and Model 1 Cross Jointed-Yielded elements*

A similar trend was shown for all the principal outputs such as  $\sigma_1$ ,  $\sigma_3$ , total displacement and yielded zones.

Regarding  $\sigma_1$  results reported in figure 7.12, four peaks of about 15000 kPa were highlighted for both the models. Four joints intersect the cavern, the above-mentioned summits are situated in correspondence to the points in which the joints cross the excavation boundaries. In general, the outputs show very similar trend, however few differences are encountered in the shapes. In particular, for the Cross Jointed model the increase of  $\sigma_1$  is more sudden respect to the equivalent continuum model, this because in the Cross Jointed model the weakness of the joints is

concentrated in a unique set of lines inside a region, while for the equivalent continuum in a strip of weaker material.

Then, concerning the  $\sigma_3$  results reported in figure 7.13, similar considerations respect to  $\sigma_1$  outcomes can be described. Thus, four peaks of about 4000-5000 kPa are highlighted, a general similar trend is pointed out between the equivalent continuum model and the Cross Jointed model.

For what concern the total displacement presented in figure 7.14 a comparable trend is shown. Even in this case four different peaks of about 4 cm are obtained. A maximum displacement of 6 cm is experienced in the Cross Jointed model in correspondence of a zone of weakness. This may be caused by the presence of a joint line that increase the movement of the cavern boundary; however, it is presented the same tendency of the equivalent continuum displacements.

Moreover, relating to the yielded elements around the excavation described in figure 7.15 it is possible to say that a comparable trend is highlighted between the two models. However, for the equivalent continuum model is experienced a more scattered behaviour around the weathered strips of jointed granite, while a more concentrated attitude is found for the Cross Jointed model. The present may be determined by the fact that the equivalent continuum model is composed by regions of weakness and so a more dispersed yielded zones are experienced, while in the Cross Jointed the yielded zones are more concentrated around the joint system.

It is also reported, for completeness, the axial force in the fully bonded bolts for what concern the continuum model and the model 1 Cross Jointed. The bolt capacity, 282 kN, is represented by the straight grey line in figure 7.16 and by the straight blue line in the figure 7.17. All the other lines are the axial force for each bolt. The maximum capacity is approached but never reached, this means that the proposed reinforcement system is capable to provide in an efficient manner the cavern's stability. The trend is similar for the two models even if for the jointed model

## RESULTS AND CONCLUSIONS

the values of axial force are generally higher, indeed due to the presence of the discontinuities.

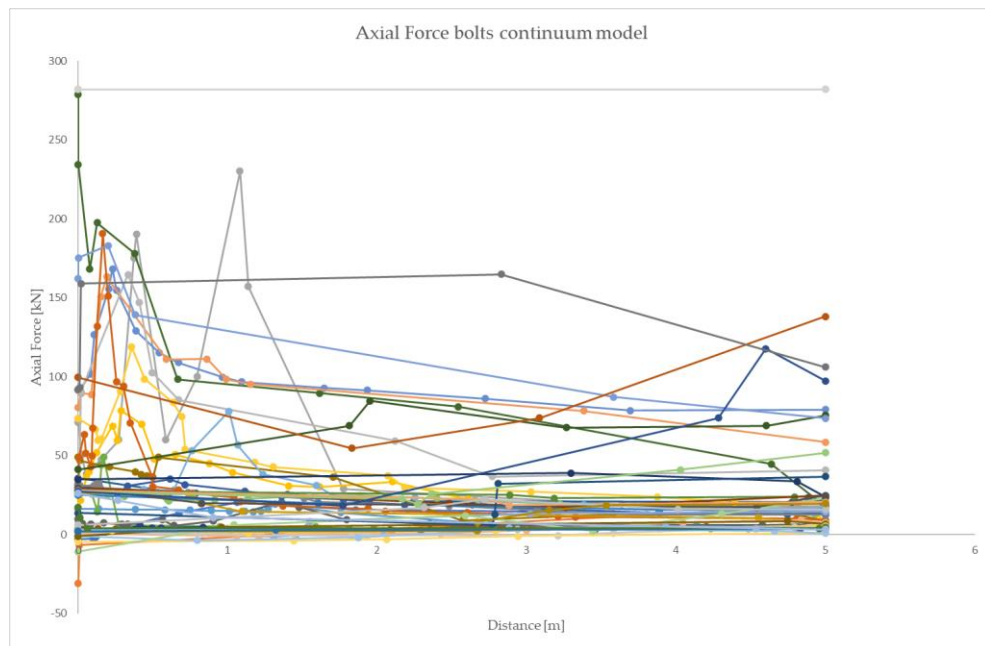


*Figure 7.16: Axial force bolts equivalent continuum*

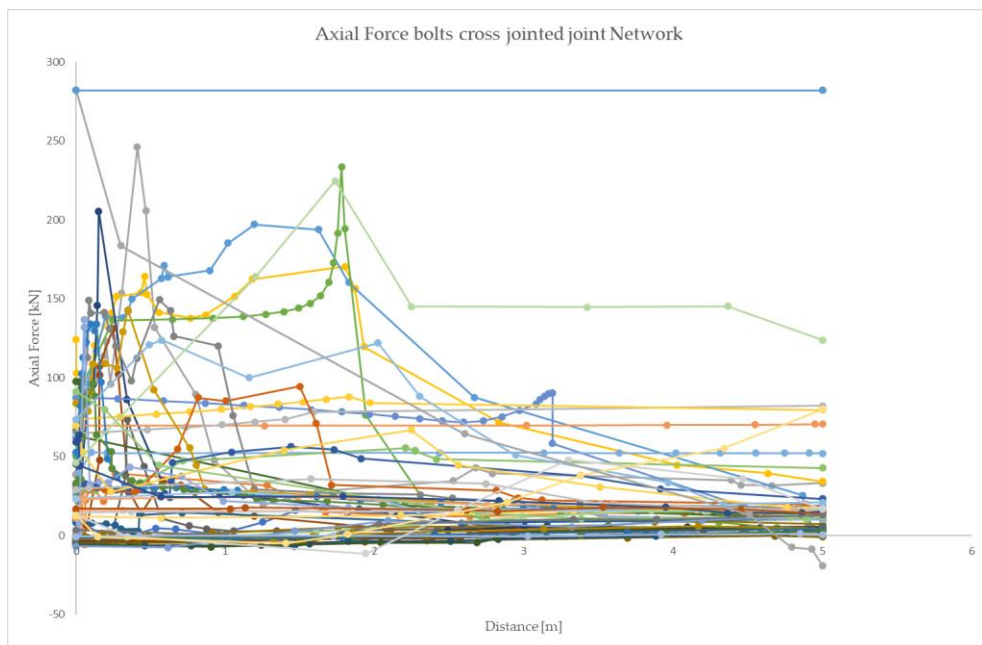


*Figure 7.17: Axial force bolts model 1 Cross Jointed*

The results show that the weathered strips with their orientations provide a discontinuum behaviour to the rock mass. Thus, the modelling of the rock mass as a homogeneous equivalent continuum is not representative of the real attitude of the

mass of rock. In fact, in the present dissertation the equivalent continuum model was implemented with different stripes of materials in a non-homogenous manner.

In the following part a brief discussion about the results of the others continuum models with joints was carried out.

The model 2 Parallel Statistical and model 3 Parallel Deterministic derive from the family of the orthogonal model, but they are slightly different respect to the Cross Jointed model. As seen, it was not possible to implement the quadrilateral shapes for the bounded joints. This fact determines differences in the results. Thus, concerning the tension outputs  $\sigma_1$ ,  $\sigma_3$  and the total displacement distant results are obtained mainly in the zones of the jointed rock mass. Moreover, regarding yielded zones they are very divergent in the joint's region compared to the one of cross jointed model and continuum model. Therefore, primarily for geometrical reasons the model 2 and the model 3 are not effective in the representation of the problem under investigation.

Then, with model 4 Veneziano joint network the application of the site of interest is difficult for the presence of distinct rock blocks, which would not be possible in a Veneziano model with not persistent joint planes, that is joint planes with less than 100% of the polygons formed by the Poisson line process marked as open joints. Therefore, this was the reason why this model was not so efficient in the case under study. Thus, for what concern the tension components  $\sigma_1$ ,  $\sigma_3$  the trend of the equivalent continuum model presents some differences compared to the Veneziano joint model, such as peaks in which the equivalent model presents 6000 kPa and the Veneziano model 200 kPa (regarding  $\sigma_3$ ). Moreover, concerning the total displacement, the Veneziano model shows higher value, as well as the yielded zones. Thus, the jointed model's results are more conservative and pessimistic compared to the model 1 and the equivalent continuum reference model.

Considering model 5 with Baecher joints network, due to fact that in this model joints terminate without respect to the joint intersection, it is not possible to

form rock block, so the Baecher model is not appropriate for joint systems in which blocks are formed at the scale of joints. This may explain the fact that with the Model 5 the results were quite different compared to the continuum reference model and the Cross Jointed joint network model. Thus, concerning  $\sigma_1$  and  $\sigma_3$  a similar trend but with lower values is obtained, while for the total displacement higher values are derived compared to the equivalent continuum model. Moreover, the yielded zones result very different in correspondence of the joints for the above-mentioned geometrical reasons. Therefore, even in this case the jointed model's results are more conservative and pessimistic compared to the model 1 and the equivalent continuum reference model.

The model 6 Voronoi, is a mosaic tessellation model, this type of model resulting appropriate for joint systems which are the result of a process of block formation in a rock mass. An example of such joint system is jointing in columnar basalts in which jointing may be formed on the faces of columns formed during the cooling of magma. Thus, the joint system of columnar basalt is very similar to that of two dimensional Voronoi tessellation. Therefore, this is the reason why this model did not follow the reference continuum model, and so was not considered for the final comparison. In fact, it shows different results for all principal outputs.

## **7.2 Three-dimensional model's results**

The results of the three-dimensional models were analysed and compared with the one derived from the two-dimensional models.

Firstly, regarding the Continuum analysis similar results were obtained comparing the two and three-dimensional models at the end of the excavations.

In figure 7.18, 7.20, and 7.22 are reported the principal results for the three-dimensional model, in term of major principal stresses, minor principal stresses and

## RESULTS AND CONCLUSIONS

total displacement. Using the feature “show excavation contour” that allows to see the results indicated around the excavation.

Regarding the  $\sigma_1$  results, they were similar to the one obtained with the two-dimensional model. In figure 7.19, it is shown the comparison between data obtained from a query on the right boundary at the end of the excavation, for the two and three-dimensional models.

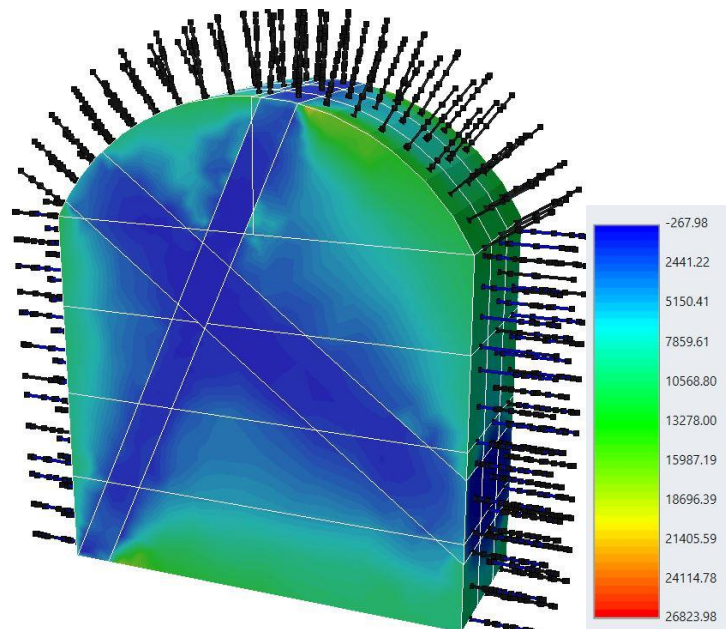


*Figure 7.18: 3D-Continuum model  $\sigma_1$  [kPa]*

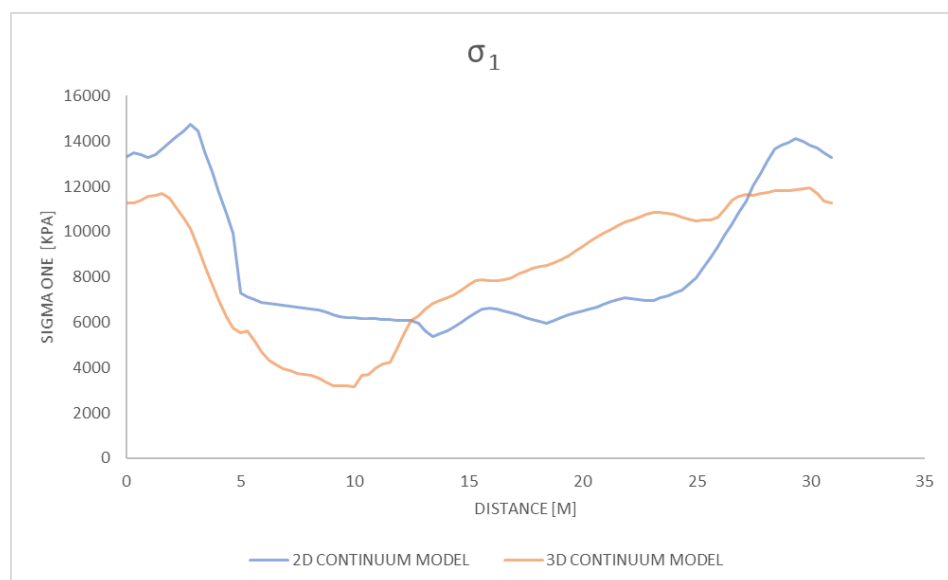


*Figure 7.19: Comparison 2D-3D Continuum model  $\sigma_1$  [kPa]*

Then, concerning the  $\sigma_3$  results, they were comparable with the one achieved with the two-dimensional model. Indeed, in figure 7.21, it is reported the comparison between data obtained from a query on the right boundary at the end of the excavation for the two and three-dimensional models.

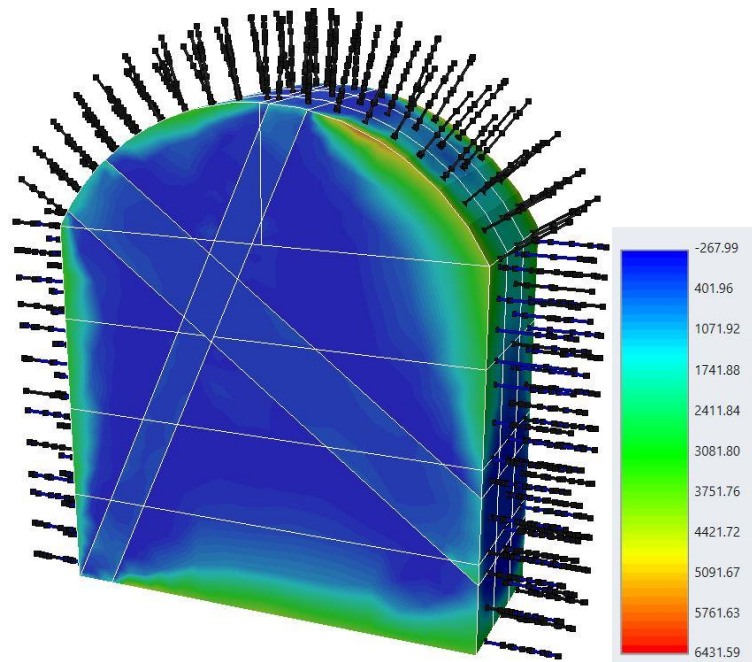


*Figure 7.20: 3D-Continuum model  $\sigma_3$ [kPa]*

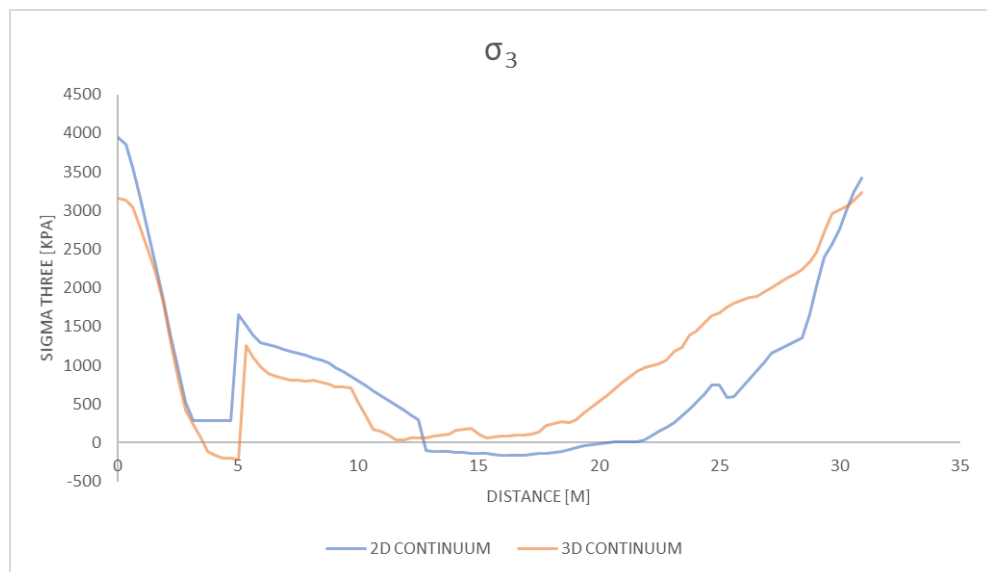


*Figure 7.21 Comparison 2D-3D Continuum model  $\sigma_3$ [kPa]*

Furthermore, regarding the total displacement results, they were close to the one derived with the two-dimensional model. In figure 7.23, it is reported the comparison between data obtained from a query on the right boundary at the end of the excavation for the two and three-dimensional models.

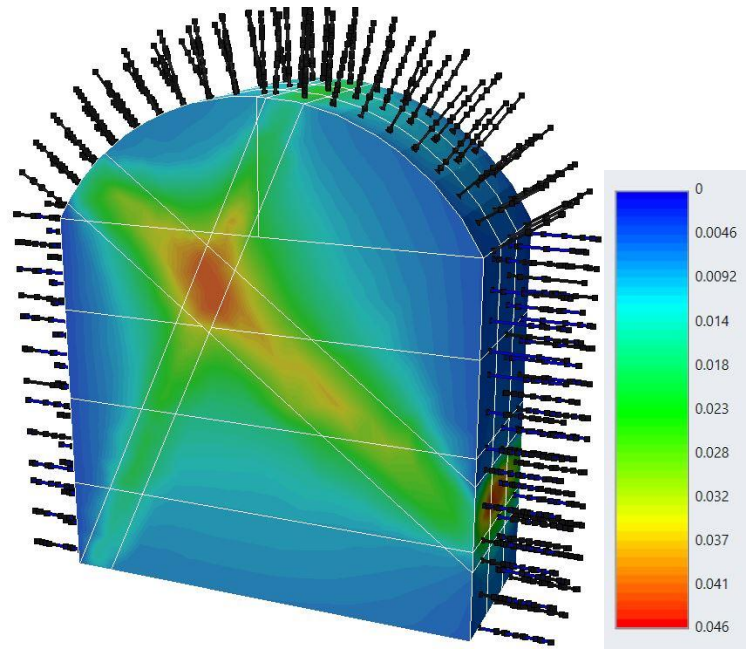


*Figure 7.22: 3D-Continuum model Total Displacement [m]*

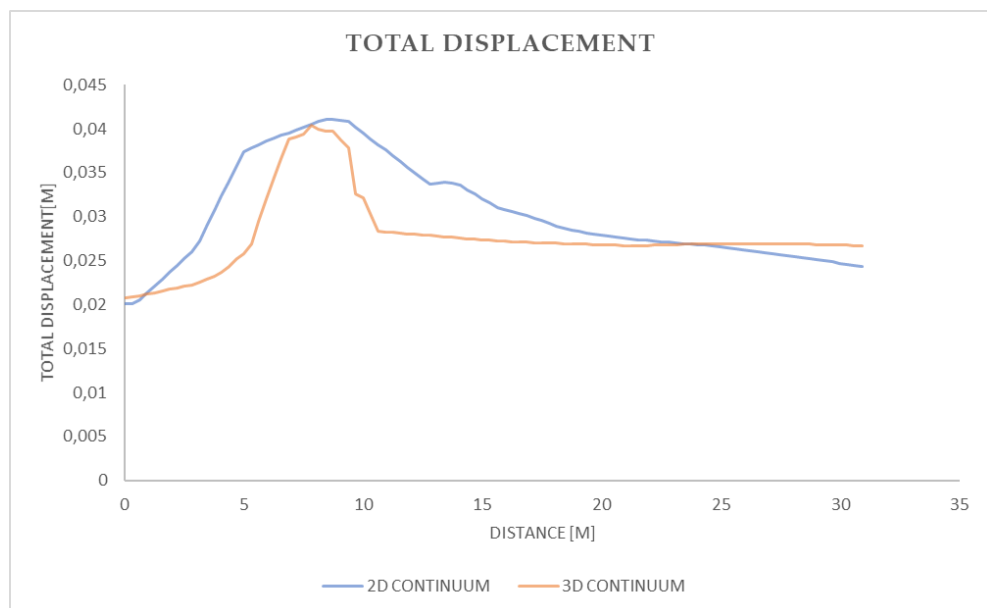


*Figure 7.23 Comparison 2D-3D Continuum model Total Displacement [m]*

Therefore, it was experienced a very similar trend for the two-dimensional and three-dimensional continuum models. This fact was not easy to assume because, although for both the models the same geometries, material properties and supports were assumed; in the three-dimensional model the confinement at the front of the excavation is automatically taken into account, while in the two-dimensional model this is considered following the assumption of plane strain conditions.

Instead, concerning the Continuum model with joints slightly different results were obtained comparing the two and three-dimensional models at the end of the excavations. This mainly due to fact that on RS<sub>3</sub> was not possible to implement joint networks. However joint planes, with the properties reported in table 4.1 and 4.3 could be implemented. Moreover, as for the two-dimensional continuum model with joints, the blue and red strips with GSI=100 that characterised the continuum model with joints were developed. Therefore, modelling joints with RS<sub>3</sub> is not effective as for RS<sub>2</sub> but still possible. By the way, in the following part, the obtained results were analysed and compared with the Cross Jointed model that, for the abovementioned reasons, was considered the reference model for the Continuum model with joints.

In figure 7.24, 7.26, and 7.28 the principal results for the three-dimensional models with joints are reported, in term of major principal stresses, minor principal stresses and total displacement.

Moreover, for what concern the  $\sigma_1$  results, they were slightly different to the one obtained with the two-dimensional Cross Jointed model, the 3D model shows a sort of plateau in the central part of the wall cavern that was not present in the Cross Jointed model. In figure 7.25, it is shown the comparison between data obtained from a query on the right boundary at the end of the excavation, for the two and three-dimensional continuum models with joints.

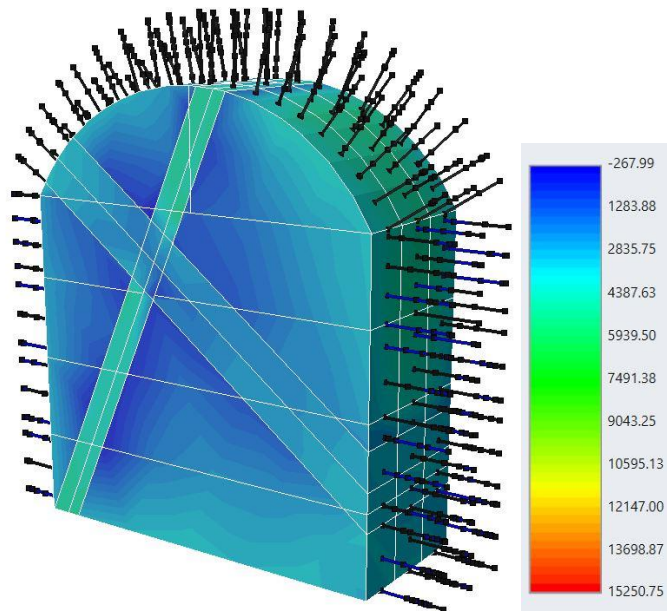


*Figure 7.24: 3D-Continuum model with joints  $\sigma_1$  [kPa]*

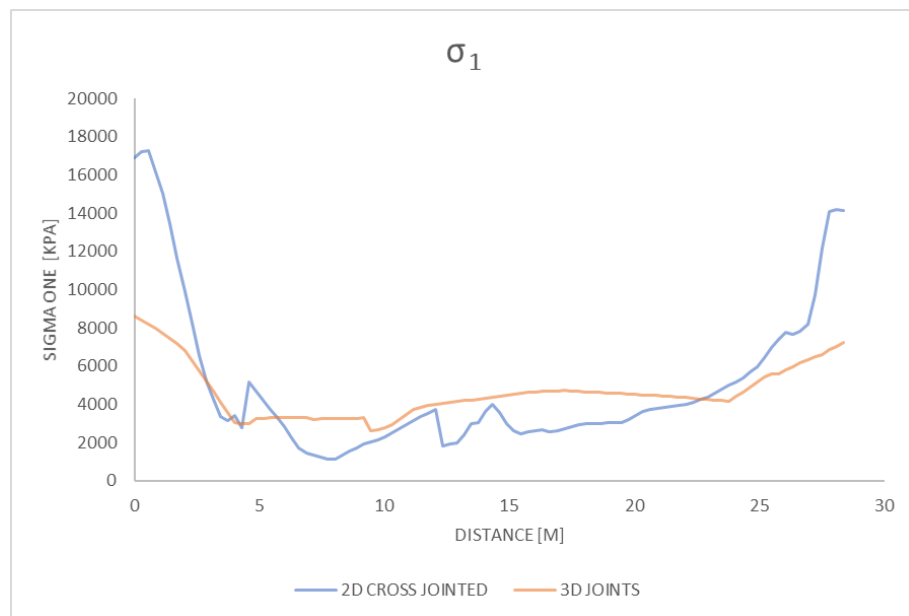


*Figure 7.25: Comparison 2D-3D Continuum model with joints  $\sigma_1$  [m]*

Then, concerning the  $\sigma_3$  results, they were more similar with the one got with the two-dimensional Cross Jointed model even if also in this case in the central part a sort of plateau with higher values is found. Indeed, in figure 7.27, it is reported the comparison between data obtained from a query on the right boundary at the end of the excavation for the two and three-dimensional models.

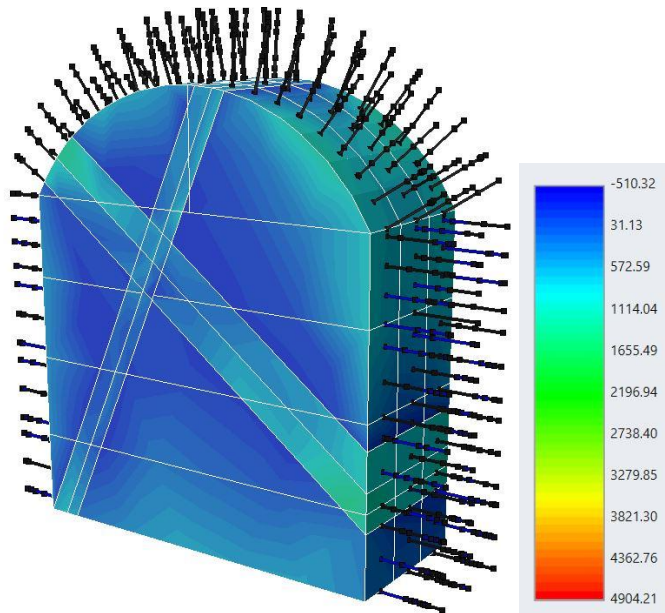


*Figure 7.26: 3D-Continuum model with joints  $\sigma_3$  [kPa]*

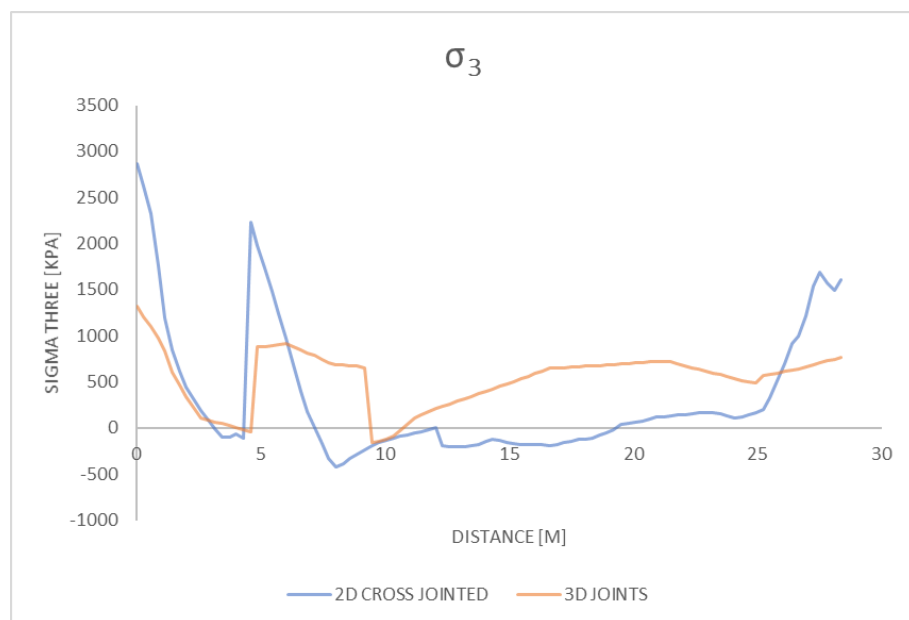


*Figure 7.27: Comparison 2D-3D Continuum model with joints  $\sigma_3$  [m]*

Furthermore, regarding the total displacement results, they show a similar trend to the one derived with the two-dimensional Cross Jointed model. However, with the Cross jointed model in correspondence to the joint a peak of 0.06 m is reached, while with the 3D model in the same point only 0.025 m. In figure 7.29, it is reported the comparison between data obtained from a query on the right boundary at the end of the excavation for the two and three-dimensional models.

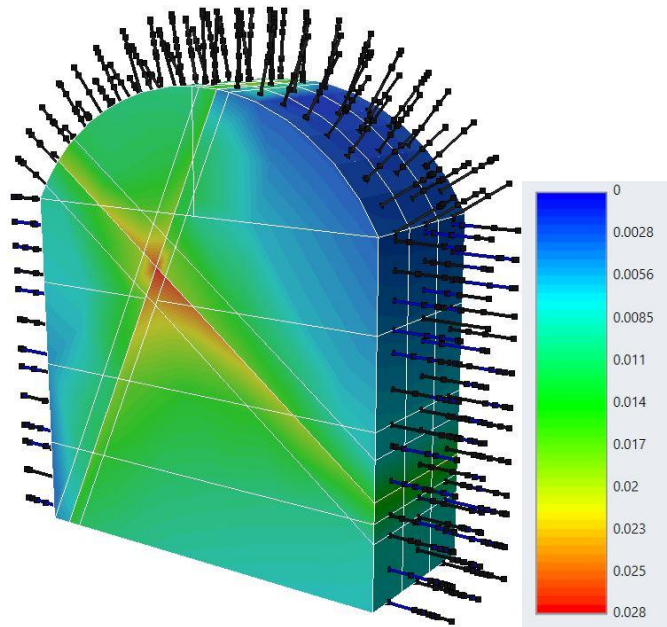


*Figure 7.28: 3D-Continuum model with joints Total displacements [m]*

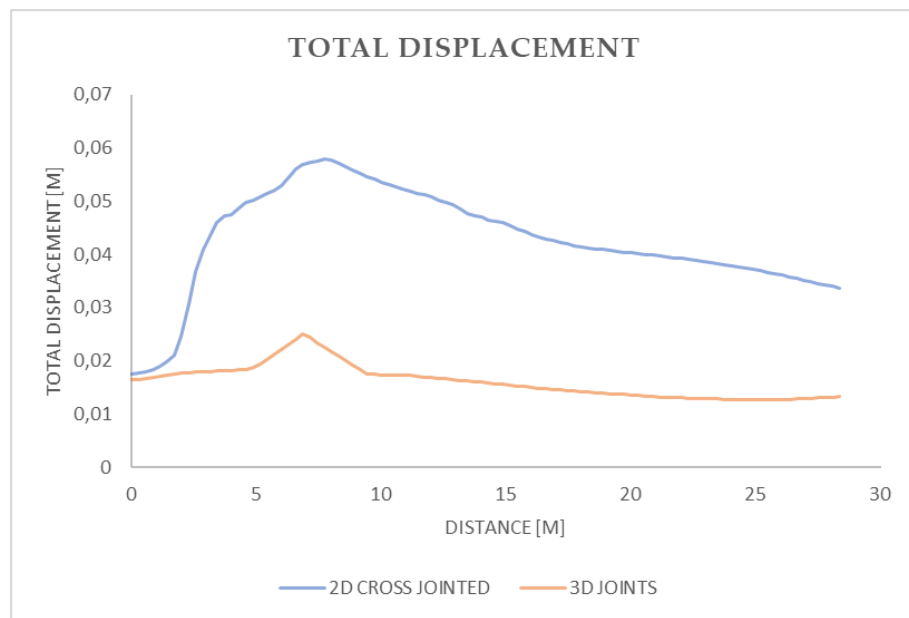


*Figure 7.29: Comparison 2D-3D Continuum model with joints Total displacement [m]*

Therefore, it was possible to conclude that this model was not able to represent in a efficient way the real conditions of the rock mass.

### **7.3 Conclusions**

In conclusion, the aim of the presented thesis was the stability analysis and modelling of an underground cavern in jointed granite using Finite Element Method, starting from a reference equivalent continuum model which takes into account the joint effects by reducing the strength and increasing the deformability of the materials.

Then, another model of jointed rock masses was implemented adopting special elements such as joint elements, also known as interface elements. In this way, it was possible to implement different continuum model with joints following the joint systems formulated by Dershowitz in 1985.

It was found that the Cross Jointed model was the one which provided results closer to that of the equivalent continuum model and better represented the real onsite conditions. Thus, in the Cross Jointed network, the fundamental assumption is that in this model, joints are defined in three mutually perpendicular sets of parallel joints.

Therefore, rock blocks are intended as rectangular prisms. Joints may be either unbounded or bounded, although bounded joints are restricted to quadrilateral shapes. It is known that in the granite at the site of interest, the cracks tend to break the rock into roughly cube-shaped blocks, thus this natural shape is well represented by the Cross Jointed joint network model represented in two dimensions by quadrilateral shapes.

This increased the validity of the reference model, because representing the jointed rock mass in a different way (using joint networks) it was derived a similar result, consistently with the natural conditions. Therefore, it is possible to conclude that using an equivalent continuum with a good geotechnical characterisation is

possible to obtain a fair approximation of the underground problem under investigation.

To do so, a careful geo-mechanical characterisation of the rock mass and of the joints was fundamental, allowing to implement a stabilisation system (systematic pattern of rock bolts) that provide efficiently the cavern stability.

Finally, the three-dimensional modelling was useful to implement in a correct way the sequences of the cavern construction and support. Moreover, the continuum three-dimensional model's results were very close to the one obtained with the two-dimensional model. However, this was not the same for the three-dimensional joint model in which the results were slightly different with respect to the Cross Jointed model.

The three-dimensional model with joints was not robust, thus modelling the joints using planes, that was the only option available in the RS<sub>3</sub> software, it was not possible to reproduce in an efficient way the current real conditions of quadrilateral shape blocks that are formed by the rock mass.

In the end, in the figures 7.30, 7.31 and 7.32 the final results for the two-dimensional and three-dimensional models, regarding the main outputs for the cavern's stability analysis, are collected in a unique solution to graphically highlight the above-mentioned conclusions.

## RESULTS AND CONCLUSIONS

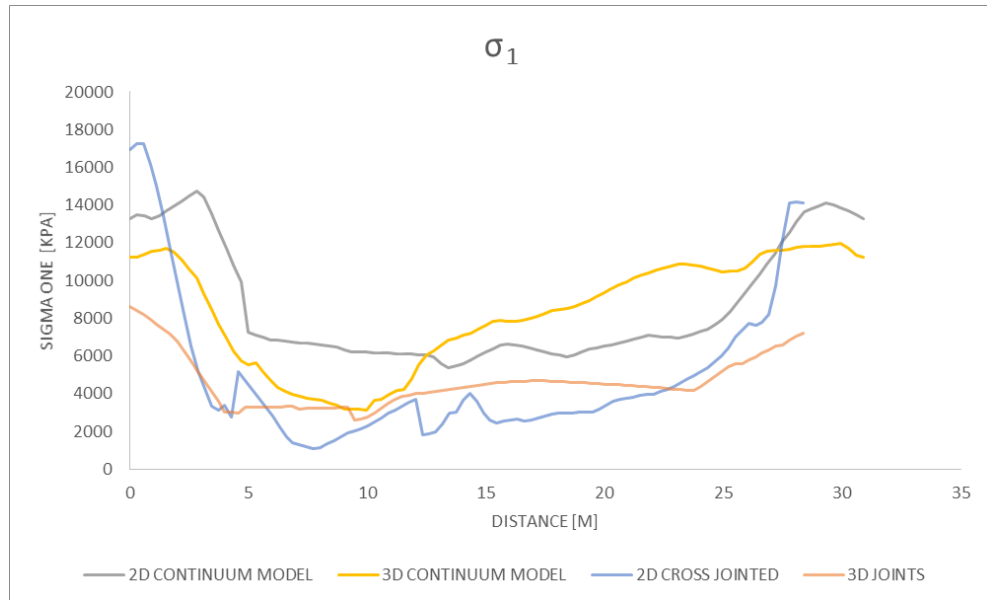


*Figure 7.30: Comparison 2D-3D models  $\sigma_1$  [m]*

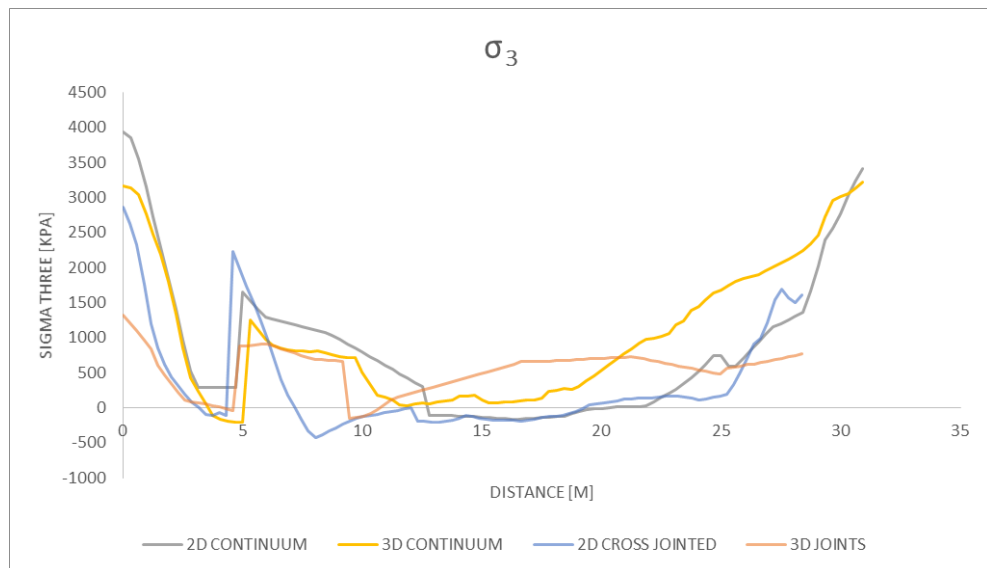


*Figure 7.31: Comparison 2D-3D models  $\sigma_3$  [m]*

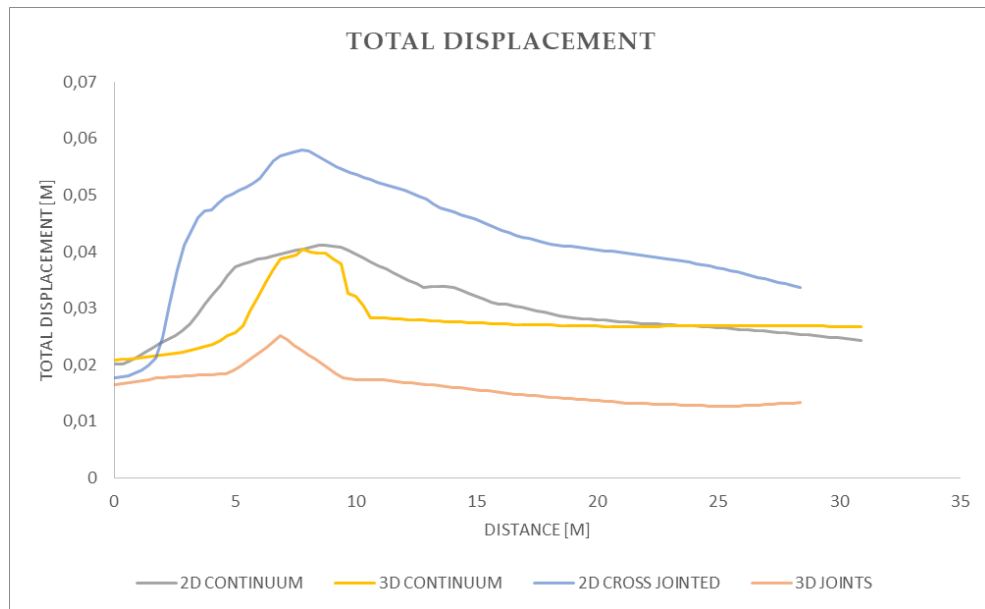


*Figure 7.32: Comparison 2D-3D models Total Displacement [m]*

## 7.4 Future research

A possible development of this master thesis could be modelling the cavern in weathered granite using Distinct Element Method, that represents the weathered domain as a set of blocks separated by fractured, it is more effective in modelling discontinuous jointed rock mass. In fact, software such as UDEC and 3DEC are two and three-dimensional programs that simulate the response of discontinuous media such as jointed rock mass. This could be interesting, mainly for what concerns the study of the discrete effect of the weathered rock mass and the relative movement and sliding between rock blocks.

By the way, in conclusion, this master thesis was very interesting and satisfying, because it was an occasion to study in the detail a topic not covered during the years of the master course.



## Chapter 8

### 8. REFERENCES

- Barton, N, Bandis, S and Bakhtar, K. 1985. Strength, Deformation and Conductivity Coupling of Rock Joints. *Int. J. Rock Mech. Min. Sci. & Geomech. Abstr.*, Vol 22, No 3, pp. 121-140.
- Barton, N.: "A model study of rock joint deformation", *IJRM*, #9 pp 579-602, (1972).
- Baecher, G.B., Lanney, N.A. and H.H. Einstein. 1978. Statistical Description of Rock Properties and Sampling. *Proceedings of the 18th U.S. Symposium on Rock Mechanics*, 5C1- 8.
- Dershowitz, W. 1985. *Rock Joint Systems*. Ph.D. Thesis, Massachusetts Institute of Technology, Cambridge, MA.
- *Guide to Cavern Engineering*, Geotechnical Engineering Office, Civil Engineering Department, 1992.
- Dershowitz, W.S., La Pointe, P.R. & T. Doe. 2000. Advances in discrete fracture network modeling. In *Proceedings of the US EPA/NGWA Fractured Rock Conference* - [info.ngwa.org](http://info.ngwa.org), 882-894.
- Beer, G. 1985. An isoparametric joint/interface element for finite element analysis. *International Journal for Numerical Methods in Engineering*, vol. 21, 585-600.
- Rocscience. 1999. A 2D finite element program for calculating stresses and estimating support around the underground excavations. *Geomechanics Software and Research*. Rocscience Inc., Toronto, Ontario, Canada.

## REFERENCES

---

- Goodman, R.E., Taylor, R.L. & T.L. Brekke. 1968. A model for the mechanics of jointed rock. *Journal of the Soil Mechanics and Foundations Division, ASCE*, 637-659.
- Manfredini, G., Martinetti, S. & R. Ribacchi. 1975. Inadequacy of limiting equilibrium methods for rock slopes design. In *Design Methods in Rock Mechanics, Proceedings of the 16th Symposium on Rock Mechanics, University of Minnesota, Minneapolis, American Society of Civil Engineers*, 35-43.
- Cundall, P., Voegele, M. & C. Fairhurst. 1975. Computerized design of rock slopes using interactive graphics for the input and output of geometrical data. In *Design Methods in Rock Mechanics, Proceedings of the 16th Symposium on Rock Mechanics*.
- Dershowitz, W.S., La Pointe, P.R. & T. Doe. 2000. Advances in discrete fracture network modeling. In *Proceedings of the US EPA/NGWA Fractured Rock Conference - info.ngwa.org*, 882-894.
- Lee, J.S., D. Veneziano & H.H Einstein, 1990. Hierarchical fracture trace mode. In *Proceedings of the 31<sup>st</sup> US Symposium on Rock Mechanics, Golden, Colorado*, 261-269.
- Hudson, J. & S.D. Priest. 1979. Discontinuities and rock mass geometry. *International Journal of Rock Mechanics, Mining Sciences & Geomechanics Abstracts*, vol. 16, 339-362
- Lee, J.S., D. Veneziano & H.H Einstein, 1990. Hierarchical fracture trace mode. In *Proceedings of the 31<sup>st</sup> US Symposium on Rock Mechanics, Golden, Colorado*, 261-269.
- Dershowitz, W., Lee, G., Geier, J. & La Pointe P. 1995. *FracMan - Interactive Discrete Feature Data Analysis, Geometric Modelling and Exploration Simulation*). User documentation. Seattle, Golder Associates Inc.
- Burland, J.B. 2007. Interaction between structural and geotechnical engineer. *The News of HSSMGE*, no. 9, 4-16.

## REFERENCES

---

- Hoek E. and Brown E.T. 1980. *Underground Excavations in Rock*. London, Instn Min. Metal, England.
- Hoek E. (1983), Strength of jointed rock masses. *Geotechnique*, Vol. 33, No. 3, 187-205.
- Zienkiewicz, O.C. and Pande G.N. 1977. Time-dependent multilaminar model of rocks-a numerical study of deformation and failure of rock masses, *International Journal for Numerical and Analytical Methods in Geomechanics*, 1(3): 219-247.
- Norwegian Soil and Rock Engineering Association (1982). *Norwegian Hard Rock Tunnelling*. Norwegian Soil and Rock Engineering Association Publication No. 1, Tapir, Trondheim, 104-135p.
- Persson, P.A., Holmberg, R., Lande, G. & Larsson, B. (1980). *Underground blasting in a city*. Proceedings of the International Symposium on Subsurface Space (Rockstore '80), Stockholm, vol. 1, pp 199-206.
- Saanio, V. (1986). Finnish design method for large rock caverns. Proceedings of the international Symposium on Large Rock Caverns, Helsinki, vol. 2, pp 1419 - 1430. Pergamon Press, Oxford.
- Stille, H. (1986). Experiences of design of large caverns in Sweden. *Proceedings of the International Symposium on Large Rock Caverns*, Helsinki, vol. 1, pp 231-242. Pergamon Press, Oxford.
- Strange, P.J. & Shaw, R. (1986). *Geology of Hung Kong Island and Kowloon*. Hong Kong Geological Survey Memoir No. 2, Geotechnical Control Office, 134 p.
- Tamrock (1986). *Handbook of Underground Drilling*. Tamrock Drills, Tampere, Finland, 328 p.
- Thomas, I.M., Coates, R. & Turner, V.D. (1986). Rock excavation for a major underground cavern in Hong Kong. Proceedings of the International Conference on, *Rock Engineering and Excavation in Urban Environments*, Hong Kong, pp 405 - 419. Institution of Mining and Metallurgy, London.

